REVIEW OF VADOSE ZONE MEASUREMENT AND MONITORING TOOLS FOR YUCCA MOUNTAIN PERFORMANCE CONFIRMATION PROGRAM

Prepared for

U.S. Nuclear Regulatory Commission
Contract NRC–02–02–012

Prepared by

Dani Or
Professor of Soil & Environmental Physics
School of Architectural, Civil and Environmental Engineering
Ecole Polytechnique Federale de Lausanne
Lausanne, Switzerland

Markus Tuller
Soil and Land Resources Division
University of Idaho
Moscow, Idaho 83844-2339

Stuart Stothoff
Center for Nuclear Waste Regulatory Analyses
San Antonio, Texas

June 2006

PREVIOUS REPORTS IN SERIES

Number	Name	Date Issued
CNWRA 2004-06	Performance Confirmation Activities Under 10 CFR Part 63 with Emphasis on Activities Potentially Significant to Waste Isolation	September 2004
CNWRA 2000-06	Assessment of Methodologies to Confirm Container Performance Model Predictions	September 2000

CONTENTS

Section Page

PREVIOUS REPORTS IN SERIES ii
FIGURES v
TABLES vii
ACKNOWLEDGMENTS ix
EXECUTIVE SUMMARY xi

1 INTRODUCTION 1-1

2 VADOSE ZONE ACTIVITIES IN THE PERFORMANCE CONFIRMATION PLAN . . . 2-1

2.1 Ongoing Activities 2-1
2.2 Future Activities (Post Construction/Operation) 2-2
2.3 Observations 2-3

3 VADOSE ZONE SENSING TECHNOLOGY 3-1

3.1 Water Content Measurement 3-1
3.1.1 Neutron Scattering 3-2
3.1.2 Time Domain Reflectometry 3-5
3.1.3 Capacitance and Frequency Domain Methods 3-10
3.1.4 Impedance Sensors (Amplitude Domain Reflectometry) 3-12
3.1.5 Phase Transmission Sensors 3-13
3.1.6 Ground-Penetrating Radar 3-14
3.2 Matric Potential Measurement 3-18
3.2.1 Background 3-18
3.2.2 Overview 3-21
3.2.3 Tensiometer 3-22
3.2.4 Heat Dissipation Sensors 3-23
3.2.5 Electrical Resistivity Sensors 3-27
3.2.6 Psychrometers 3-28
3.3 Pore Water Extraction 3-32
3.3.1 Suction Cups 3-33
3.3.2 Combined Solution Sampling—Tensiometer Probes 3-34
3.3.3 Lysimeters 3-36
3.3.4 Passive Capillary Samplers 3-38
3.3.5 Capillary Absorbers 3-39
3.3.6 Solution Extraction from Soil and Rock Samples 3-41
3.4 Indirect Water Content Measurement 3-41
3.4.1 Electrical Resistivity Methods 3-41
3.4.2 Electromagnetic Induction Methods 3-47
3.4.3 Fiber Optic Sensors 3-50
3.5 Temperature Measurement 3-51
3.5.1 Thermocouples 3-51
3.5.2 Resistance Temperature Detectors 3-52
3.5.3 Thermistors 3-54

CONTENTS (continued)

Section Page

3.5.4 Fiber Optic Thermometry 3-55
3.6 Relative Humidity Measurement in Cavities 3-55
3.6.1 Psychrometers 3-58
3.6.2 Chilled Mirror Hygrometers (Dew-Point Technique) 3-59
3.6.3 Capacitive Humidity Sensors 3-61
3.6.4 Resistive Humidity Sensors 3-62
3.6.5 Thermal Conductivity Humidity Sensors 3-63
3.7 *In Situ* Water Flux Measurement 3-63
3.7.1 Water Flux Meter 3-63
3.7.2 Heat Pulse Sensors—Water Content, Thermal Properties, and Water Flux 3-64
3.8 *In Situ* Gas Flux Measurement 3-67
3.9 Sensor Pairing for *In Situ* Characterization and Monitoring 3-67
3.10 Characterization and Monitoring in the Vadose Zone 3-72

4 EXAMPLE APPLICATIONS USING CURRENT TECHNOLOGY 4-1

4.1 Tracers and Fractured Rock 4-1
4.1.1 Tracers 4-1
4.1.2 Measurement and Sampling in Fractured Rock 4-3
4.2 Near-Surface Water Fluxes 4-5

5 SUMMARY AND RECOMMENDATIONS 5-1

5.1 Summary of Measurement Technology 5-1
5.2 Discussion 5-2

6 REFERENCES 6-1

FIGURES

Figure		Page
3-1	An Illustration of a Neutron Probe Lowered Into an Access Tube for Repetitive *In Situ* Water Content Measurements	3-2
3-2	Calibration Curve for CPN 502 Neutron Probe in Millville Silt Loam Soil, Logan, Utah	3-3
3-3	Applications of Neutron Scattering for Monitoring Water Content	3-6
3-4	Time Domain Reflectometry Cable Tester with Three-Rod Probe Embedded Vertically in Surface Soil Layer	3-7
3-5	Time Domain Reflectometry Waveforms Increase in Travel Time as the Permittivity of the Fluid Medium Increases	3-7
3-6	Calibration Approaches for Establishing Relationships Between Bulk Dielectric Permittivity and θ_v	3-8
3-7	Commonly Used Time Domain Reflectometry Systems	3-11
3-8	Commercially Available Capacitance Sensors	3-13
3-9	Commercially Available Frequency Domain Sensor	3-14
3-10	Commercially Available Impedance Sensor	3-15
3-11	Commercially Available Phase Transmission Sensor	3-16
3-12	Ground-Penetrating Radar Operation	3-17
3-13	Cross Borehole Ground-Penetrating Radar Measurement Layout and Comparison Between Ground Penetrating Radar and Neutron Probe Measurements	3-19
3-14	Illustration of Typical Tensiometers for Matric Potential Measurement Using Vacuum Gauges and Electronic Pressure Transducers	3-22
3-15	An Advanced Tensiometer for Large Depths Installed in a PVC Guide Pipe	3-24
3-16	A Schematic of the CSI 229 Heat Dissipation Sensor	3-26
3-17	Water Potential Dynamics Measured by Heat Dissipation Sensor, Tensiometer, and Psychrometer During a Laboratory Experiment	3-27
3-18	Commercially Available Electrical Resistance Sensors	3-29
3-19	Psychrometers	3-31
3-20	Typical Setup of Soil Water Samplers (Suction Cups)	3-34
3-21	Combined Solution Sampling	3-35
3-22	Design of a Refilled Suction Lysimeter	3-37
3-23	Design of a Passive Capillary Sampler	3-38
3-24	Deployment Sequence for Capillary Absorbers	3-40
3-25	Surface Electrical Resistivity	3-43
3-26	Multi-Electrode Resistivity	3-45
3-27	Electromagnetic Induction Method	3-46
3-28	Commercially Available Electromagnetic Induction Meter	3-49
3-29	Design of a Fiber Optic Miniprobe Measurement System	3-50
3-30	Thermocouples Connected to a Datalogger and Embedded in the Soil	3-53
3-31	Commercially Available Resistance Temperature Detector Probe	3-54
3-32	Fiber Optic Thermometry	3-56
3-33	Fiber Optic Probes	3-57
3-34	Design of a Psychrometer Used for Porous Media Applications	3-58
3-35	Chilled Mirror Hygrometer Method	3-60
3-36	Commercially Available Chilled Mirror Dewpoint Sensor	3-60
3-37	Commercially Available Capacitive Relative Humidity Sensor	3-62

FIGURES (continued)

Figure Page

3-38 Water Flux Meter Proposed by Gee, et al. (2005) 3-64
3-39 Dual Probe Heat Pulse Sensor 3-65
3-40 Gas-Flux Sensors 3-68
3-41 The Effective Measurement Range of Commonly Used Matric Potential Measurement Methods 3-69
3-42 Vertical Flux Estimates from a Site in Idaho Exhibiting a Unit Gradient 3-70
3-43 Time Domain Reflectometry Probes and Tensiometers Combined to Continuously Monitor Soil Water Dynamics in the Plant Root Zone 3-71
3-44 The Instantaneous Profile Method for Measurement of Hydraulic Conductivity *In Situ* Using Concurrent Measurements 3-72

4-1 Fluorobenzoate Tracers 4-3
4-2 Potential Design and Placement of Capillary Absorbers for Solution Sampling From Boreholes 4-4
4-3 A Setup for Air Permeability Mapping in a Borehole Using Inflatable Packers 4-5
4-4 Indirect Flux Measurement Using Tensiometers and a Neutron Probe (Right), and Direct Flux Measurement Using Deep Tensiometers and a Lysimeter (Left) 4-6

TABLES

Table Page

3-1 Units, Dimensions and Common Symbols for Potential Energy of Soil Water 3-21

3-2 Measurement Range and Calibration Coefficients for E, J, K, R, S, and T-Type Thermocouples 3-52

ACKNOWLEDGMENTS

This report was prepared to document work performed by the Center for Nuclear Waste Regulatory Analyses (CNWRA) for the U.S. Nuclear Regulatory Commission (NRC) under Contract No. NRC–02–02–012. The activities reported here were performed on behalf of the NRC Office of Nuclear Material Safety and Safeguards, Division of High-Level Waste Repository Safety. This report is an independent product of CNWRA and does not necessarily reflect the view or regulatory position of NRC.

The authors acknowledge R. Fedors and C. Dinwiddie for their thorough technical review and useful insight, and G. Wittmeyer for his editorial and programmatic reviews. The administrative support provided by J. Gonzalez and P. Houston is greatly appreciated.

QUALITY OF DATA, ANALYSES, AND CODE DEVELOPMENT

DATA: All CNWRA-generated original data contained in this report meet quality assurance requirements described in the CNWRA Quality Assurance Manual. Sources for other data should be consulted for determining the level of quality for those data. No original data were generated from the analyses presented in this report.

ANALYSES AND CODES: No codes were used in the analyses contained in this report.

PRODUCT DESCRIPTION: Most methods discussed in this report are illustrated with at least one example to demonstrate how the method is implemented. There is no intent to provide an exhaustive catalog of manufacturers or products. Any use of trade, product, or firm names in this publication is for descriptive or illustrative purposes only and does not imply endorsement by CNWRA or NRC.

EXECUTIVE SUMMARY

The U.S. Department of Energy (DOE) Performance Confirmation Plan (Bechtel SAIC Company, LLC, 2004) documents recent DOE intentions for performance confirmation activities at the potential repository at Yucca Mountain. The Performance Confirmation Plan does not represent a final plan for confirmation activities, and technical details of the activities have not been fully developed. A preliminary review of the Performance Confirmation Plan identified several ongoing and planned future performance confirmation activities that would occur in the vadose zone. All of the planned vadose-zone activities are identified as occurring in facilities at the repository horizon. By implication, all characterization and monitoring activities in the vadose zone during performance confirmation will use sensors emplaced in fractured rock (most likely within boreholes drilled from the repository) or cavities in the rock (e.g., drifts, niches, and alcoves). Many of the sensors used for performance confirmation will experience elevated temperatures in the thermally accelerated drifts that will be used to mimic postclosure conditions, in which access for maintenance and upgrades may be severely restricted.

The activities listed in the Performance Confirmation Plan suggest that DOE may wish to use sensors for measuring water content, matric potential, temperature, relative humidity, and water and gas fluxes, and DOE may also wish to obtain pore water for additional analyses. The current state of the art in sensor technology for these applications is reviewed in this document to provide baseline information on the suite of sensors that are available for characterization and monitoring activities in the vadose zone.

The review of available sensor technology suggests that the technology for measuring water content, matric potential, and water and gas fluxes, as well as for obtaining pore water samples, is most fully developed for unconsolidated porous media, as soil science is the primary area of application and development. Findings from the technology review include:

- Water content sensors: A wide variety of approaches are brought to bear on measuring water content. The available methods resolve water content over a wide range in porous media, but some of the methods may not be suitable for fractured rock. Sensor development is proceeding rapidly in some areas. It is not clear how robust these sensors are under elevated temperatures.

- Matric potential sensors: Matric potential is also determined with a variety of methods, but no single method works over the entire range of potentials that may be observed in the field. Each of the methods may be applied to the rock matrix. It is not clear how robust these sensors are under elevated temperatures.

- Pore water samplers: Several sampling techniques are available for extracting pore water. *In situ* techniques may be extremely slow to extract water from the rock matrix.

- Temperature sensors: Temperature sensors infer temperature from the known response of an engineered component to temperature. Industrial applications have provided relatively robust, reliable, and maintenance-free sensors that may be applied over the range of temperatures that may be observed in the field.

- Relative humidity sensors: A variety of methods are used to measure relative humidity. Industrial applications have provided relatively robust, reliable, and maintenance-free sensors. It is not clear how well these sensors perform under elevated temperatures.

- Water flux sensors: Two methods are available to directly measure *in situ* water flux, but significant development is required before either would be applied to fractured rock. It is not clear how well these sensors would perform under elevated temperatures.

- Gas flux sensors: No method exists for directly estimating *in situ* gas flux, although a device is available to estimate transfer between a porous medium and the atmosphere.

Two examples were presented to illustrate how current vadose-zone technology might be deployed to address measurement of percolation fluxes in the subsurface. One example shows how applied tracers might be used to estimate deep percolation fluxes, fast pathways, and lateral diversion. The other example documents several approaches that have been used to estimate shallow infiltration.

The review suggests that measurement activities occurring in fractured vadose-zone rock under ambient temperatures, with time horizons up to perhaps a few years, may be able to use current technology with little modification as long as appropriate maintenance access is available. It is reasonable to expect that the normal pace of technological development will continue to produce enhanced sensors and methodology for the shallow subsurface that may be adapted to hard and fractured rock, even if the rock applications themselves do not drive sensor development.

The review further suggests that current technology may not be adequate for some measurement activities with time horizons of years to decades, particularly if maintenance access is not available or elevated temperatures will occur. Sensors adapted from industry, such as temperature and relative humidity sensors, may be relatively robust and reliable under these conditions. Sensors with a less wide-spread applicability, such as water content, matric potential, water and gas flux sensors, and pore water samplers, may require significant additional development before the technology is capable of handling extended emplacement, especially under elevated temperatures. As there is a quite limited market for such products, it is reasonable to expect that technological development may only slowly produce enhanced sensors and methodology suitable for these more-demanding conditions.

<u>Reference</u>

Bechtel SAIC Company, LLC. “Performance Confirmation Plan.” TDR–PCS–SE–000001. Rev. 05 ICN 00. Las Vegas, Nevada: Bechtel SAIC Company, LLC. 2004.

1 INTRODUCTION

Regulations governing the disposal of high-level radioactive waste at 10 CFR 63, Subpart F, require development of a Performance Confirmation Program for a potential repository in Yucca Mountain. The goal of the program is to confirm that the actual subsurface conditions and potential changes in these conditions during construction and waste emplacement operations are within the limits assumed during the licensing review. The Center for Nuclear Waste Regulatory Analyses (CNWRA), at the direction of the U.S. Nuclear Regulatory Commission (NRC), has reviewed the U.S. Department of Energy (DOE) proposed Performance Confirmation Program for long-term monitoring in the vadose zone. The DOE articulated their preliminary Performance Confirmation Plan (Bechtel SAIC Company, LLC, 2004) for the Performance Confirmation Program. The preliminary Performance Confirmation Plan (Bechtel SAIC Company, LLC, 2004) is referred to as the Performance Confirmation Plan, or Plan for short, throughout this report.

Section 2.1 of the Performance Confirmation Plan summarized the DOE interpretation of the regulatory requirements for the Performance Confirmation Program as

- Confirm that subsurface conditions, geotechnical and design parameters are as anticipated and that changes to these parameters are within limits assumed in the License Application
- Confirm that the waste retrieval option is preserved
- Evaluate information used to assess whether natural and engineered barriers function as intended
- Evaluate effectiveness of design features intended to perform a postclosure function during repository operation and development
- Monitor waste package condition

Vadose zone conditions played an important role in the selection of the potential repository location. Section 3.2 of the Performance Confirmation Plan identified the following vadose zone characteristics as being particularly important:

- A semiarid climate with limited precipitation
- A thickness of rock and soil above the repository of approximately 215 to 450 meters [705 to 1,480 ft]
- Hydrogeologic and geochemical characteristics that limit radionuclide movement
- Depth to groundwater below repository emplacement drifts from more than 215 meters to nearly 365 meters [705 to 1,200 ft]

These characteristics strongly influence the natural and engineered barriers intended to isolate waste, by minimizing contact with naturally occurring water fluxes and by retarding radionuclide

transport (by sorption and drift shadow) in the event of a breach of a waste package at the repository level.

The Performance Confirmation Program is an important component of the overall Yucca Mountain Project, assuring that the potential repository will perform as envisioned. The Performance Confirmation Plan (Bechtel SAIC Company, LLC, 2004) articulates the approaches that DOE intends to take for performance confirmation. The Performance Confirmation Plan is the initial attempt by DOE to define the activities that will occur during performance confirmation, and is subject to revision. Although the specific details of each activity remain to be finalized, the Plan suggests that DOE vadose zone performance confirmation activities will focus on *in situ* and in-drift moisture and energy balances at and below the repository horizon, and will consider conditions in and near thermally accelerated drifts. The activities listed in the Performance Confirmation Plan are summarized in Section 2 for reference.

DOE will emplace suites of sensors to carry out the performance confirmation activities. Based on the types of activities listed in the Performance Confirmation Plan, it is reasonable to assume that DOE may wish to consider sensors for water content, matric potential, temperature, relative humidity, and water and gas fluxes, and DOE may also wish to obtain pore water for additional analyses. Section 3, the bulk of this report, is a review of the techniques that are used for performing these types of measurements in the vadose zone, providing a snapshot of the strengths and weaknesses of current technology. Section 4 illustrates some of the capabilities of current technology with examples of hypothetical activities that might occur at a geologic repository, and Section 5 summarizes the findings on vadose zone characterization and monitoring methods.

2 VADOSE ZONE ACTIVITIES IN THE PERFORMANCE CONFIRMATION PLAN

The U.S. Department of Energy (DOE) developed a Performance Confirmation Plan (Bechtel SAIC Company, LLC, 2004) to ensure that repository performance lies within estimated or predicted parameters. Section 1.3 of the Performance Confirmation Plan defines eight stages for developing the Performance Confirmation Program:

(1) Select performance confirmation parameters and test methods
(2) Predict performance and establish a baseline
(3) Establish bounds and tolerances for key parameters
(4) Establish test completion criteria and variance guidelines
(5) Plan activities, and construct and implement the Performance Confirmation Program
(6) Monitor, test, and collect data
(7) Analyze and evaluate data
(8) Recommend corrective action in the case of variance

DOE narrowed the list of performance characterization activities to eleven ongoing and nine future activities as the basis for their proposed Performance Confirmation Plan, based on an evaluation of various aspects and alternatives related to repository performance and potential impact on total system performance. Sections 2.1 and 2.2 below quote the summary of these processes found in the Executive Summary of the Performance Confirmation Plan [bold italics (added) denote vadose zone processes].

2.1 Ongoing Activities

(1) Precipitation monitoring (precipitation quantities and composition measured at the Yucca Mountain site)

(2) ***Seepage monitoring (seepage monitoring and analysis in alcoves on the repository intake side and in repository thermally accelerated drifts)***

(3) ***Subsurface water and rock testing (chloride mass balance and isotope chemistry analysis of water samples collected at selected underground locations)***

(4) ***Unsaturated zone testing (field testing of transport and sorptive properties of unsaturated zone rock in an ambient seepage alcove or a drift with no waste packages emplaced)***

(5) Saturated zone monitoring (measurements of water level, electrochemical potential, hydrogen potential, and background radionuclide concentrations in saturated zone wells at the repository site and in Nye County)

(6) Saturated zone alluvium testing (tracer testing of alluvium transport properties in the Alluvial Test Complex)

(7) ***Subsurface mapping (mapping of fractures, faults, stratigraphic contacts and lithophysal characteristics of rock in the underground openings)***

(8) Seismicity monitoring (monitoring of regional seismic activity and observation of fault displacements following significant seismic events)

(9) Construction effect monitoring (measurement of construction deformation of underground openings/confirmation of related rock mechanical properties)

(10) Corrosion testing (laboratory samples testing of waste package, waste package pallet, and drip shield materials corrosion behavior in the range of expected repository environments)

(11) Waste form testing (laboratory testing of waste form dissolution and waste package coupled effects including use of scale mockups of waste package)

2.2 Future Activities (Post Construction/Operation)

(12) Saturated zone fault zone hydrology testing (hydraulic and tracer testing in fault zones)

(13) Drift inspection (periodic inspection of emplacement drifts and thermally accelerated drifts using remote inspection and measurement techniques)

(14) ***Thermally accelerated drift near-field monitoring (monitoring of rock mass and water properties in the near-field of a thermally accelerated emplacement drift)***

(15) Dust buildup monitoring (monitoring and laboratory evaluation of the quantity and composition of dust on engineered barrier surfaces and samples)

(16) ***Thermally accelerated drift environment monitoring (monitoring and laboratory evaluations of environmental conditions in a thermally accelerated drift including gas and water compositions, temperatures, film depositions, microbes, radiation and radiolysis effects using remote techniques)***

(17) Thermally accelerated drift thermal-mechanical effects monitoring (monitoring of drift and invert degradation in a thermally accelerated drift)

(18) Seal testing (testing of effectiveness of borehole seals in the laboratory, shaft and ramp seals in the field, and backfill emplacement techniques)

(19) Waste package monitoring (monitoring of integrity of waste packages using visual inspection and/or internal pressure measurement employing remote monitoring techniques)

(20) Corrosion testing of thermally accelerated drift samples (laboratory testing of waste package, waste package pallet, and drip shield samples obtained from a thermally accelerated drift)

2.3 Observations

The Performance Confirmation Plan conceptually describes repository performance as attributable to three barriers: (i) the Upper Natural Barrier, including infiltration, unsaturated zone flow, ambient seepage, and thermal seepage; (ii) the Engineered Barrier System; and (iii) the Lower Natural Barrier, including unsaturated zone flow, radionuclide transport in the unsaturated zone, saturated zone flow, and saturated zone transport. Each of the activities summarized in Sections 2.1 and 2.2 are intended to help confirm that one or more of the barriers is performing within the limits assumed during the License Application. The Upper and Lower Natural Barriers both have components within the vadose zone.

The activity descriptions in the Plan appear to focus on quality assurance and safety issues, and the technical details of the planned activities are not fully determined. Aside from precipitation observations, hydrology-related performance confirmation activities listed in the Plan are either activities related to near-drift processes or activities related to the saturated zone. Most of the proposed near-drift activities are intended to consider processes in and near thermally accelerated drifts. By omission, it appears that DOE intends to not perform activities confirming that infiltration rates and unsaturated zone fluxes from the ground surface to the repository are within the limits assumed during the License Application.

Based on the activities described in the Performance Confirmation Plan, many vadose zone measurement sensors used for performance confirmation will be placed within boreholes drilled into fractured rock from drifts, alcoves, and niches. The remaining sensors would be placed directly within drifts, alcoves, and niches. Many of the sensors will encounter high temperatures in and near thermally accelerated drifts, which are drifts that will be heavily instrumented, closed to ventilation using bulkheads, and allowed to heat up prior to closure in order to examine system responses to conditions expected in the repository during the postclosure thermal period. There is no activity described in the Plan that would place vadose zone measurement sensors within an unconsolidated porous medium.

3 VADOSE ZONE SENSING TECHNOLOGY

Vadose zone sensing technology largely has been driven by soil scientists, although industrial activity has also driven sensor development in some areas (e.g., temperature and humidity sensors). Vadose zone sensing technology has only rarely been applied within rock masses (e.g., Yucca Mountain), and typically these applications are modifications of techniques developed for soil science. Most vadose zone sensing methodologies can be applied to soil, rock, and industry-specific porous media. All such media are generically referred to as porous media in this report.

The sensor methods discussed in this report are divided into eight general sensor categories: (i) water content measurement, (ii) matric potential measurement, (iii) pore water extraction, (iv) indirect water content measurement, (v) temperature measurement, (vi) relative humidity measurement in cavities, (vii) in situ water flux measurement, and (viii) *in situ* gas flux measurement. Several sensors may be used to measure more than one physical quantity, and in some cases multiple sensors are bundled into one probe. Sensors with multiple capabilities are presented in the section related to the most advanced of the sensor's capabilities. Characteristics of methods with wide exposure and particular applicability to the Yucca Mountain Project are summarized in a Summary Box.

Most methods discussed in this report are illustrated with at least one example to provide a visual example of how the method is implemented. There is no intent to provide an exhaustive catalog of commercial products, and any use of trade, product, or firm names in this publication is for descriptive or illustrative purposes only and does not imply endorsement by the Center for Nuclear Waste Regulatory Analyses or the U.S. Nuclear Regulatory Commission.

3.1 Water Content Measurement

The amount of water in a porous medium and the forces by which water is held in the pores (matric or capillary potential) are important attributes of liquid water in a porous medium. These attributes are related to each other through a characteristic curve. The liquid-phase characteristics affect the gaseous phase in the pore space and the rates of exchange between the liquid and gas phases; these characteristics also affect other transport properties such as hydraulic conductivity.

Many geotechnical and hydrologic practices and studies require knowledge of the amount of water contained in soil or in rock formations. Some of the methods used to determine water content are described in this section, focusing on methods for performing continuous and measurements relevant to long-term monitoring and the U.S. Department of Energy (DOE) Performance Confirmation Plan. The neutron scattering approach emits neutrons into the porous medium and measures characteristics of reflected neutrons. The remaining methods are all based on measurement of the bulk dielectric permittivity or the dielectric constant (ε_b) of the porous medium (Hilhorst, et al., 2001). The dielectric constant of rock and soil is dominated by the presence of liquid water, due to its high dielectric constant (~81) relative to other constituents such as soil and rock minerals (2 to 5), frozen or bound water (~3), and air (1). Dielectric methods rely on interactions between porous media and applied electromagnetic waves or fields to deduce the dielectric permittivity of the medium under study. These methods include time domain reflectometry, capacitance and frequency domain methods, impedance sensors, phase transmission sensors, and ground-penetrating radar.

3.1.1 Neutron Scattering

The neutron scattering method is commonly used for field measurement of volumetric water content and in some industrial and construction applications (e.g., see applications at www.berthold.com). The method is based on the propensity of hydrogen nuclei to slow (thermalize) high energy fast neutrons. A typical neutron moisture meter consists of (i) a probe containing a radioactive source that emits high-energy (2 to 4 MeV) fast {1,600 km/s [994 mi/s]} neutrons and a detector of slow neutrons; (ii) a scaler to monitor the flux of slow neutrons, and, optionally, (iii) a datalogger for storing and retrieving data. The neutron probe method is illustrated in Figure 3-1. The radioactive source commonly contains a mixture of Americium-241 and Beryllium in 10 to 50 millicurie amounts. The alpha particles emitted by the decay of the Americium-241 collide with the light Beryllium nuclei, resulting in emission of fast neutrons.

Fast neutrons are emitted spherically from the radioactive source into the surrounding medium, where they collide with various atomic nuclei. Collisions with most nuclei are virtually elastic (i.e., resulting in only minor losses of kinetic energy by the fast neutrons). However, collisions with light hydrogen nuclei, which have mass similar to neutrons, cause significant loss of kinetic energy and slow the fast neutrons. When the speed of fast neutrons diminishes to that of particles at ambient temperature {approximately 2.7 km/s [1.7 mi/s]}, with corresponding energies of approximately 0.03 eV, the neutrons are called thermalized or slow neutrons. Thermalized neutrons rapidly form a “cloud” of nearly constant density near the detector that measures the return flux of the slow neutrons. The average kinetic energy loss (the relative number of slow neutrons returning to the detector) is linearly dependent on the amount of

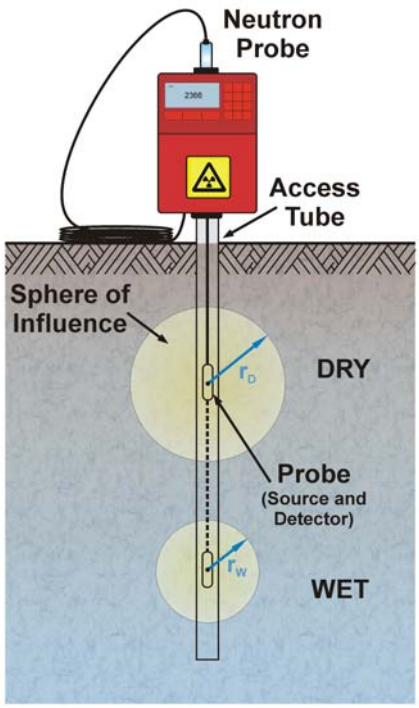

Figure 3-1. An Illustration of a Neutron Probe Lowered Into an Access Tube for Repetitive *In Situ* Water Content Measurements. Note the Different Sphere of Influence for Measurements in Wet and Dry Soil.

hydrogen nuclei in the soil, and the primary source of hydrogen in soil (and the most variable in time) is water. Several other nonhydrogen substances effectively thermalize fast neutrons and are present in trace amounts in some media; these substances generally may be compensated for using medium-specific calibration.

Calibration of the neutron probe to account for background hydrogen sources and other local effects (e.g., local bulk density, trace neutron attenuators, etc.) is conveniently achieved by simultaneous measurement of water content (from samples acquired during installation of an access tube or from nearby destructive sampling) and actual neutron probe counts at the same locations. The calibration curve (Figure 3-2) is typically linear and relates volumetric water content, θ_v, to slow neutron counts or count ratio

$$\theta_v = a + b \ (CR) \tag{3-1}$$

where

CR	—	ratio of slow neutron counts at a specific location in the soil to a standard count obtained with the probe in its shield
a and *b*	—	fitting constants

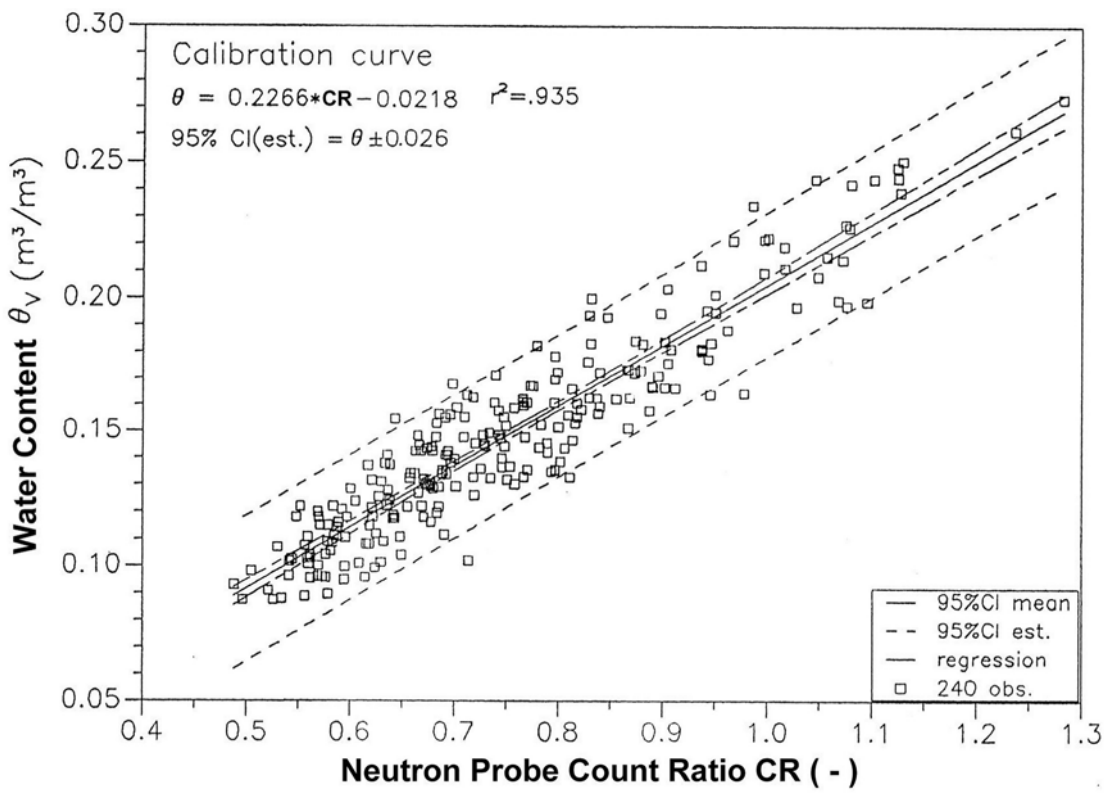

Figure 3-2. Calibration Curve for CPN 502 Neutron Probe in Millville Silt Loam Soil, Logan, Utah. The Dashed Lines Represent the 95 Percent Confidence Interval About the Regression Line. [Reproduced From Or (1990) With Permission]

The calibration coefficients are similar for many soils. The sphere of influence of the radiation source, which varies from approximately 15 cm [0.49 ft] (wet soil) to approximately 70 cm [2.3 ft] (very dry soil), depends on how far fast neutrons travel before becoming thermalized (see illustrated sphere of influence in Figure 3-1). An approximation for the radius of influence, *r* (in centimeters), as a function of ambient water content is given by

$$r = 15\left(\theta_v\right)^{-1/3} \tag{3-2}$$

The neutron scattering method is unsuitable for measurements near the soil surface or rock cavities because a portion of the neutrons may escape. Reliable measurements are typically obtained at depths (or distances from a rock wall) exceeding 15 to 20 cm [0.49 to 0.66 ft]. Limitations or disadvantages of this method include the radiation hazard and associated licensing requirements, uncertain spatial resolution, unsuitability for near-surface measurements, and medium-specific calibration requirement. Characteristics of the method relevant to performance confirmation are summarized in Summary Box 1.

Summary Box 1. The Neutron Scattering Method

Measurement Range

- Entire range of water contents

Accuracy

- ±2 percent volumetric water content with calibration

Limitations

- Radiation hazards and licensing requirements
- Requires site specific calibration
- Variable volume of measurement
- Not suitable for near-surface measurements
- Provides “snap shots”
- Difficult to automate
- Installation and measurements are labor intensive

Advantages

- Repetitive and nondestructive measurements at the same locations
- Reliable and robust measurements (following calibration)
- Cost effective: one device can serve many access tubes
- Measurement of total water content for entire θ range is not sensitive to phase and energy state of water (liquid, bound, and frozen water)

Applicability for the Performance Confirmation Program

- May be used for monitoring near-field variations in water content
- May be used to independently quantify percolation flux in the shallow subsurface in combination with deep (advanced) tensiometers

3.1.2 Time Domain Reflectometry

Time domain reflectometry is a relatively new method for water content measurement (Topp, et al., 1980). The main advantages of the time domain reflectometry method over other methods for repetitive water content measurement (e.g., neutron scattering) are (i) accuracy to within 1 to 2 percent of volumetric water content, (ii) minimal calibration requirements—in many cases medium-specific calibration is not needed, (iii) no radiation hazard, (iv) good spatial resolution, (v) measurements are simple to obtain, and (vi) the method is capable of providing continuous water content measurements through automation and multiplexing. Figure 3-3 depicts currently available time domain reflectometry systems.

The propagation velocity, v, of an electromagnetic wave along a transmission line (probe or waveguide) of length L (Figure 3-4) embedded in a porous matrix is determined from the time response of the system to a pulse generated by the time domain reflectometry cable tester. The propagation velocity ($v = 2L/t$) is a function of the bulk dielectric constant (ε_b) according to

$$\varepsilon_b = \left(\frac{c}{v}\right)^2 = \left(\frac{ct}{2L}\right)^2 \tag{3-3}$$

where

c — velocity of electromagnetic waves in vacuum (3×10^8 m/s)
t — time for a wave to traverse the length of the embedded waveguide and return (out and back distance = $2L$)

The definition of the dielectric constant is given in Eq. (3-3); this equation states that the dielectric constant of a medium is the squared ratio of wave propagation velocity in vacuum to the propagation velocity in the medium. The method is relatively insensitive to soil composition and texture because the bulk dielectric constant (ε_b) is controlled by the dielectric constant of liquid water, thus is a good method for measuring liquid water content. The bulk dielectric permittivity is determined from analyses of time domain reflectometry waveforms (reflection coefficient versus time or distance) as depicted in Figure 3-5.

Two basic approaches are used to establish the relationships between ε_b and volumetric water content (θ_v). The first approach is empirical, whereby mathematical expressions are simply fitted to observed data without using any particular physical model. Such an approach was employed by Topp, et al. (1980), who fitted a third-order polynomial to the observed relationships between ε_b and θ_v for multiple soils (Figure 3-6a). The second approach is physically based, using a mixing model of the dielectric constants and the volume fractions of each of the soil components to derive a relationship between the composite (bulk) dielectric constant and the amount of soil water (i.e., a specific component). Dielectric mixing models were developed by Birchak, et al. (1974), Dobson, et al. (1985), and Roth, et al. (1990).

Time domain reflectometry calibration establishes the relationship between ε_b and θ_v. For example, calibration might be conducted in a fairly uniform soil without abrupt changes in water content along the waveguide. The empirical relationship for mineral soils (soils with low organic matter content), as proposed by Topp, et al. (1980), is

$$\theta_v = -5.3 \times 10^{-2} + 2.92 \times 10^{-2}\,\varepsilon_b - 5.5 \times 10^{-4}\,\varepsilon_b^2 + 4.3 \times 10^{-6}\,\varepsilon_b^3 \tag{3-4}$$

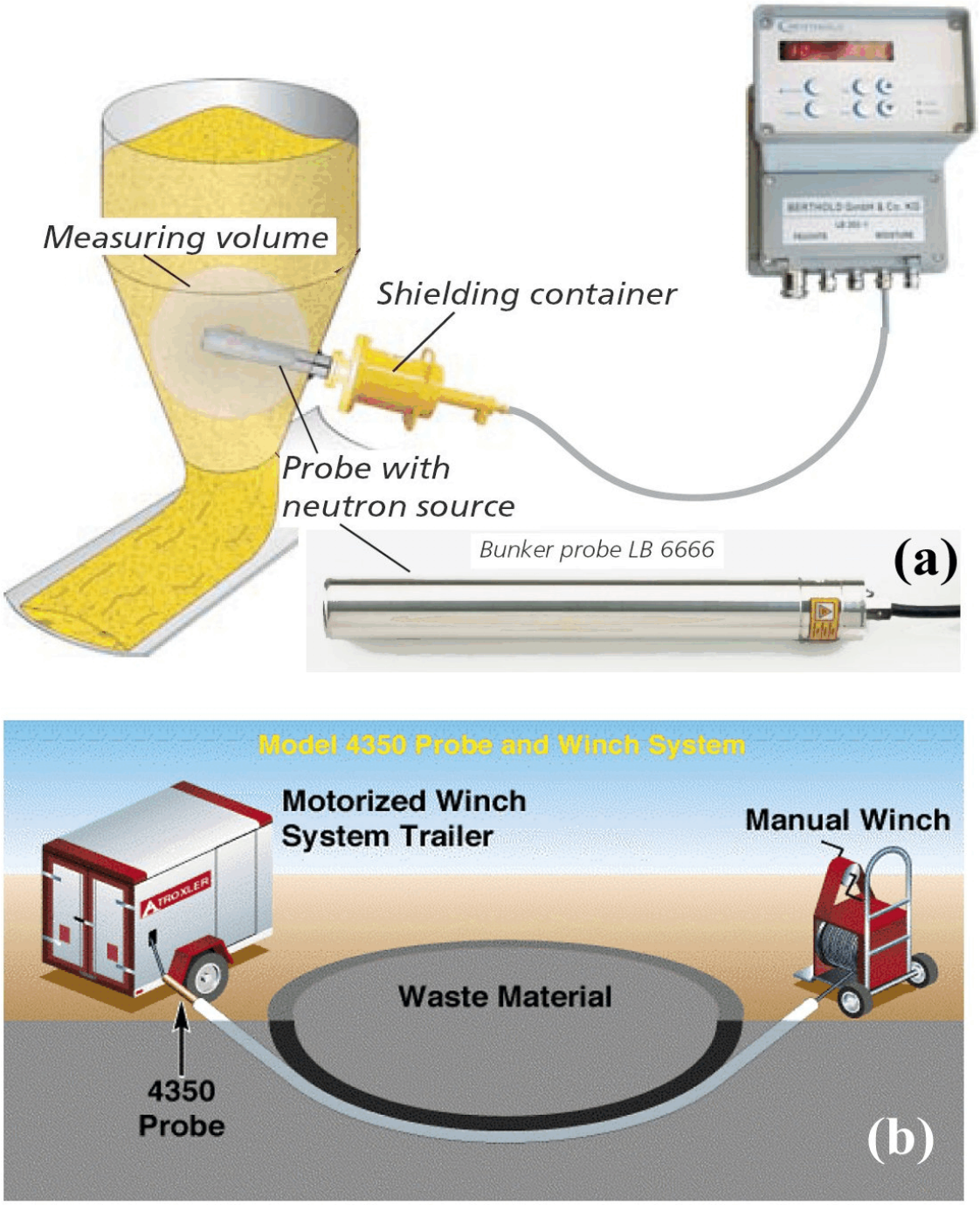

Figure 3-3. Applications of Neutron Scattering for Monitoring Water Content: (a) A Stand-Alone Probe in Industrial Applications, and (b) Automated Scanning Through a Horizontal Access Tube With a Manual or Motorized Winch. [Illustration (a) Courtesy of Berthold Technologies U.S.A., LLC; (b) Reproduced with Permission from T. Burford, Sandia National Laboratories]

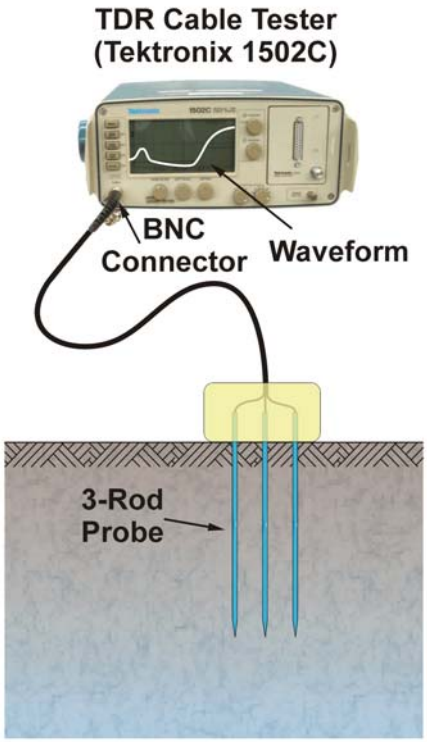

Figure 3-4. Time Domain Reflectometry Cable Tester With Three-Rod Probe Embedded Vertically in Surface Soil Layer

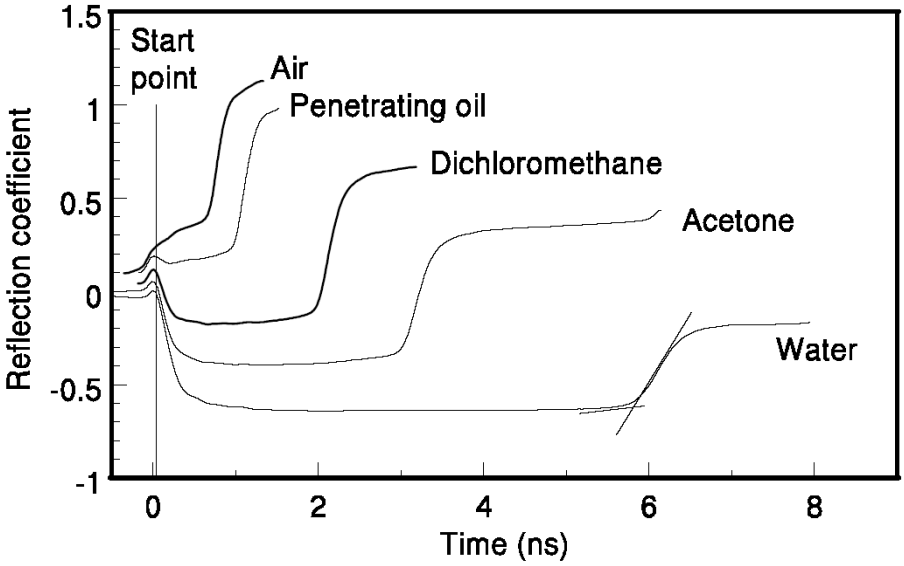

Figure 3-5. Time Domain Reflectometry Waveforms Increase in Travel Time as the Permittivity of the Fluid Medium Increases. Travel Time for the Water Waveform is Determined Using The Intersection of the Two Tangent Lines. [Reproduced From Robinson, et al. (2003) With Permission]

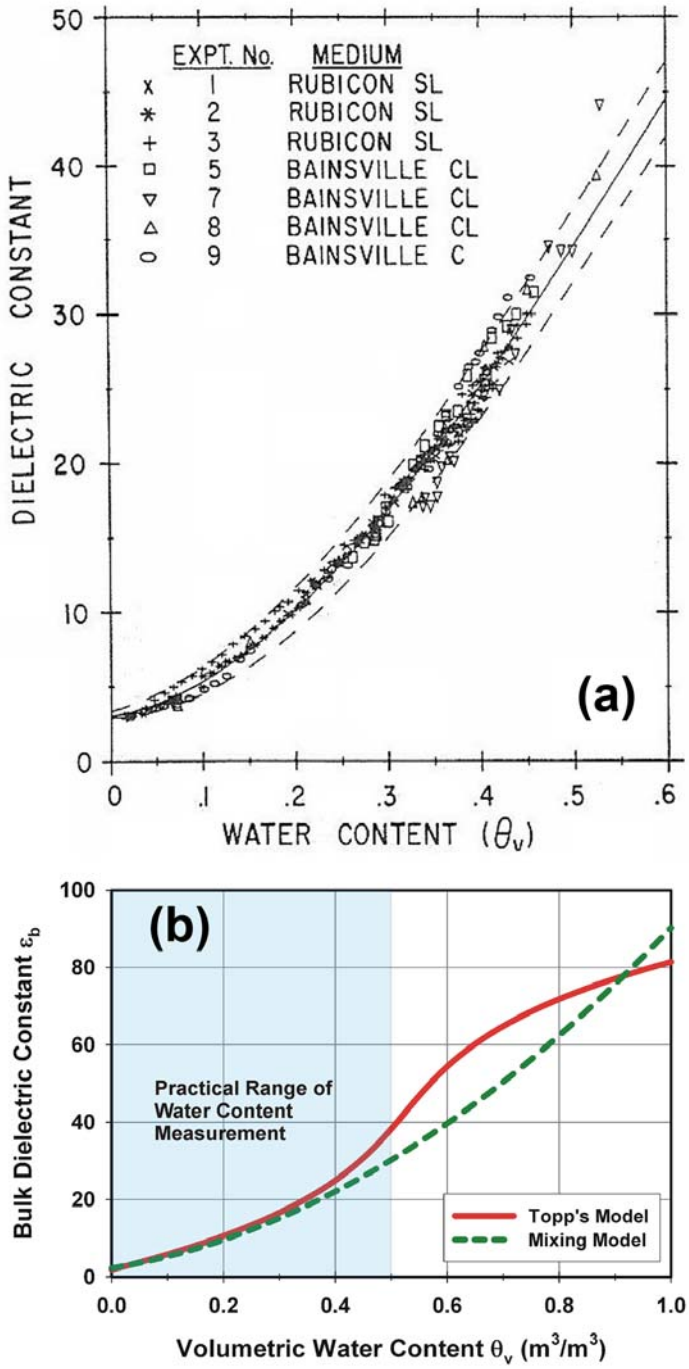

Figure 3-6. Calibration Approaches for Establishing Relationships Between Bulk Dielectric Permittivity and θ_v: (a) The Empirical Expression of Topp, et al. (1980) Fitted to Experimental Results; and (b) Comparison Between Topp's Empirical Expression and a Physically-Based Dielectric Mixing Model.
Note: SL–Silt and CL–Clay
[(a) Reproduced From Topp, et al. (1980) With Permission]

This relationship provides adequate description for water contents less than 0.5 (covering most of the range of interest in many soils), with an estimation error for θ_v of approximately 0.013. However, Eq. (3-4) does not adequately describe the relationship between ε_b and θ_v for water contents exceeding 0.5 and for soils containing appreciable amounts of organic matter (see Figure 3-6b).

A physically-based calibration model employing dielectric mixing of the constituents and their geometric arrangement expresses the bulk dielectric constant of a three-phase system (Roth, et al., 1990) as:

$$\varepsilon_b = \left[\theta_v \varepsilon_w^{\beta} + (1-n)\varepsilon_s^{\beta} + (n-\theta_v)\varepsilon_a^{\beta}]\right]^{\frac{1}{\beta}} \tag{3-5}$$

where

n	—	soil porosity
$1-n$	—	volume fraction of the solid phase: $(1-n) = V_s/V_T$, where V_s is volume of solids and V_T is total sample volume
θ_v	—	volume fraction of the aqueous phase: $\theta_v = V_w/V_T$, where V_w is volume of water
$n - \theta_v$	—	volume fraction of the gaseous phases: $(n-\theta_v) = V_a/V_T$, where V_a is volume of air
ε_s	—	dielectric constant of the solid phase
ε_w	—	dielectric constant of the aqueous phase
ε_a	—	dielectric constant of the gaseous phase
β	—	factor summarizing the geometry of the medium relative to the axial direction of the wave guide ($-1 \le \beta \le 1$; $\beta = 1$ for an electric field parallel to soil layering, $\beta = -1$ for a perpendicular electrical field, and $\beta = 0.5$ for an isotropic two-phase mixed medium)

Note that the volume fractions sum to unity.

Rearranging Eq. (3-5) and solving for θ_v yields

$$\theta_v = \frac{\varepsilon_b^{\beta} - (1-n)\,\varepsilon_s^{\beta} - n\varepsilon_a^{\beta}}{\varepsilon_w^{\beta} - \varepsilon_a^{\beta}} \tag{3-6}$$

which links θ_v to the value of ε_b measured by time domain reflectometry. Many have used $\beta = 0.5$, which is shown by Roth, et al. (1990) to produce a calibration curve very similar to the third-order polynomial proposed by Topp, et al. (1980) over the water content range of $0 < \theta_v < 0.5$. If common values are assumed for the various constituents such as $\beta = 0.5$, $\varepsilon_w = 81$, $\varepsilon_s = 4$, and $\varepsilon_a = 1$ into Eq. (3-6), the resulting form is

$$\theta_v = \frac{\sqrt{\varepsilon_b} - (2-n)}{8} \tag{3-7}$$

Note that the porosity of the material must be known or estimated when using the mixing model approach. A comparison between the Topp, et al. (1980) expression [Eq.(3-4)] and a calibration

curve based on Eq. (3-7) with n = 0.5 is depicted in Figure 3-6b. In summary, Eq. (3-4) establishes an empirical relationship between bulk soil dielectric and volumetric water content, whereas Eq. (3-6) is based on physical and geometrical considerations and Eq. (3-7) is a simplified version of Eq. (3-6).

Several commonly used time domain reflectometry systems are shown in Figure 3-7. Limitations or disadvantages of the time domain reflectometry method include relatively high equipment expense, potentially limited applicability under saline conditions due to signal attenuation, and the need for media-specific calibration for media having large amounts of bound water or high organic matter contents. Characteristics of the method relevant to performance confirmation are summarized in Summary Box 2.

Summary Box 2. The Time Domain Reflectometry Method

Measurement Range

- Entire range of water contents

Accuracy

- ± 1 to 2 percent volumetric water content

Advantages

- Superior accuracy to within 1 to 2 percent of the actual volumetric water content
- Minimal calibration requirements (usually no medium-specific calibration necessary)
- No radiation hazard
- Excellent spatial and temporal resolution
- Continuous measurements through automation and multiplexing

Limitations

- Expensive—typical system costs approximately $4,000
- Limited performance in saline porous media (for bulk electrical conductivity values in excess of 0.02 to 0.03 S/m)
- Potential temperature effects
- Specialized—no “off-the-shelf” systems; requires training

Applicability for the Performance Confirmation Program

- Monitoring near field and in-drift variations in water content (using large probes for fracture integration)
- May be used to independently quantify percolation flux in the shallow subsurface [paired with deep (advanced) tensiometers]
- Confirmation of drift shadow below the repository

3.1.3 Capacitance and Frequency Domain Methods

Two electrodes (parallel plates or rods) inserted into a porous medium form a capacitor (the porous medium is the dielectric). Capacitance is strongly dependent on the dielectric constant, which is dominated by the amount of water in the porous medium. The relationship between

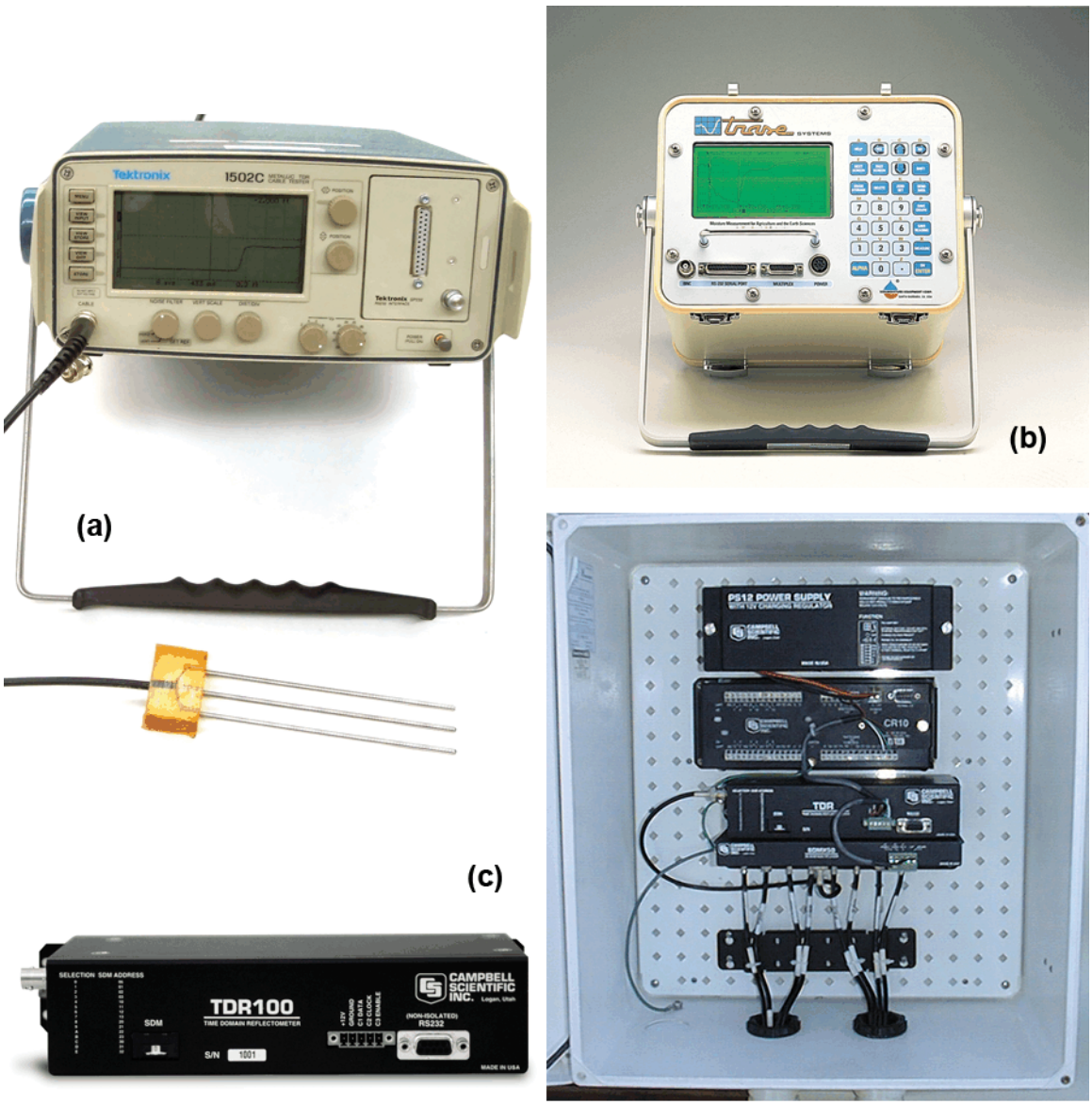

Figure 3-7. Commonly Used Time Domain Reflectometry Systems: (a) Tektronix 1502c General Purpose Cable Tester, (b) Trase System (Soilmoisture Equipment Corp.), and (c) TDR100 (Campbell Scientific, Inc.) by Itself (Left) and TDR100 Installed in Enclosure (Right). [Photograph in (a) by M. Tuller, Image in (b) Courtesy Soilmoisture Equipment Corp., and Images in (c) Courtesy of Campbell Scientific, Inc.]

dielectric constant and electrical capacitance between two parallel plates of area *A* and spacing *d* is

$$C = \frac{A\,\varepsilon^{*}\varepsilon_0}{d} \tag{3-8}$$

where

ε^*	—	complex dielectric constant of the soil or rock
ε_0	—	free space permittivity
C	—	capacitance

The complex dielectric constant contains both real (ε') and imaginary (ε'') components, with $\varepsilon^* = \varepsilon' - i\,\varepsilon''$ and $i = \sqrt{-1}$. In most applications only the real part of the dielectric constant is considered.

When the capacitor is connected to an oscillator to form a tuned electrical circuit, changes in soil moisture can be detected through changes in operating frequency. This basic frequency domain theory is applied in capacitance and frequency domain reflectometry sensors. In capacitance sensors the dielectric permittivity of a medium is determined by measuring the charge time of a capacitor. In frequency domain reflectometry sensors the oscillator frequency is modulated within a certain range to find the resonant frequency (greatest amplitude), which is related to the medium's water content.

A material-specific calibration is typically necessary because the operating frequency of these devices is generally below 100 MHz, and at these low frequencies the bulk permittivity may be affected by minerals. Furthermore, effects of temperature, salinity, bulk density, and clay content are more pronounced than for high frequency techniques such as time domain reflectometry. Commercially available capacitance sensors include HYDRA probes (Stevens Water Monitoring Systems, Inc.), ECH_2O probes (Decagon Devices, Inc.), CS616-L Water Content Reflectometers and CS620 HydroSense® probes (Campbell Scientific, Inc.). Commercially available frequency domain reflectometry sensors include the Sentry 200-AP probe (Troxler, North Carolina, USA) and the EnviroScan© sensor (Sentek Sensor Technologies, 2001). Representative capacitance sensors are shown in Figure 3-8, with the EnviroScan© sensor illustrated in Figure 3-9.

The measurement range and accuracy vary considerably among this family of sensors (Evett and Steiner, 1995; Paltineanu and Starr, 1997). For example, Evett and Steiner (1995) found measurement errors with the Sentry 200AP to be three times larger than comparable measurement errors using a neutron probe.

3.1.4 Impedance Sensors (Amplitude Domain Reflectometry)

Electrical impedance represents the total opposition of a system to an alternating current at a given frequency. Impedance is a complex quantity with the real component called resistance and the imaginary component called inductive or capacitive reactance. When an electromagnetic wave traveling along a transmission line reaches a section of the line with a

Figure 3-8. Commercially Available Capacitance Sensors: (a) HYDRA Probe (Stevens Water Monitoring Systems, Inc.), (b) CS620 HydroSense® Probe (Campbell Scientific, Inc.), and (c) ECH$_2$O (Decagon Devices Inc.). [Image (a) Courtesy of Stevens Water Monitoring Systems, Inc.; Image (b) Courtesy of Campbell Scientific, Inc.; and Image (c) Courtesy of Decagon Devices. Photocredit: photobay.biz; Reproduced With Permission From Decagon Devices Inc.]

different impedance, part of the transmitted energy is reflected back toward the source. The reflected wave interacts with the incident wave, producing a voltage standing wave along the transmission line (i.e., change of wave amplitude along the length of the transmission line).

The impedance change due to a combination of a probe and porous medium can be estimated by measuring the change in amplitude (Gaskin and Miller, 1996; Nakashima, et al., 1998). These sensors improve the estimates of water content in the surrounding medium by using a measurement frequency that reduces the influence of the electrical conductivity in the surrounding medium. Impedance sensors use an oscillator to generate a sinusoidal signal at a fixed frequency (e.g., 100 MHz), which is applied to a coaxial transmission line that extends into the porous medium through an array of parallel metal rods; the outer rod forms an electrical shield around the central signal rod. This rod arrangement acts as an additional section of the transmission line, having impedance that depends on the dielectric constant of the soil between the rods. An example of an impedance sensor is shown in Figure 3-10.

3.1.5 Phase Transmission Sensors

A sinusoidal electromagnetic wave shifts phase as it moves away from the source. This phase shift depends on travel distance, wave frequency, and propagation velocity. Given the wave frequency and travel distance, the water content can be determined based on the magnitude of

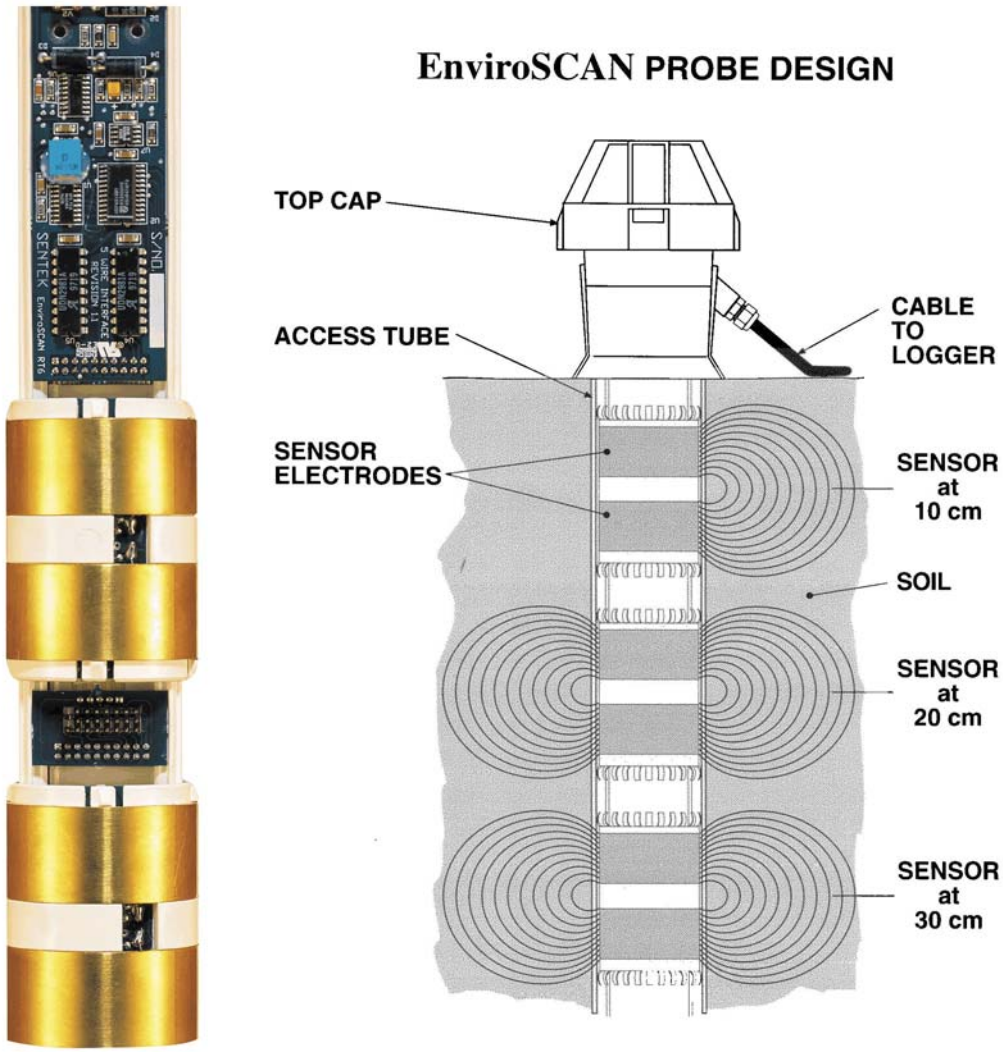

Figure 3-9. Commercially Available Frequency Domain Sensor: Sentek EnviroSCAN® Sensor for Profiling Water Content Along an Access Tube [Images Reproduced With Permission From Sentek Pty Ltd. Copyright Sentek Pty Ltd 2001. EnviroSCAN® Is a Registered Trademark of Sentek Pty Ltd]

phase shift because propagation velocity is related to the water content of the medium. The probe uses a particular waveguide design (two concentric metal, opened rings) so that phase shift is measured at the beginning and end of the waveguides. An example of a phase transmission sensor is shown in Figure 3-11.

3.1.6 Ground-Penetrating Radar

Ground-penetrating radar is a geophysical technique used in reflection mode to non-invasively image the shallow subsurface (Davis and Annan, 1989). An example of how the technique may

Figure 3-10. Commercially Available Impedance Sensor: (a) ThetaProbe ML2x Soil Moisture Sensor and HH2 Moisture Meter (Photograph Courtesy Delta-T Devices, Ltd.—www.delta-t.co.uk), and (b) Field Application of a Bank of Soil Moisture Sensors. [Photograph Reproduced From Calder, et al. (2002) With Permission]

be applied in the field using a mobile unit is shown in Figure 3-12a. Ground-penetrating radar is an antenna-based tool that transmits short electromagnetic waves into the ground, and in return, receives backscattered radar echoes from subsurface interfaces, as indicated by Figure 3-12b. The reflection strength of each echo and the two-way travel time needed to send the pulse and receive each echo are recorded. Common mid-point soundings are used to estimate the average velocity of electromagnetic waves in a given subsurface environment, thus providing a conversion factor for associating each subsurface reflection with a particular depth [recall Eq. (3-3)]. A cross section of subsurface reflectors as a function of lateral and vertical distance is then built using common offset profiling, which consists of repeatedly pulsing the transmitter and receiving the echoes at incremental positions along a transect. Figure 3-12c shows a typical tracegram with distinct reflectors.

Radar reflections originate primarily at discontinuities of relative dielectric constant where the electromagnetic wave undergoes an abrupt change in velocity. The relative dielectric constant of a given geologic unit determines the velocity of radar waves in that unit. The relative dielectric constant of a material is a measure of its capacity to store electrical charge. Good dielectric materials store electrical charge (e.g., $\varepsilon^* = 1$); thus, water ($\varepsilon^* = 81$) is a poor dielectric, given that it easily conducts charge when subject to an electric field. On this basis, ground-penetrating radar is potentially useful for estimating the water content of the subsurface, because the velocity of electromagnetic waves is very fast in dry material, solid ice, and air, and is slow in water-saturated material. Empirical models and mixing models may be used to estimate water content, just as with Time Domain Reflectometry, as discussed in detail in Section 3.1.2.

Figure 3-11. Commercially Available Phase Transmission Sensor: VIRRIB® Soil Moisture Sensor. [Reproduced From Bulletin 343, Institute of Food and Agricultural Sciences, University of Florida (2004) With Permission]

Two important aspects of ground-penetrating radar are resolution and penetration depth. Ground-penetrating radar resolution is determined by the period of the emitted pulse, which is controlled by the frequency bandwidth of the system. Because impulse radar systems are designed with bandwidths that are approximately equal to the center frequency, the resolution of ground-penetrating radar increases with increasing center frequency (Davis and Annan, 1989).

Ground-penetrating radar penetration depth is dependent on the center frequency of the system, the electrical conductivity of the subsurface environment, and on the scattering properties of the geology.

Radar energy is significantly attenuated in materials having elevated electrical conductivity, such as silts, clays, and low to moderate water content material with high concentrations of total dissolved solids or salts (from evaporative losses in desert environments, for example). In low conductivity media, such as porous dry sands and sandstone, gravel or ice, low-frequency antennas (<100 MHz) can achieve signal penetration to depths exceeding several tens of meters, and mid- to high-frequency antennas (>100 MHz) can achieve signal penetration up to several meters.

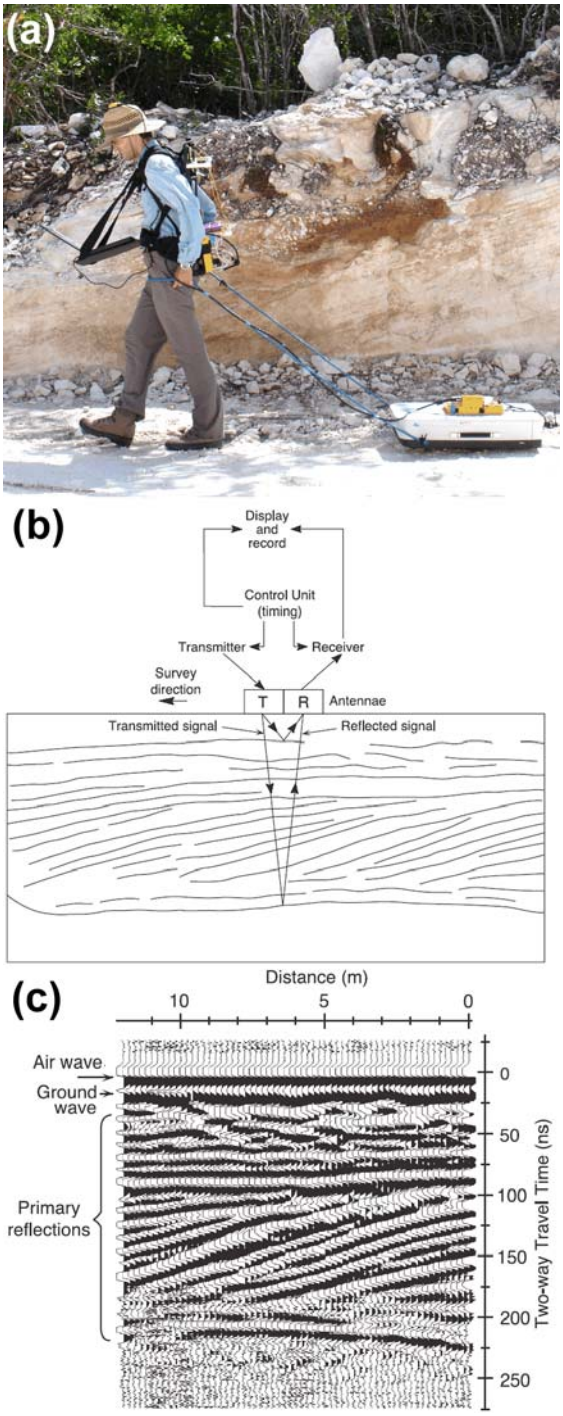

Figure 3-12. Ground-Penetrating Radar Operation: (a) Field Application of a Mobile Unit, (b) Illustration of Operational Setup, and (c) a Typical Radar Cross-Section of a Subsurface Formation. [(a) Photograph Courtesy of M. Grasmueck, Rosentiel School of Marine and Atmospheric Science, University of Miami; (b) and (c) Reprinted From Earth-Science Reviews, 66, A. Neal, Ground-Penetrating Radar and Its Use in Sedimentology: Principles, Problems and Progress, Page 266, Copyright (2004), With Permission From Elsevier]

The Tumalo Tuff (Oregon) and the Bishop Tuff (California) have both been demonstrated to scatter radar waves (Rust and Russell, 2006; Grimm, et al., 2006); the Bandelier Tuff (New Mexico) is known to be opaque to radar waves.[1] In sum, radar techniques are sensitive to changes in physical and mineral properties, including permittivity, magnetic permeability, electrical conductivity, porosity and density. This sensitivity does reduce the range of subsurface environments in which the ground-penetrating radar method can be successfully applied.

In addition to surface application, ground-penetrating radar may also be used in boreholes by, for example, lowering a transmitter into a borehole and recording signal strength at a receiver at the ground surface or in another borehole. An example of this procedure is shown in Figure 3-13, in which the cross-borehole application of ground-penetrating radar is compared to neutron-probe observations. Cross borehole radar tomography (ground-penetrating radar used in transmission mode) was used at Yucca Mountain during Site Characterization. These data are only now undergoing analysis (Kowalsky, et al., 2005).

3.2 Matric Potential Measurement

3.2.1 Background

Water held in the pore space of a porous medium is subjected to several force fields. The combined effects of these forces result in a deviation in potential energy relative to the reference state, called the total water potential, ψ_T, defined as the amount of work that an infinitesimal unit quantity of water at equilibrium is capable of doing when it moves (isothermally and reversibly) to a pool of water at similar standard (reference) state (i.e., similar pressure, elevation, temperature, and chemical composition). There are alternative definitions of water potential using concepts of chemical potential or specific free energy of the chemical species. The water chemical species is just one component of the solution called the water phase; the methods documented in this report typically consider the water phase, not the water species. Some of the arguments concerning the definitions and their scales of application are presented by Corey and Klute (1985), Iwata, et al. (1988), and Nitao and Bear (1996). Because these fundamental concepts are subject to ongoing debate, simple and widely accepted definitions are presented that are applicable at macroscopic scales and yield an appropriate framework for practical applications.

The primary forces acting on water held within a rigid porous matrix under isothermal conditions can be conveniently grouped (Day, et al., 1967) as (i) matric forces resulting from interactions of the solid phase with the liquid and gaseous phases; (ii) osmotic forces owing to differences in the chemical composition of the water solution across a semi-permeable membrane, which will be neglected in this report; and (iii) body forces induced by gravitational and other (e.g., centrifugal) inertial force fields.

The thermodynamic approach, whereby potential energy is considered rather than forces, is particularly useful for equilibrium and flow considerations. Forces are extremely difficult to measure, and vector balances are computationally difficult to work with. Potential energy is a

[1]P. Annan. Personal communication to C. Dinwiddie, Geosciences and Engineering Division, Southwest Research Institute. Mississauga, Ontario, Canada: Sensors & Software, Inc. 2005.

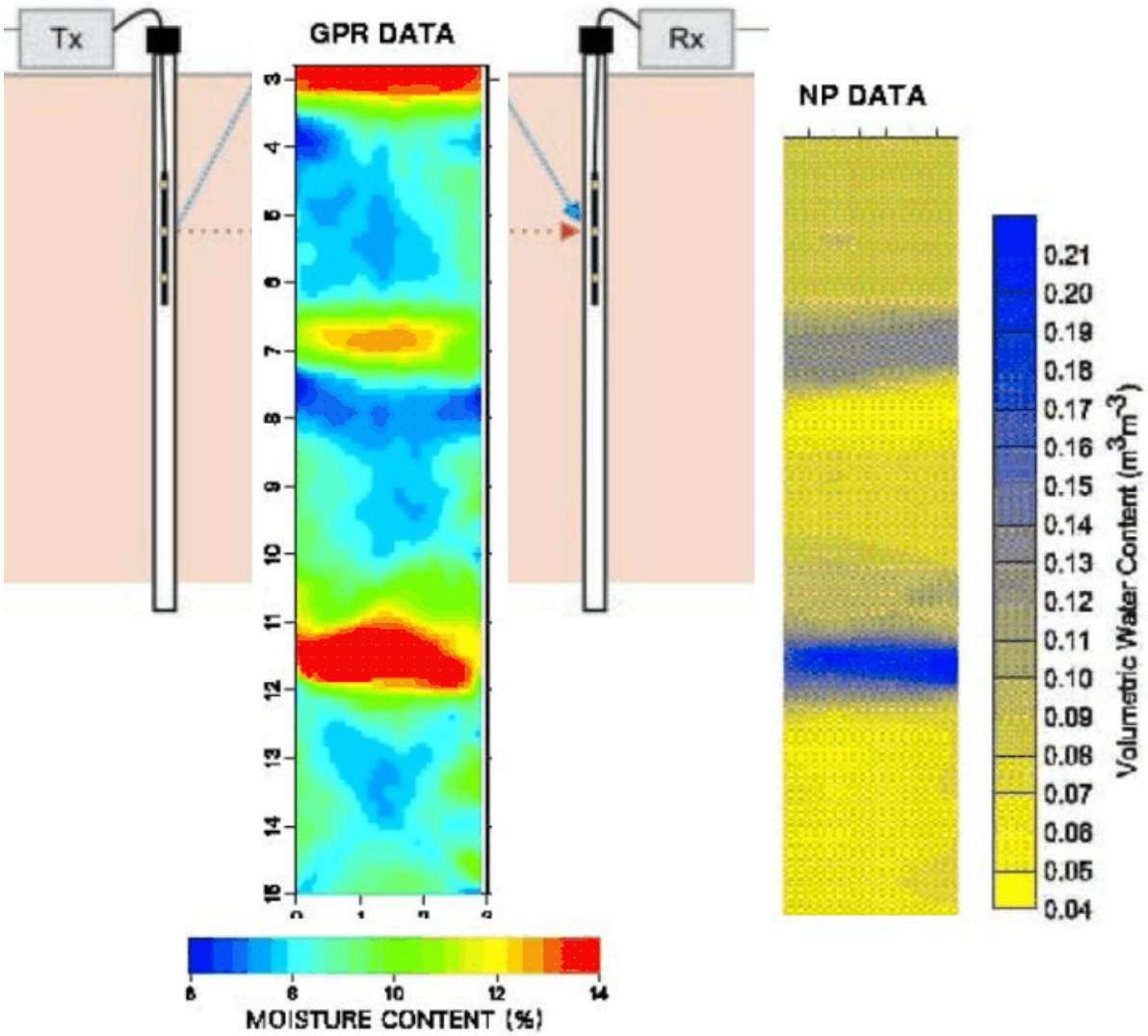

Figure 3-13. Cross Borehole Ground-Penetrating Radar Measurement Layout and Comparison Between Ground Penetrating Radar and Neutron Probe Measurements From the Same Domain [Modified From Majer, et al. (2002) and Ferré, et al. (2003) With Permission]

scalar quantity, defined as the negative integral of the force over the path taken by an infinitesimal amount of water when it moves from a reference location to the point under consideration. Consequently, the hydraulic potential (ψ_h, or the total potential neglecting the osmotic component) can be expressed as the algebraic sum of the component potentials corresponding to the different fields acting on soil water, or

$$\psi_h = \psi_m + \psi_p + \psi_z \tag{3-9}$$

where

ψ_m — is the matric potential
ψ_p — is the pressure potential
ψ_z — is the gravitational potential

The matric potential, ψ_m, results from the combined effects of capillarity and adsorptive forces within the porous matrix. The primary mechanisms for these effects include (i) capillarity caused by liquid-gas interfaces forming and interacting within the irregular soil pore geometry, (ii) adhesion of water molecules to solid surfaces due to short-range London-van der Waals forces and extension of these effects by cohesion through hydrogen bonds formed in the liquid, and (iii) ion hydration and water participating in diffuse double layers (particularly near clay surfaces). There is some disagreement regarding the practical definition of this component of the total potential. Some researchers consider all contributions other than gravity and solute interactions (at a reference atmospheric pressure). Others use a device known as a tensiometer (discussed in Section 3.2.3) to provide a practical definition of the matric potential for water in contact with its porous cup (Hanks, 1992). The value of ψ_m ranges from zero, when the soil is saturated, to increasingly negative values as the soil becomes drier {note that ψ_m = 0 mm [0 in] is greater than ψ_m = −1,000 mm [−39.4 in]}.

The pressure potential, ψ_p, is defined as the hydrostatic pressure exerted by the column of unsupported water above a point of interest divided by the density of water. Using units of energy per unit weight provides a simple and practical definition of ψ_p, which is the vertical distance from the point of interest to the free water surface (unconfined water table elevation). The convention used here is that ψ_p is always positive below a water table and zero at or above the water table. With this convention, nonzero magnitudes of ψ_p and ψ_m are mutually exclusive: either ψ_p is positive and ψ_m is zero (saturated conditions), or ψ_m is negative and ψ_p is zero (unsaturated conditions), or $\psi_p = \psi_m = 0$ at the free water table elevation. Note that some researchers prefer to combine the pressure and matric components into a single term, which assumes positive values under saturated conditions and negative values under unsaturated conditions. Based on operational and explanatory considerations, the more commonly used separate-components convention is adopted here.

The gravitational potential, ψ_z, is determined solely by the elevation of a point relative to some arbitrary reference datum, and is equal to the work needed to raise a body against the earth's gravitational pull from the reference datum to its present position. When expressed as energy per unit weight, the gravitational potential is simply the vertical distance from the reference datum to the point of interest. The numerical value of ψ_z itself is not important (it is defined with respect to an arbitrary reference datum)—what is important is the difference (or gradient) in ψ_z between any two points of interest. This difference is independent of the reference datum.

Total water potential and its components may be expressed in several ways depending on the definition of a "unit quantity of water." Potential may be expressed as (i) energy per unit of mass, (ii) energy per unit of volume, or (iii) energy per unit of weight. A summary of the resulting dimensions, common symbols, and units are presented in Table 3-1. The various expressions of soil water energy status are equivalent, with

$$\mu = \frac{\psi}{\rho_w} = gh \tag{3-10}$$

where

ρ_w — density of water
g — gravitational acceleration

Only μ has actual units of potential; ψ has units of pressure and h has units of length (representing the height of water over a datum). However, each of these expressions is widely used in earth sciences in a generic sense to refer to potential.

3.2.2 Overview

Four techniques are commonly used to measure matric potential, each with different ranges of applicability. Tensiometers rely on a direct hydraulic connection between an engineered porous medium and the surrounding medium, thus are appropriate for relatively wet conditions but are subject to failure under dry conditions. Heat dissipation sensors also rely on a direct hydraulic connection between an engineered porous medium and the surrounding medium; however, compared to tensiometers, heat dissipation sensors are slower to equilibrate, may not be as accurate in the range of potentials where tensiometers are valid, but are less prone to fail and can consider drier conditions. Electrical resistivity sensors are akin to heat dissipation sensors, except matric potential is inferred from electrical resistivity within the engineered medium and the sensor may be affected by the ionic composition of the surrounding medium. Psychrometers work with water vapor rather than liquid water, unlike the other matric-potential sensor types, obviating the need for liquid-phase connectivity between the bulk medium and sensor. Psychrometers measure relative humidity, estimating matric potential using the known equilibrium between water vapor and liquid water. Psychrometers are appropriate for dry conditions, but are inaccurate under wet conditions. There is little overlap between tensiometer and psychrometer measurement ranges.

Table 3-1. Units, Dimensions and Common Symbols for Potential Energy of Soil Water

Units	Symbol	Name	Dimensions*	SI Units
Energy/Mass	μ	Chemical Potential	L^2/T^2	J/kg
Energy/Volume	ψ	Soil water potential, suction, or tension	$M/(LT^2)$	N/m^2 (Pa)
Energy/Weight	h	Pressure head	L	m

*L is length, M is mass, and T is time.

3.2.3 Tensiometer

Tensiometers directly measure the water potential in the surrounding porous medium. A tensiometer consists of a porous cup, usually made of ceramic (or sintered metal) with very fine pores, connected to a vacuum gauge through a water-filled tube, as shown in Figure 3-14. The porous cup is placed in intimate contact with the bulk porous medium at the desired measurement location. When the matric potential of the surrounding medium is lower (more negative) than the potential inside the tensiometer, water moves from the tensiometer to the surrounding medium through the saturated porous cup in response to the difference in potential, thereby creating suction measured by the gauge. Water flow continues until the suction inside the tensiometer equals the bulk matric potential. Flow may occur in either direction. The volume of exchanged water is typically very small because water is essentially incompressible and air is excluded from the tensiometer. Because the tensiometer actually measures the pressure difference between the atmosphere and the water inside the tensiometer, it is straightforward to consider both matric potential and pressure potential (i.e., saturated conditions) with the same device.

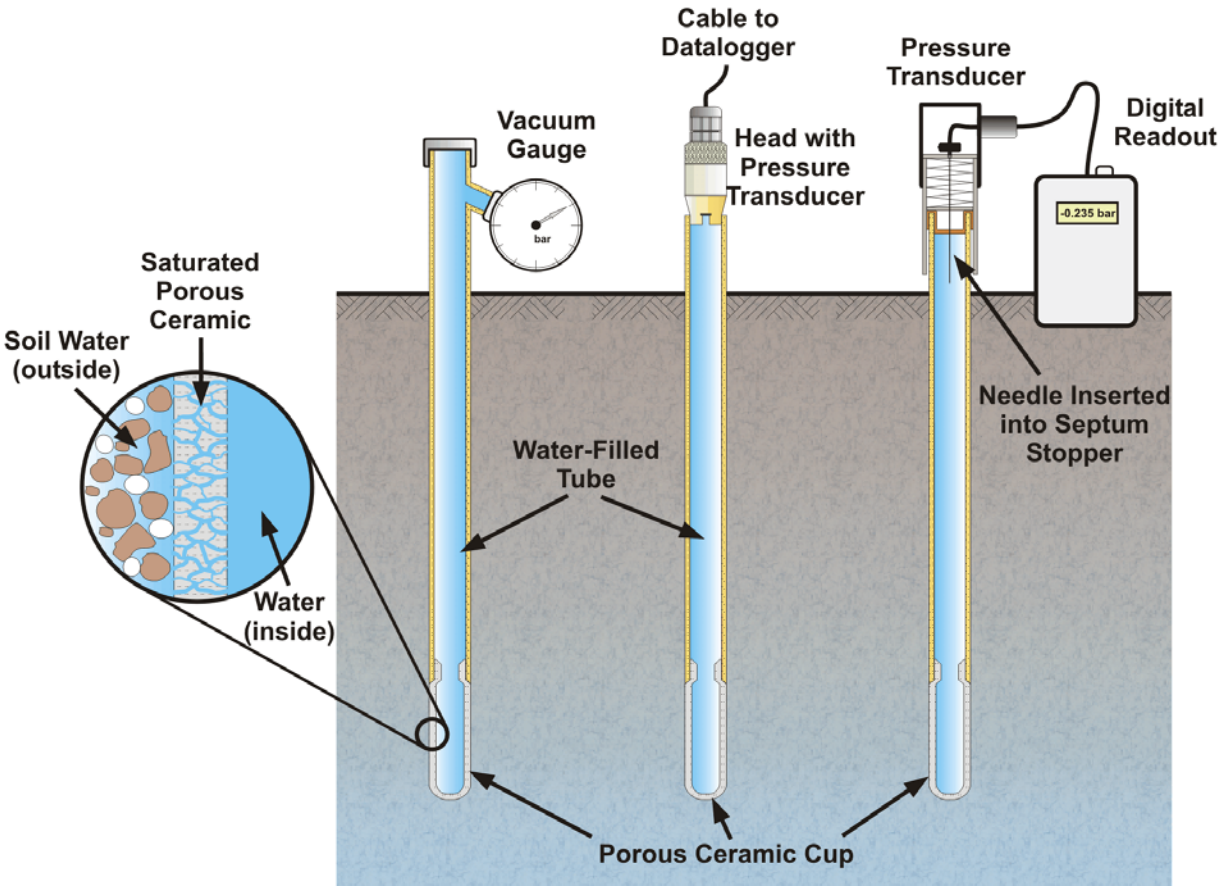

Figure 3-14. Illustration of Typical Tensiometers for Matric Potential Measurement Using Vacuum Gauges and Electronic Pressure Transducers. [Illustration Copyright 2005 From "Field Methods for Monitoring Solute Transport" by Tuller and Islam, 2005. Reproduced by Permission of Routledge/Taylor & Francis Group, LLC.]

A tensiometer fails if a gas bubble forms inside the device, because the connection with the bulk soil is no longer almost incompressible. Spontaneous cavitation of water occurs as the water tension nears 8 to 10 m [26.2 to 32.8 ft] under typical pressure and temperature conditions, with impurities and small entrapped gas bubbles serving as nuclei for cavitation. Porous cups for tensiometers are usually designed with sufficiently small pores that cavitation occurs before air penetrates the porous cup. Despite efforts to extend the range of tensiometric measurements by delaying onset of cavitation, the practical range for these devices remains limited to suction (negative matric potential) less than 100 kPa [1 bar] {i.e., 10 m [32.8 ft] head of water}, and other techniques must be used for matric potential measurement under drier conditions.

Tensiometer maintenance demands for deep monitoring are reduced with the suggested tensiometer proposed by McElroy and Hubbell (2004), as shown in Figure 3-15. The advanced tensiometer has a relatively small water reservoir adjacent to the porous cup, reducing the need for refilling, and instrument accuracy is enhanced by placing the pressure transducer adjacent to the reservoir where temperatures are relatively stable.

Tensiometers must maintain direct hydraulic connection between the vacuum gauge and the surrounding bulk medium or the device fails, so proper tensiometer installation is critical to sensor performance. Prior to installation, porous cups should be soaked for 24 to 48 hours, followed by thorough testing of the tensiometers under controlled laboratory conditions, to ensure that the device is free of bubbles. The orientation of the installation borehole is not important, but it should be only slightly larger than the tensiometer to better maintain hydraulic connection between tensiometer and the bulk medium. A tight hydraulic connection is formed by pressing the tensiometer into a slurry emplaced at the measurement location. The slurry is preferably formed of the native granular material cored from the measurement location during borehole installation, but silica flour may replace the native material for installation in rock. In expansive soils, a bentonite collar should be poured and compacted around the top portion of the sampler to prevent water from seeping through gaps between the sampler and installation borehole.

Macropores or highly structured and coarse porous media may limit the application of tensiometric measurements.

Characteristics of the tensiometer method are summarized in Summary Box 3.

3.2.4 Heat Dissipation Sensors

Heat dissipation sensors are akin to electrical resistivity sensors (Section 3.2.5), in that the technique relies on measurements within a medium with known characteristics emplaced within the bulk medium. As with electrical resistivity methods, it may take a long time for the emplaced medium to come to complete equilibration with the surrounding bulk medium, particularly under dry conditions.

Heat dissipation sensors characterize matric potential by analyzing the thermal response of the emplaced rigid porous medium. Heat dissipation sensors contain heating elements in line source or point source configurations embedded in a rigid porous matrix with fixed pore space. A heat pulse is created by applying a constant current through the heating element for a specified time period, with the thermal response measured by a thermocouple placed at a certain distance from the heating source (Phene, et al., 1971; Bristow, et al., 1993). The rate of

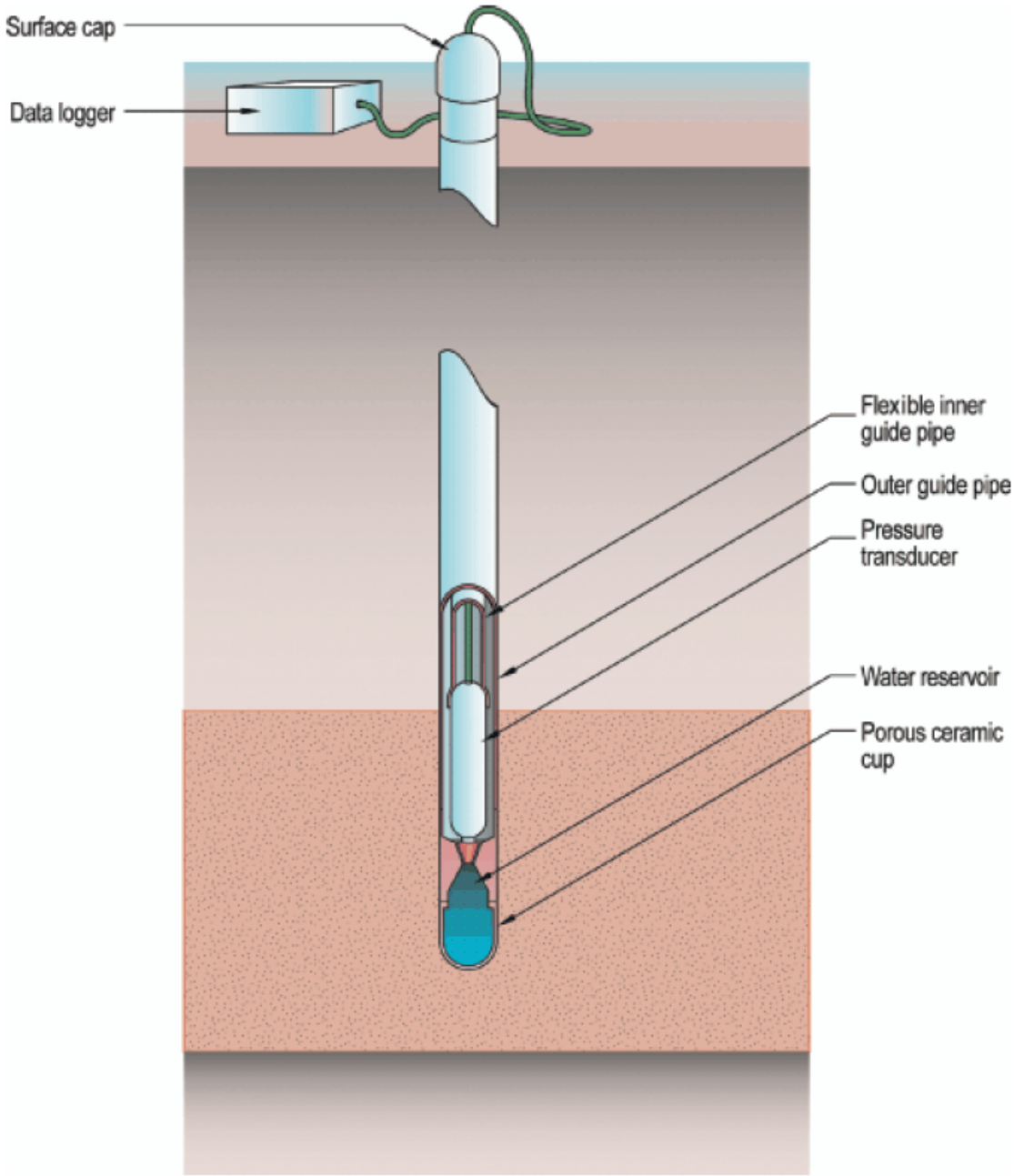

Figure 3-15. An Advanced Tensiometer for Large Depths Installed in a PVC Guide Pipe [Reproduced From McElroy and Hubbell (2004) With Permission]

Summary Box 3. Tensiometers
Measurement Range • Typically from 0 to −10 m [0 to −32.8 ft] of pressure head (some can measure positive pressure) **Accuracy** • Dependent on pressure gauge and response time, typically within ± 10 mm [± 0.4 in] **Limitations** • Frequent maintenance (newly designed advanced tensiometers depicted in Figure 3-16 reduce maintenance) • Limited measurement range • Small measurement volume **Advantages** • Repetitive and nondestructive measurements at a location • Most direct measurement of capillary/matric potential (at appropriate range) • Automation and remote monitoring and service (advanced design) • Low cost **Applicability for the Performance Confirmation Program** • May be used to independent quantify percolation flux in the shallow subsurface (combined with neutron probes or time domain reflectometry) • Perhaps the most sensitive sensor for *in situ* assessment of local hydraulic gradients associated with capillary diversion around drifts

heat dissipation in a porous medium is dependent on the specific heat capacity, thermal conductivity, and density of the medium. All three quantities increase with increasing water content, which in turn increases with increasing matric potential. These relationships are determined before sensor emplacement. The thermocouple response following a pulse allows the thermal properties of the emplaced medium to be estimated, which in turn allows determination of matric potential. Often the magnitude of temperature increase following a pulse is linearly related to the natural logarithm of matric potential, with a larger temperature increase occurring under drier conditions.

A line source sensor is shown in Figure 3-16. This sensor has a fine-wire heating element axially centered in a cylindrical ceramic matrix, with a matrix radius of 1.5 cm [0.59 in] and a matrix length of 3.2 cm [1.26 in]. A thermocouple is located adjacent to the heating element at mid-length. Both the heating wire and the thermocouple are contained in the shaft portion of a hypodermic needle. A comparison between heat dissipation, tensiometer, and psychrometer measurements of matric potential within the same soil volume in a laboratory experiment (Reece, 1996) is shown in Figure 3-17. The heat dissipation measurements follow the tensiometer measurements in the wet range and the psychrometer measurements in the dry range, suggesting that the heat dissipation approach may be appropriate in the intermediate range where neither of the other two methods are accurate.

Characteristics of heat dissipation sensors are summarized in Summary Box 4.

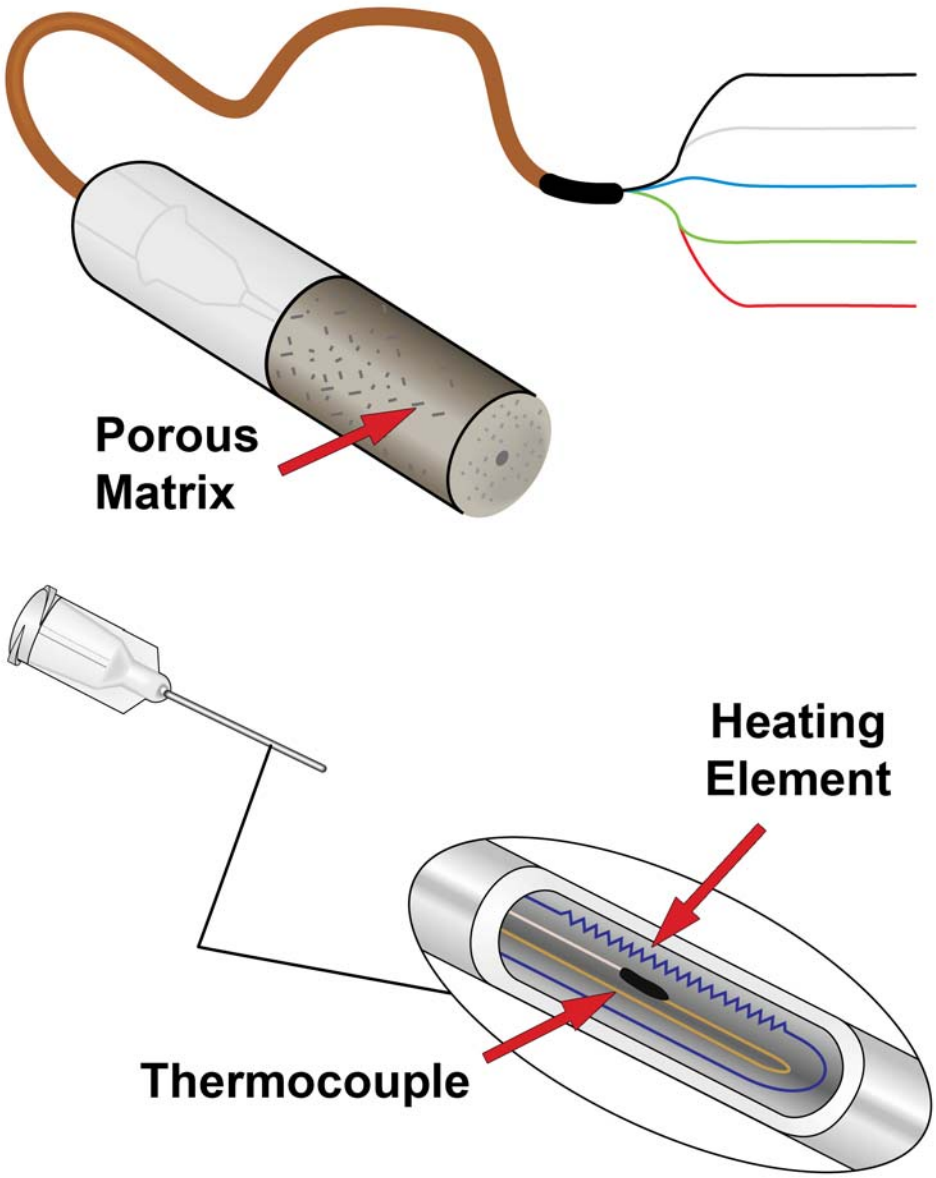

Figure 3-16. A Schematic of the CSI 229 Heat Dissipation Sensor (Campbell Scientific, Inc.) [Illustration Courtesy of Campbell Scientific, Inc.]

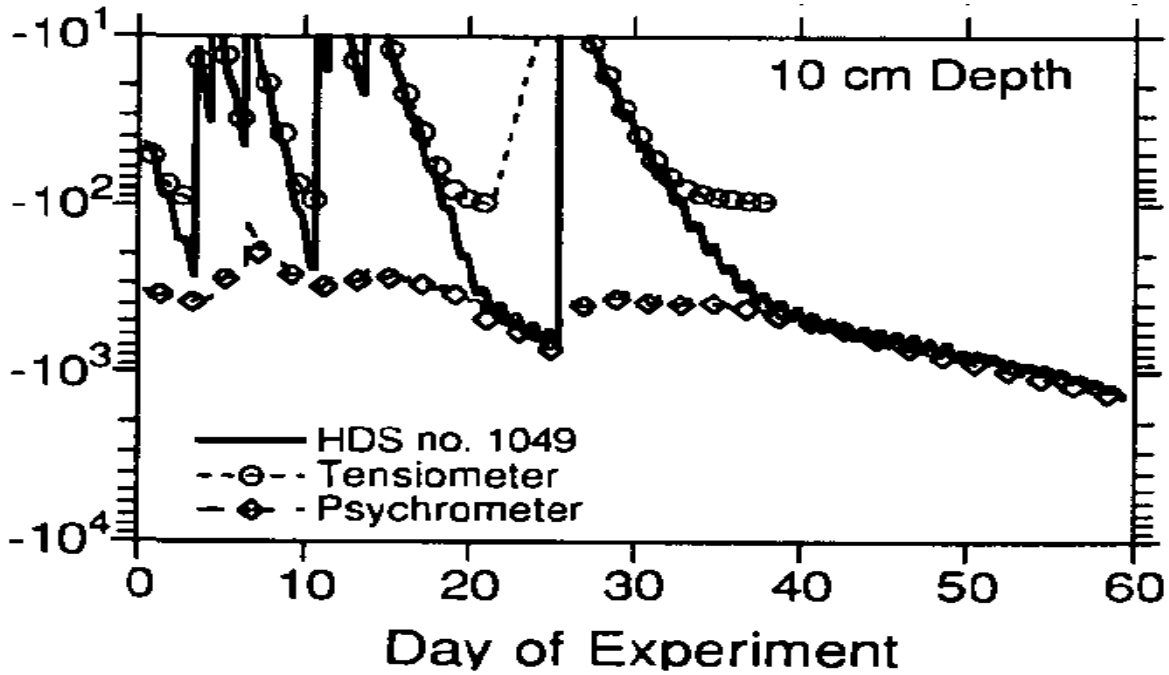

Figure 3-17. Water Potential Dynamics Measured by Heat Dissipation Sensor, Tensiometer, and Psychrometer During a Laboratory Experiment. The Tensiometer and Psychrometer Ranges do not Overlap, but the Heat Dissipation Sensor Bridges the Gap. [Reproduced From Reece (1996) With Permission]

3.2.5 Electrical Resistivity Sensors

The electrical resistivity of a porous medium depends on the water content and soluble ionic constituents. Simple and inexpensive sensors, such as the sensor shown in Figure 3-18, have been developed to infer water status using the dependance of resistivity on water content. These sensors usually consist of concentric cylindrical or flat parallel electrodes embedded in an engineered porous matrix and connected to lead wires. Resistance is measured within the engineered porous matrix, and the relationship between resistance and water potential obtained from calibration prior to installation is used to determine water potential. The commonly used term ‘gypsum block' arises from early models, which were made of gypsum to buffer ionic effects from the surrounding medium (Buoyoucos and Mick, 1940), and from the practice of using gypsum as a buffer for many sensors using some other material for the porous matrix. As with tensiometers and heat dissipation sensors, the sensor is embedded in the surrounding medium and allowed to equilibrate.

Under equilibrium conditions, the sensor matric potential is equal to the surrounding water matric potential, but the sensor water content may be different than water content of the surrounding medium. Electrical resistivity measurements are often used to estimate soil water content, either by using a known relationship between soil matric potential and soil water content (Gardner, 1986) or by inferring soil water content directly with proper calibration for a particular soil (Kutilek and Nielsen, 1994).

Summary Box 4. Heat Dissipation Sensors
Measurement Range • Typical matric potential range from −0.01 to −1 MPa [−0.1 to −10 bar] {Flint, et al. (2002) claim an upper range of −100 MPa [−1000 bar], which seems highly unlikely for many soils} **Accuracy** • Measurement sensitivity is proportional to matric potential value. The data of Flint, et al. (2002) suggest 20 percent absolute in the range of −0.01 and −35 MPa [−0.1 and −350 bar], while the data considered by Reece (1996) place the value at approximately ± 7 percent **Limitations** • Limited accuracy • Slow response time • Hydraulic decoupling with surrounding porous media under dry conditions • Indirect measurement of matric potential • Requires calibration **Advantages** • Simple installation • Low maintenance • Remote monitoring • Automation • Low cost **Applicability for the Performance Confirmation Program** • A potential backup sensor for tensiometers under dry conditions

The primary advantages of electrical resistance sensors are their low cost and simple measurement requirements. Measurements may be obtained using a simple resistance meter, or more conveniently acquired automatically using a data logger. However, each electrical resistance sensor must be calibrated before use, which can be a significant effort, because the sensors can be affected by the ionic composition of the surrounding solution. Moreover, the method is inaccurate under wet conditions, thus this measurement method is appropriate mostly as a qualitative indicator of water status (Spaans and Baker, 1992).

3.2.6 Psychrometers

Psychrometric measurements are based on equilibrium between liquid water and water vapor in the ambient pore space. Water potential in the gaseous phase is related to relative humidity, through the Kelvin equation (Or and Wraith, 2002)

$$\mathrm{RH} = \frac{e}{e_0} = \exp\left(\frac{M_w g h}{RT}\right) \tag{3-11}$$

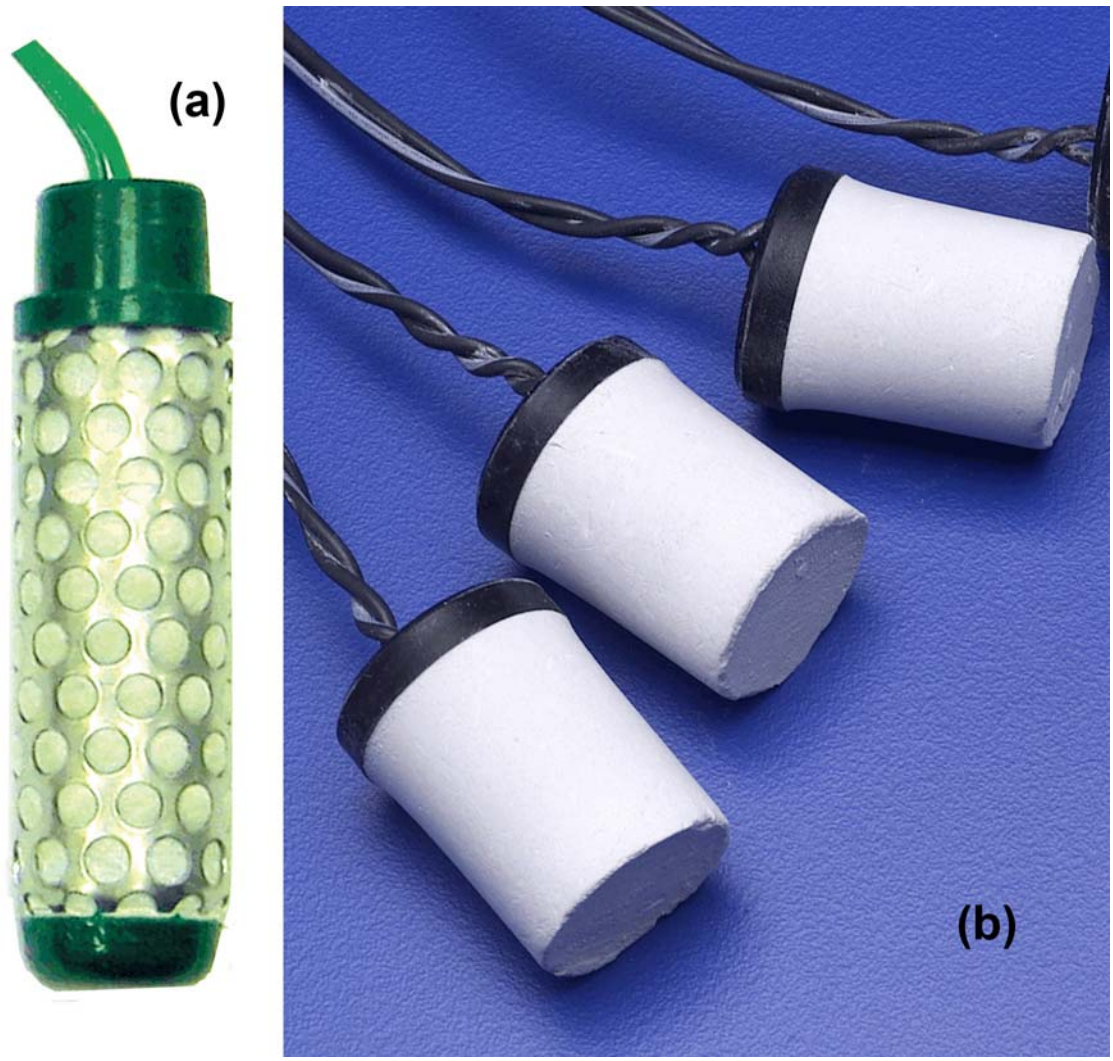

Figure 3-18. Commercially Available Electrical Resistance Sensors: (a) 253-L Watermark Soil Matric Potential Block (Irrometer Company, Inc.), and (b) Gypsum Blocks (Delmhorst Instrument Co.). [Image (a) Watermark Sensors, Irrometer Company, Riverside, California, Reproduced With Permission; Image (b) Courtesy of Delmhorst Insturment Co.]

where

RH	—	relative humidity
e	—	water vapor pressure
e_0	—	saturated vapor pressure at the same temperature
M_w	—	molecular weight of water (0.018 kg mol^{-1})
g	—	gravitational acceleration (9.81 m s^{-2} at sea level)
h	—	water potential (m)
R	—	ideal gas constant (8.31 J K^{-1} mol^{-1})
T	—	absolute temperature (K)

Note that h includes both the matric potential and the osmotic potential because air is an effective diffusion barrier for most solutes. Rearranging Eq. (3-11) and taking a log-transformation leads to

$$h = \frac{RT}{M_w g} \ln\left(\frac{e}{e_0}\right) \tag{3-12}$$

When e/e_0 is close to 1, which is usually the case in the vadose zone in humid climates or at large depths in arid areas, the logarithm in Eq. (3-12) can be linearized with little loss of accuracy, resulting in

$$h = \frac{RT}{M_w g}\left(\frac{e}{e_0} - 1\right) = 471T\left(\frac{e}{e_0} - 1\right) \tag{3-13}$$

for h in meters. Accuracy deteriorates approximately linearly with h; the linearized relationship has an error of approximately 7.5 percent for $h = -150$ m, which is roughly the wilting point for many plant species.

Psychrometers typically measure the difference between a dry bulb, and wet bulb temperature. The dry bulb is at the temperature of the surrounding medium. An evaporating surface fixes the temperature of the wet bulb, with the difference in temperature between dry and wet bulbs dependent on evaporation rate, which is in turn dependent on the relative humidity of the gas phase. The difference in temperatures between the wet and dry bulb is related to the relative humidity by the psychrometric equation

$$\frac{e}{e_0} = 1 - \left(\frac{s + \gamma}{e_0}\right)\Delta T \tag{3-14}$$

where

s	—	slope of the saturation water vapor pressure curve ($s = de_0/dT$)
γ	—	psychrometric constant {~0.067 kPa K^{-1} at 20 °C [68 °F]}
ΔT	—	temperature difference (°C) between the dry and wet bulb

A thermocouple is a double junction of two dissimilar metals. A thermocouple psychrometer uses a fine-wire chromel-constantan or other bimetallic thermocouple. When the two junctions are subject to different temperatures, they generate a voltage difference (the Seebeck effect) (Seebeck, 1921). Conversely, when an electrical current is applied, the junction is heated or cooled, depending on the direction of the current (the Peltier effect). In typical use, one junction of the thermocouple is suspended in a thin-walled porous ceramic or stainless steel screen cup buried in the medium of interest, while another is embedded in an insulated plug to measure the ambient temperature at the same location (Figure 3-19). An electrical current cools the suspended thermocouple below the dew point until water condenses on the junction, whereupon the cooling current is stopped. The wet bulb temperature is achieved during subsequent evaporation from the junction.

An accurate measurement of the temperature difference plays a critical role in psychrometric water potential determinations. For example, temperature-difference measurements must be

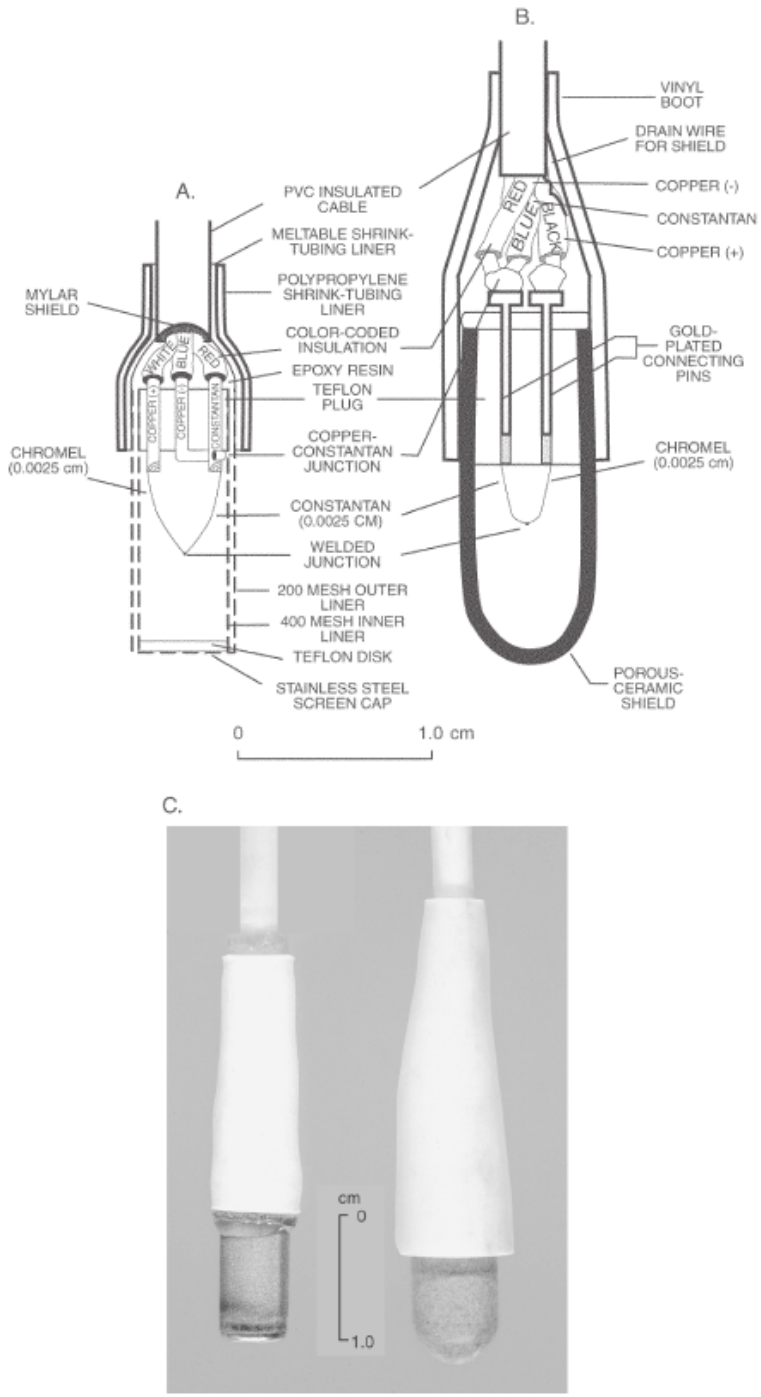

Figure 3-19. Psychrometers: Schematics of (a) Screen-Caged Psychrometer Sensor (b) Ceramic-Cupped Psychrometer Sensor, and (c) Photograph of Commercially Available Sensors. [Reproduced From Andraski and Scanlon (2002) With Permission]

accurate to 0.005 °C [0.009 °F] for water potential measurements to be accurate to ~10^4 m. Psychrometers are, therefore, highly susceptible to thermal gradient effects and do not perform well when significantly affected by diurnal temperature variations. Psychrometers have a relatively slow response time, because the method requires that the vapor and liquid phase must come to equilibrium. Psychrometers may be buried and left for long periods, although corrosion is a problem in some environments.

Recently introduced water activity measurement devices (Decagon Devices, Inc., Pullman, Washington) rely on a *chilled mirror* sensor to measure water potential to as low as −300 MPa [−3,000 bar] following equilibration of liquid and vapor phases of water in a sample within a closed chamber. A thermoelectric (Peltier) cooler controls the mirror temperature. An infrared light beam is directed onto the mirror and reflected to a photodetector, which detects the change in reflectance when condensation occurs on the mirror (wet bulb temperature). A thermocouple attached to the mirror accurately measures the dew-point temperature.

Characteristics of psychrometers are summarized in Summary Box 5.

Summary Box 5. Psychrometers

Measurement Range

- Andraski and Scanlon (2002) state that the upper measurement limit of a psychrometer is approximately −0.03 to −0.2 MPa [−0.3 to −2 bar]. The lower limit of routine measurements made with Peltier sensors is approximately −8 MPa [−80 bar]. At lower water potentials, the dew-point temperature is more than 0.6 °C [33 °F] below ambient temperature and Peltier cooling is too inefficient to condense sufficient water on the sensing junction for stable readings. The lower limit of water potential measurements with wet-loop sensors (where a large drop of water is placed on the sensing junction) is approximately −300 MPa [−3,000 bar] because water application produces readings that are more stable than achieved by Peltier cooling sensors. A typical range for field sensors is −0.1 to −10 MPa (e.g., Wescor PST–55).

Accuracy

- ± 2 percent {at best, −0.01 MPa [−0.1 bar]}
- Dependent on relative humidity or matric potential

Limitations

- Limited measurement range
- Coarse resolution at the wet end

Advantages

- Good *in situ* measurement capability in the dry (low relative humidity) range

Applicability for Performance Confirmation Program

- Extends the range of *in situ* matric potential measurement in the dry range
- Supports water content measurement in drying regions

3.3 Pore Water Extraction

The importance of collecting pore water solution for measuring the concentrations of dissolved constituents, and conducting environmental studies in general, was recognized by Joffe (1932), who described the soil water solution as the “blood circulating in the soil body.” Soil scientists,

hydrologists, geochemists, ecologists, engineers, and health safety specialists have major interest in the chemical composition of the soil solution, as it provides crucial information regarding the distribution of plant nutrients and hazardous chemicals in the vadose zone. Water quality monitoring below waste disposal sites, for example, is important for detection of contaminant plumes migrating from leaking liners, and allows early initiation of remedial measures. A wide variety of extraction techniques and devices are available.

Six common techniques for extracting pore water are discussed in this section, including suction cups, combined tensiometers and suction cups, suction lysimeters, passive capillary samplers, capillary absorbers, and extraction from samples.

3.3.1 Suction Cups

Briggs and McCall (1904) were among the first to introduce a method for extracting soil water through porous ceramic cups. Numerous modifications to the initial design of the suction cup have been made since its invention almost a century ago. Cole (1968) introduced automated soil solution samplers. Chow (1977) developed a vacuum sampler that automatically shuts down after collecting a specific volume of soil solution. Additional improvements were introduced by Parizek and Lane (1970) and Wood (1973). Stone and Robl (1996) designed a heavy duty device to withstand soil compaction due to farm equipment.

The most commonly applied devices for collection of solution from unsaturated soils are vacuum soil water samplers (Rhoades and Oster, 1986), such as suction cups or suction lysimeters. These instruments operate under the same principle. A porous material (cup or plate) is brought into hydraulic contact with the surrounding soil, the sampler is evacuated to a pressure slightly below the matric potential in the surrounding medium to induce a pressure gradient, and pore water flows into the sampler and collection containers. It is important to adjust the applied vacuum (usually based on tensiometer measurements) to prevent high gradients and the development of preferential flow paths towards the cup. Accordingly, soil water samplers are commonly installed in combination with tensiometers, or the sampler and tensiometer are combined in one instrument, as discussed in Section 3.3.2. The potential field developing around a suction cup was measured with tensiometers by Krone, et al. (1951).

The time required for solution collection depends on the volume necessary for chemical analysis, the hydraulic conductivity and water content (matric potential) of the medium, and the applied gradient (Rhoades and Oster, 1986). A sandy soil close to field capacity (i.e., shortly after gravity drainage ceases following saturation) will provide sufficient sample volume for most analyses within a few hours, while less permeable or drier media may require considerably more time to extract the same volume. Note that automated sampling stations (Cepuder and Tuller, 1996) enable continuous sampling.

A typical soil water collection system contains three main functional units: the suction cups or plates, sampling bottles, and a vacuum container connected to a vacuum pump, as illustrated in Figure 3-20. The applicable range of soil water samplers is limited to suction values (vacuum) of less than 10 m [32.8 ft] head of water due to onset of cavitation in the metastable solution at subatmospheric pressure and the propensity of air to enter porous materials. Installation of suction cups closely follows procedures discussed for tensiometers, because the two devices have similar operational characteristics.

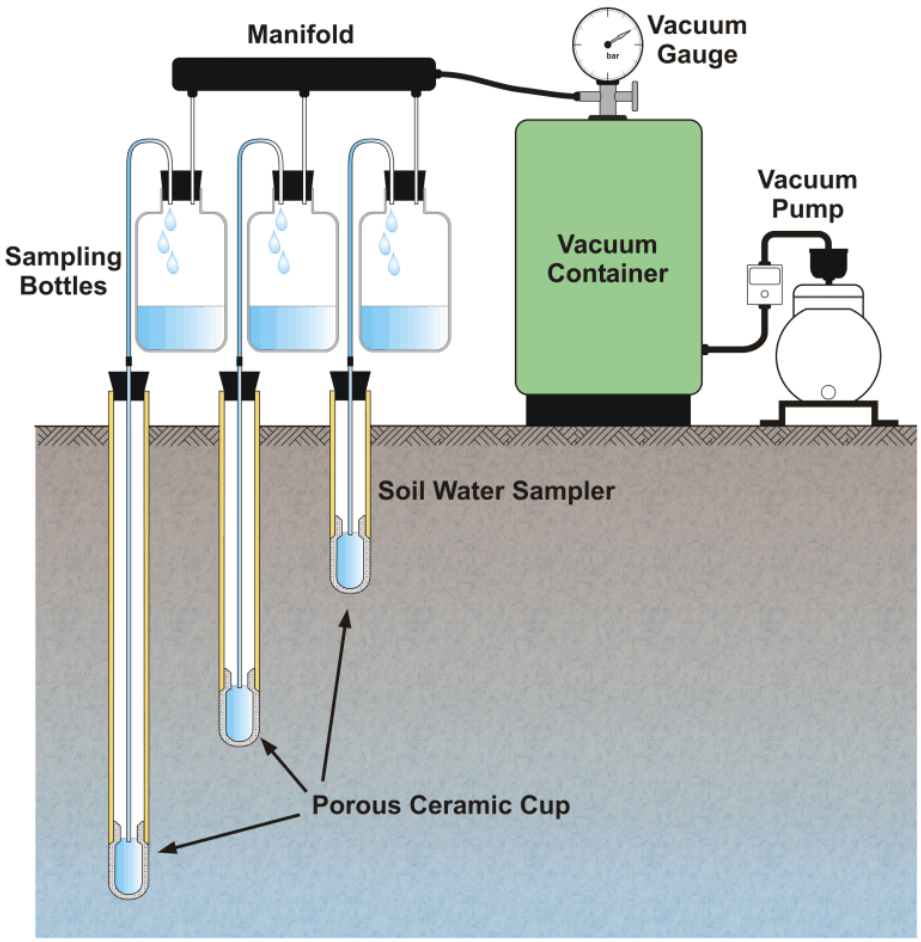

Figure 3-20. Typical Setup of Soil Water Samplers (Suction Cups) [Illustration Copyright 2005 From "Field Methods for Monitoring Solute Transport" by Tuller and Islam, 2005. Reproduced by Permission of Routledge/Taylor & Francis Group, LLC.]

Suction samplers primarily differ in the shape and size of the devices, and in the chemical and physical properties of the porous materials used to establish hydraulic contact with the surrounding soil. A large number of porous materials such as ceramic (perhaps the most widely used), polytetrafluoroethylene, polyethylene, stainless steel, nylon, polyvinyl chloride, polypropylene, polyvinylidene fluoride, Teflon®, and glass may be used for suction cups or plates. The porous material is often selected based on cost, durability, and minimization of chemical interactions with components in pore water. There is conflicting evidence concerning the applicability of ceramic samplers for collecting pore water for chemical analyses, probably due to differences in chemical composition and physical properties of the ceramic materials used in the devices and differences in chemical composition of soil solution.

3.3.2 Combined Solution Sampling—Tensiometer Probes

Characterization of solute transport in the vadose zone requires measurement of spatial and temporal changes in both solute concentration and water content (or matric potential). These

observations are commonly made using suction samplers and tensiometers. It is convenient to combine these devices into one probe to take advantage of the similarities in the basic design of the two devices.

Moutonnet, et al. (1989) introduced a modified tensiometer they call the Tensionic probe (shown in Figure 3-21a) that allows concurrent measurement of matric potential and extraction of pore water. The Tensionic probe uses a porous ceramic cup to contact the surrounding medium, just like a standard tensiometer. The ceramic cup is placed at the tip of a polyvinyl chloride shaft. The shaft protects three tubes entering the cup, with one tube connected to a sealed compartment in the upper portion of the shaft that contains the tensiometer sensor, and two tubes forming a conduit to the surface for priming and sample extraction. The tensiometer is primed with de-aired and deionized water at the start of each sampling cycle. Once the Tensionic probe equilibrates matric potential with the surrounding medium, the Tensionic probe operates in tensiometer mode like any tensiometer. Ions present in the pore water continually

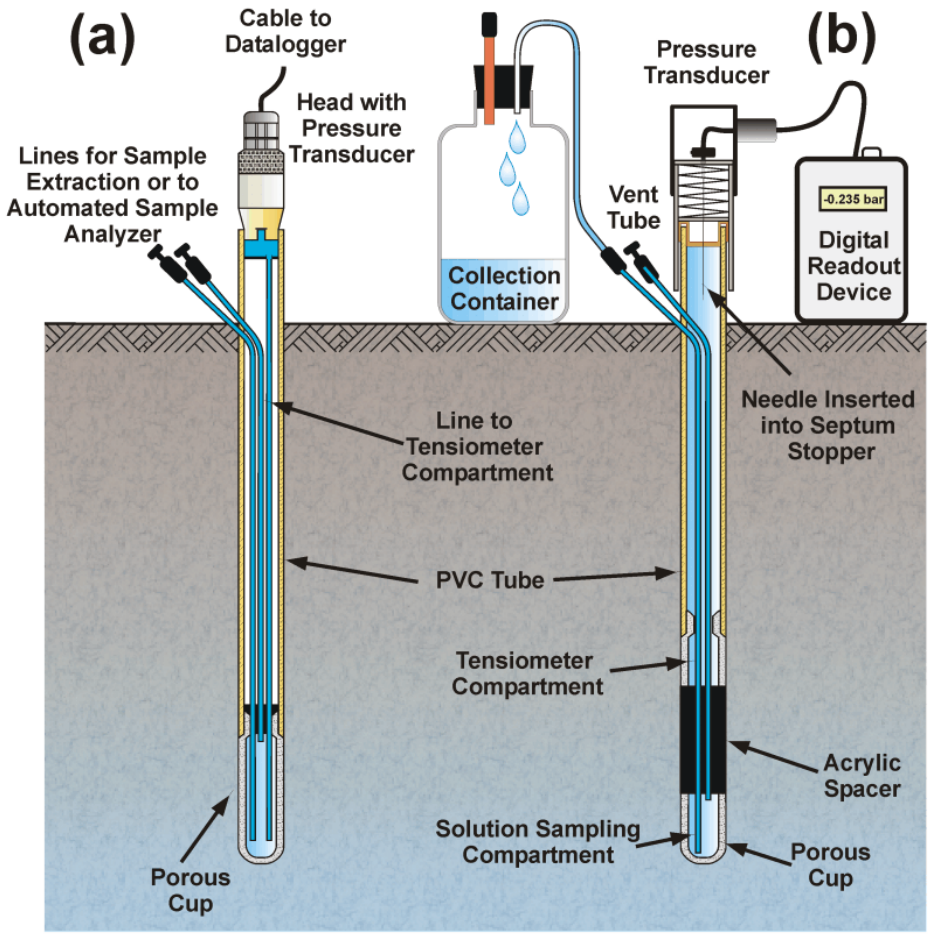

Figure 3-21. Combined Solution Sampling: (a) The Tensionic Probe (Moutonnet, et al., 1993), and (b) A Probe with Separated Sampling and Tensiometer Compartments (Essert and Hopmans, 1998). [Illustration Copyright 2005 From "Field Methods for Monitoring Solute Transport" by Tuller and Islam, 2005. Reproduced by Permission of Routledge/Taylor & Francis Group, LLC.]

diffuse through the porous cup while the Tensionic probe is in place, and ultimately the water inside the tensiometer attains chemical equilibrium with the surrounding pore water. Moutonnet, et al. (1993) report that 8 to 10 days were required for equilibrium to occur for NO_3. Once chemical equilibrium is reached, the sample is extracted and the tensiometer is flushed and refilled with de-aired and deionized water to start another sampling cycle. Moutonnet, et al. (1993) and Moutonnet and Fardeau (1997) used automated Tensionic probes to determine concentrations of NO_3-N, NO_2-N, and NH_4-N under maize. Similar devices were applied by Morrison, et al. (1983) and Rehm, et al. (1986) to characterize contaminant migration under waste disposal sites. Major drawbacks of the Tensionic probe are the lack of control over the sample volume, which is largely dependent on water content (Saragoni, et al., 1990), and uncertainty regarding the time required for chemical equilibration.

Essert and Hopmans (1998) took a different design approach when combining a tensiometer and pore water sampler. They separated the porous cup with an acrylic barrier into two compartments, as shown in Figure 3-21b. The bottom compartment is used for sample extraction, while the top compartment operates as a tensiometer. Interactions between the two compartments would interfere with the operational modes, and may occur due to (i) reduction of the matric potential in the surrounding medium as water is removed during solute extraction, and (ii) change of solute concentration due to exchange with the tensiometer compartment. Essert and Hopmans (1998) recommend separating the compartments with a 10 cm [3.9 in] spacer to overcome these biases. This distance is somewhat arbitrary, although it is supported by theoretical considerations (Warrick and Amoozegar-Fard, 1977).

3.3.3 Lysimeters

Lysimeter studies date back to the late 18th century when scientists investigated the fate of precipitation in soils (Joffe, 1932). The term “lysimeter” originated from the Greek words “lusis” (loosening) and “meter” (measuring), and is somewhat misused today. Lysimeters were originally developed to study complex soil-plant-atmospheric relationships, with solute transport being only one component. In its original application, a lysimeter is a large soil or rock block surrounded by a casing, with its lower boundary separated from the parent material (Bergström, 1990), and often mounted on a large balance for monitoring inputs and losses (e.g., evapotranspiration) as functions of atmospheric and hydrologic conditions. Many lysimeter designs and sizes with varying boundary conditions and application areas are reported in the literature. In this section lysimeters designed for collection of pore water are described.

One basic type of lysimeter contains an undisturbed soil or rock monolith, and the other basic type is filled with a disturbed porous matrix. A lysimeter may extend from the surface to depths of as much as 2 to 3 m [6.6 to 9.8 ft]; it may be buried (Cepuder and Tuller, 1996) or installed from a trench sidewall. Lysimeters may be isolated from the surrounding medium via impermeable sidewalls or may maintain hydraulic contact with the parent material. Casings may be round, square, or rectangular, and made of concrete, steel, fiberglass or polyvinyl chloride (ASTM International, 1998; Best and Weber, 1974; Furth, 1985; Weber, 1995).

Pore water within the lysimeter is commonly obtained at the bottom of the lysimeter, either through gravity drainage or through suction through a porous material (like suction samplers). Note that suction samplers are sometimes referred to as lysimeters because of this similarity. Suction lysimeters are often more useful than gravity drainage lysimeters for vadose-zone

studies, particularly in arid environments, because gravity drainage only occurs when the bottom of the lysimeter is saturated, while suction can be applied in a more controlled fashion.

Suction lysimeters (such as the device illustrated in Figure 3-22) and gravity drainage lysimeters have been applied in numerous studies related to monitoring transport of agrochemicals and water movement (Bergström, 1990; Jemison and Fox, 1994; Tyler and Thomas, 1977; Winton and Weber, 1996; Joffe, 1932; Kilmer, et al., 1944; Kohnke, et al., 1940; McMahon and Thomas, 1974; Karnok and Kucharski, 1982; Dolan, et al., 1993; Cepuder and Tuller, 1996; Moyer, et al., 1996). Lysimeters have also been applied to investigate colloid-facilitated transport of organic compounds and heavy metals (Thompson and Scharf, 1994) and the fate and cycling of ^{15}N (Reeder, 1986).

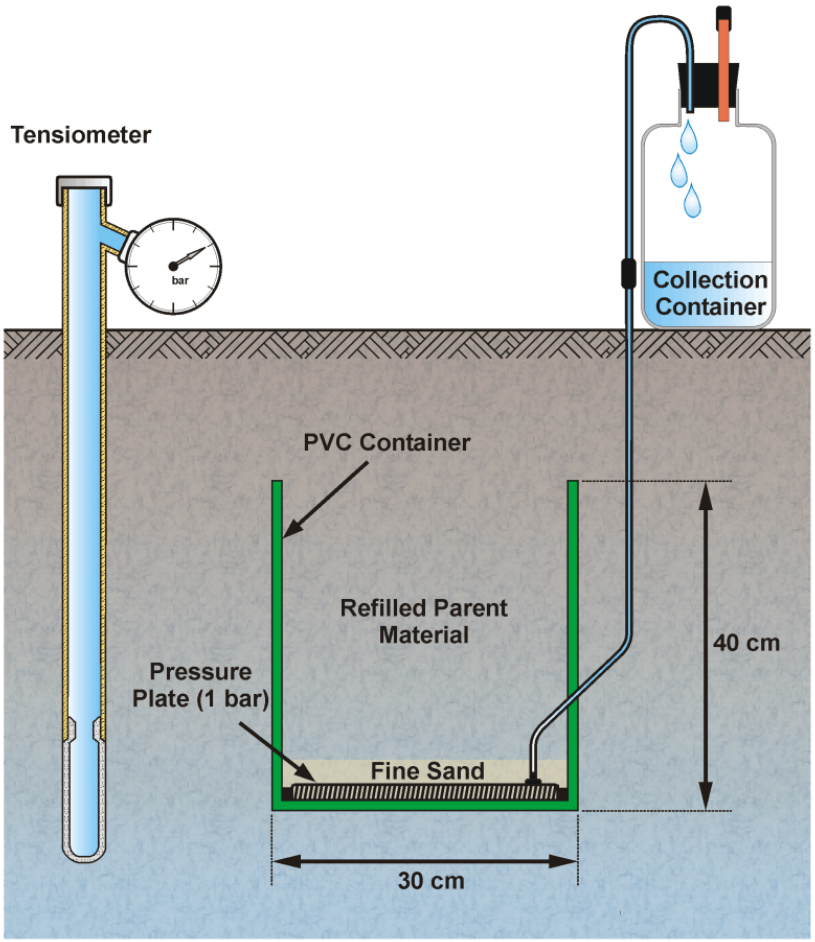

Figure 3-22. Design of a Refilled Suction Lysimeter (Installed With a Tensiometer for Monitoring Soil Matric Potential) (Tuller and Islam, 2005). A Similar Design Was Used by Cepuder and Tuller (1996) for Nitrate Leaching Studies. [Illustration Copyright 2005 From "Field Methods for Monitoring Solute Transport" by Tuller and Islam, 2005. Reproduced by Permission of Routledge/Taylor & Francis Group, LLC.]

3.3.4 Passive Capillary Samplers

Passive capillary samplers, first introduced by Brown, et al. (1986), use tension developed in a hanging wick to passively extract pore solution from the porous medium above a sampling pan, as shown in Figure 3-23. Passive capillary samplers directly measure water flux density (Selker, 2002), a distinct advantage over suction cups or lysimeters. Recent advances in passive capillary sampler design include wick selection and design equations (Boll, et al., 1992; Knutson and Selker, 1994; Rimmer, et al., 1995) and wick pretreatment methods (Knutson, et al., 1993).

Passive capillary samplers are designed for long-term operation using environmentally stable, nonadsorbing materials such as stainless steel, fiberglass, and high density polyethylene (Topp and Smith, 1992). The sampler consists of a fiberglass or high-density polyethylene container supporting a stainless steel or high-density polyethylene top panel. The panel is divided into multiple compartments, with holes for a wick in each section (Louie, et al., 2000). The wick is cut to the desired length, and one end is separated into individual strands and

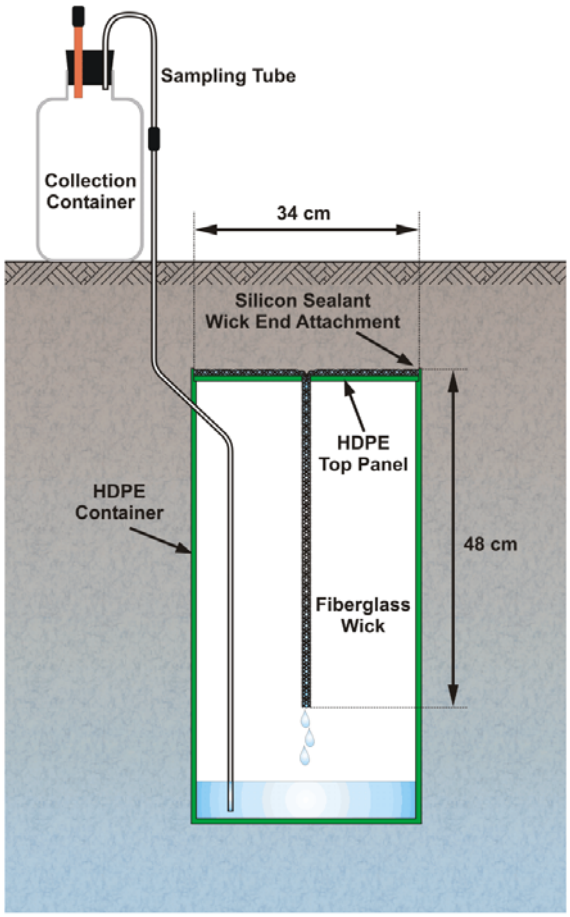

Figure 3-23. Design of a Passive Capillary Sampler [Illustration Copyright 2005 From "Field Methods for Monitoring Solute Transport" by Tuller and Islam, 2005. Reproduced by Permission of Routledge/Taylor & Francis Group, LLC.]

cleaned by kiln combustion according to Knutson, et al. (1993). The wick is guided through the center hole, the filaments of the open end are flared radially on the top of the panel, and the filaments are glued into place with silicone.

Most wicks used for passive capillary samplers are products for furnace isolation and are available in a variety of dimensions, weaves, and densities applicable to a wide range of soil and rock textures (Selker, 2002). Some wick materials follow exponential relationships between hydraulic conductivity and pressure, as tabulated by Knutson and Selker (1994). From these tabulated values and the unsaturated hydraulic conductivity of the host porous medium, certain design criteria for passive capillary samplers (e.g., length, type, and number of wicks for sampling a given area) can be calculated. Binding agents (e.g., starch) applied during the manufacturing process may reduce wick wettability, limiting the range of tension that the wick can use to draw water from the overlying soil. Kiln combustion at 450 °C [842 °F] was found to be the most effective procedure for removal of various coatings (Knutson, et al., 1993). However, kiln combustion may induce contamination of the wick surface with ash, which is undesirable especially if the collected solution is intended to be analyzed for trace elements. As with other samplers, thorough laboratory testing and wick cleaning with acid and deionized water is imperative before field installation.

Passive capillary samplers are commonly installed from soil trenches. A tunnel only slightly larger than the sampling device is excavated perpendicular to the trench at the desired sampling depth. The top panel is filled with slightly compacted native soil, then the sampler is carefully pushed into the tunnel and elevated with wedges to achieve tight hydraulic contact between the tunnel ceiling and the soil layer in the top panel (Louie, et al., 2000). A bentonite layer is applied to hydraulically isolate the sampler from the trench. The tubing for sample extraction is brought aboveground and the trench is refilled and compacted. The pore water collected at the bottom of the sampler is extracted with a manual or battery-operated vacuum pump, either at predetermined time intervals or triggered by monitored matric potential or water content.

Passive capillary samplers have been successfully tested in laboratory experiments (Knutson and Selker, 1996; Rimmer, et al., 1995), and applied in a number of field trials (Brandi-Dohrn, et al., 1996; Louie, et al., 2000; Holder, et al., 1991; Boll, et al., 1991).

3.3.5 Capillary Absorbers

When two porous materials with differing water potential are brought into hydraulic contact, water flows from the medium with higher potential energy to the medium with lower potential energy. This physical phenomenon is used in capillary absorbers, where a porous membrane (absorber) is brought in close hydraulic contact with the wall of a borehole. Pore water is wicked into the absorber because of the difference in water potential, the membrane is allowed to equilibrate with the surrounding medium, the membrane is retrieved, and the solution extracted for chemical analyses (Keller and Hendrickx, 2002).

The effective permeability of the host/membrane system controls the flow rate of the liquid into the absorbing material. Time to equilibration may vary widely between different media, and strongly depends on the moisture content of the host medium (Keller and Travis, 1993), so it may be quite uncertain whether equilibrium has been reached for a given sample. Keller and Hendrickx (2002) developed an approach using changes in the electrical resistance of the absorber during wicking to infer equilibrium.

Tight contact between soil and absorber must be established to prevent evaporation losses during equilibration, which could cause an increase in solute concentration. Furthermore, it is important to prevent evaporation losses and cross-contamination during absorber retrieval.

Potential problems with absorber placement, borehole isolation, and absorber retrieval are eliminated with an advanced installation method that employs an impermeable balloon-shaped liner to which the absorber material is glued (Keller and Hendrickx, 2002; Koglin, et al, 1995). Absorbers may be circular or annular patches, or may cover the entire liner surface. The inverted liner (i.e., turned outside in) and attached tether is wound onto a reel as shown in Figure 3-24a. The liner unrolls from the reel as it is lowered into the borehole, with the absorber facing the borehole wall as shown in Figure 3-24b. The inside of the liner is filled with pressurized gas or water to establish tight contact between absorber and wall, isolating individual absorbers if patches are used. The liner is inverted again and rolled back onto the reel when retrieving the absorber, avoiding cross-contamination and minimizing exposure of personnel to hazardous chemicals.

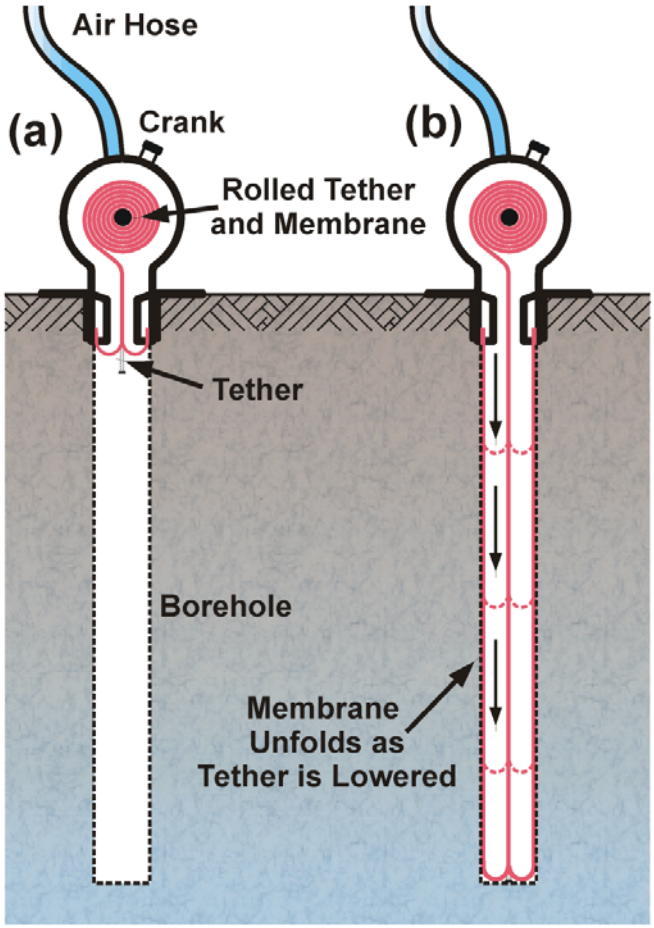

Figure 3-24. Deployment Sequence for Capillary Absorbers: (a) Canister Placed on Surface Casing, and (b) Membrane Lowered Into the Borehole and Pushed Against the Borehole Wall Using Pressurized Air (Koglin, et al., 1995) [Illustration Copyright 2005 From "Field Methods for Monitoring Solute Transport" by Tuller and Islam, 2005. Reproduced by Permission of Routledge/Taylor & Francis Group, LLC.]

3.3.6 Solution Extraction from Soil and Rock Samples

In situ sampling techniques may be supplemented by extraction of pore water from soil and rock samples collected in the field by means of coring or simple excavation. Such destructive testing may be desirable when sampling is too slow or inconvenient. Detailed discussion of extraction from soil and rock samples is beyond the scope of this report, but the possibility is mentioned for completeness.

There is a variety of single and sequential extraction techniques, including column displacement and centrifugation, or a combination of both (Adams, et al., 1980; Fuentes, et al., 2004; Martens, 2002; Pueyo, et al., 2003; Villar-Mir, et al., 2002). The selection of method is mainly based on the chemical species under investigation and the sample volume required for a particular analysis technique. Adams, et al. (1980) compare the ionic composition of solutions extracted from loam and clayey soils by means of column displacement with a $CaSO_4$-KCNS solution, centrifugation of moist soil with carbon tetrachloride (CCl_4) added, and simple centrifugation of moist soil. They conclude that the composition of the extracted solution was not affected by the method employed. Alberts, et al. (1977) and Villar-Mir, et al. (2002) describe extraction techniques suitable for NO_3-N determination. Fuentes, et al. (2004) and Pueyo, et al. (2003) present single and sequential extraction techniques to determine heavy metals in sewage sludge and contaminated soils.

3.4 Indirect Water Content Measurement

Dielectric and electric measurement methods discussed in Sections 3.1 and 3.2.5 typically use sensors embedded in an engineered porous medium having a calibrated relationship between the measured and desired quantities. The engineered medium is placed within the natural porous medium of interest and allowed to equilibrate before measurements are made. The same physical principles can be applied using indirect methods, where the sensors interrogate the porous medium of interest without the relationship between water content and a sensed quantity afforded by a calibrated engineered medium.

Electrical resistivity, electromagnetic inductance, and fiber optic methods are reviewed in this section. Electrical resistivity and electromagnetic inductance methods may be applied to indirectly estimate bulk electrical conductivity at a much larger scale than the methods discussed in Sections 3.1 and 3.2.5. Electrical conductivity is related to water content, the hydrologic quantity of interest, as discussed in Section 3.1. Fiber optic sensors are an emerging area that offers the potential for estimating several hydrologic properties, including water content, using optical sensors.

3.4.1 Electrical Resistivity Methods

The basic principle of electrical resistivity measurements may be explained using the relationship between electrical resistance and electrical resistivity of a wire

$$R = \rho \frac{L}{A} \tag{3-15}$$

where

R — electrical resistance of the wire (Ω)

ρ	—	electrical resistivity (Ω·m)
L	—	wire length (m)
A	—	cross-sectional area of the wire (m^2)

Ohm's law relates the electromotive force V (volts) to current flow I (amperes) using the expression $V = IR$. Substituting this expression into Eq. (3-15) and rearranging yields an explicit expression for resistivity

$$\rho = \frac{A}{L} \cdot \frac{V}{I} \tag{3-16}$$

Equation (3-16) illustrates that the resistivity is a function of the ratio of voltage drop to current and the conductor dimensions. This principle can be applied to measure resistivity of a porous medium acting as a conductor between two or more electrodes. The resistivity of natural porous media is highly dependent on water content, solute concentration (or on total dissolved solids), texture, and structure. In general, increasing water content in a pore space leads to a decrease in resistivity as low-resistivity water displaces high-resistivity air. Coarse-textured soils usually have higher resistivity than fine-textured soils at the same water content due to less grain-to-grain contact area per unit volume.

The first soil electrical resistivity measurements date back to geophysical prospecting in the 1920s, when a linear array with two current electrodes (outer pair) and two potential electrodes (inner pair) was installed in the soil or rock formation. The electrical potential (voltage) is measured across the inner pair while a constant current is maintained through the outer electrode pair, as shown in Figure 3-25. The most common electrode array configurations are (i) the Wenner array, with equally spaced electrodes; (ii) the Schlumberger array, with the spacing between the potential electrodes smaller than the spacing between current electrodes; and (iii) the dipole-dipole array, where the potential and current electrode pairs do not overlap (Furman, et al., 2003). The spacing between the potential and current electrodes in the dipole-dipole array is the same (a), but the spacing between pairs is na, where n is an integer. The resistivity is a function of electrode spacing (a,b) (Figure 3-25) given as

$$\text{Wenner array: } \rho = 2\pi a R \tag{3-17}$$

$$\text{Schlumberger array: } \rho = \pi \frac{(a^2 + ab)}{b} R \tag{3-18}$$

$$\text{Dipole - dipole array: } \rho = \pi a n (n+1)(n+2) R \tag{3-19}$$

The bulk soil/rock electrical conductivity (EC_a) is the inverse of the resistivity as illustrated for the Wenner array

$$EC_a = \frac{1}{2\pi a R} \tag{3-20}$$

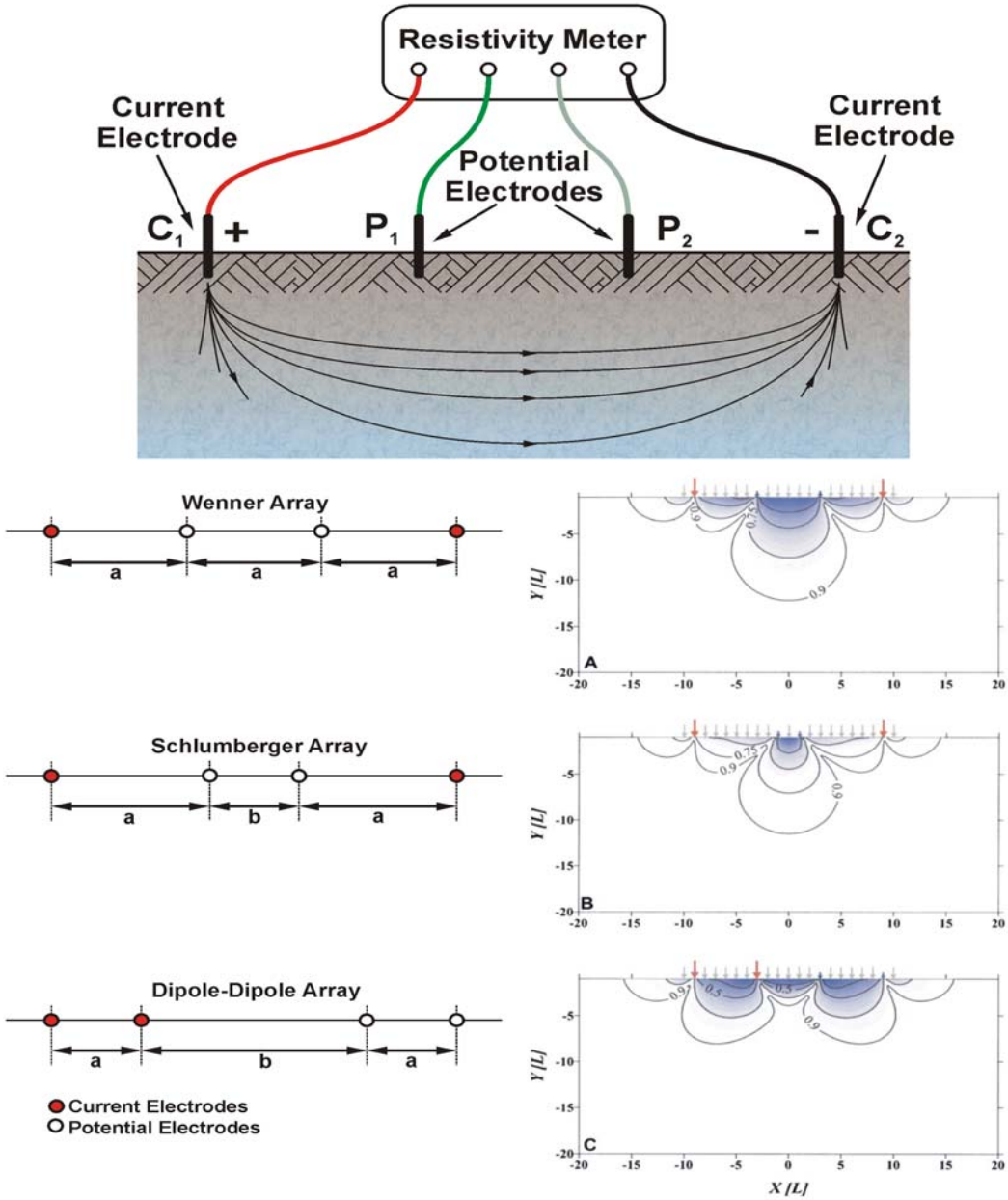

Figure 3-25. Surface Electrical Resistivity: (a) The Current Electrode Pair Is Spaced Outside the Potential Electrode Pair, (b) Three Common Electrode Configurations (Measurement Arrays) for Surface Electrical Resistivity, and (c) Corresponding Measurement Spatial Sensitivity (Contours Represent Cumulative Relative Sensitivity) [Illustration Copyright 2005 From "Field Methods for Monitoring Solute Transport" by Tuller and Islam, 2005. Reproduced by Permission of Routledge/Taylor & Francis Group, LLC. Sensitivity Maps Reproduced From Furman, et al., 2003.]

A calibration relationship between water content and R is used to obtain water content from EC_a given known geometric parameters, as with all other methods that measure bulk electrical conductivity (e.g., time domain reflectometry, electromagnetic induction).

The depth of current penetration for the Wenner array electrode configuration is approximately equal to the inner electrode spacing (Rhoades and Ingvalson, 1971; Rhoades and van Schilfgaarde, 1976; Rhoades, 1978). Nadler (1980) theoretically and experimentally determined the soil volume influenced by the applied electrical field and found that the depth sensed with a Wenner array is greater than the inner electrode spacing for most field situations, especially under highly variable conductivity conditions with depth caused by varying water content and solute concentrations. Recent analyses by Furman, et al. (2003) have established spatial weighting functions for the various arrays in homogeneous and heterogeneous formations.

The electrodes are placed in a linear array based on the applied configuration scheme (see Figure 3-26 for an example), with the separation distance based on the desired depth and volume of influence (Rhoades, 1978; Nadler, 1980). Metal electrodes are typically pushed into the ground when conducting surveys in soil, while aluminum screen covered with wet or moist vermiculite can be used for rock. It may be advantageous to mount the electrodes, current source, resistance meter, and datalogger on a nonconducting frame for monitoring surveys with fixed electrode spacing, to allow rapid repositioning when a large number of measurements are required. Frame-mounted electrical resistivity systems equipped with global positioning system and dataloggers are commercially available from a number of companies (e.g., GEOSCAN Research, VERIS Technologies, GEONICS Limited) but can be easily assembled from scratch (Rhoades and Halvorson, 1977). The basic components consist of a battery-powered constant-current-source resistance meter with a range from 0.1 to 1000 Ω, four metal electrodes, and connecting wire.

By successively increasing electrode separation distance around a point of interest, EC_a can be determined for discrete depth intervals (Halvorson and Rhoades, 1974). Assuming that the penetration depth is equal to the separation distance, the volume measured may be considered as a uniform lateral layer to which deeper layers are added successively as the separation distance increases. These layers may be treated as parallel resistors with EC_x, the bulk electrical conductivity for the xth layer, calculated by (Barnes, 1952)

$$EC_x = EC_{(a_i - a_{i-1})} = \frac{EC_{a_i} \cdot a_i - EC_{a_{i-1}} \cdot a_{i-1}}{a_i - a_{i-1}} \tag{3-21}$$

where

a_i — sampling depth i
a_{i-1} — prior sampling depth

Two- and three-dimensional EC_a distributions can be readily obtained using the multielectrode resistivity method with an array of a large number of evenly spaced electrodes. Multiplexers are used to activate four electrodes at a time in any feasible array configuration (Figure 3-27). A three-dimensional distribution of bulk electrical conductivity is obtained by varying electrode separation distances in the two-dimensional electrode array.

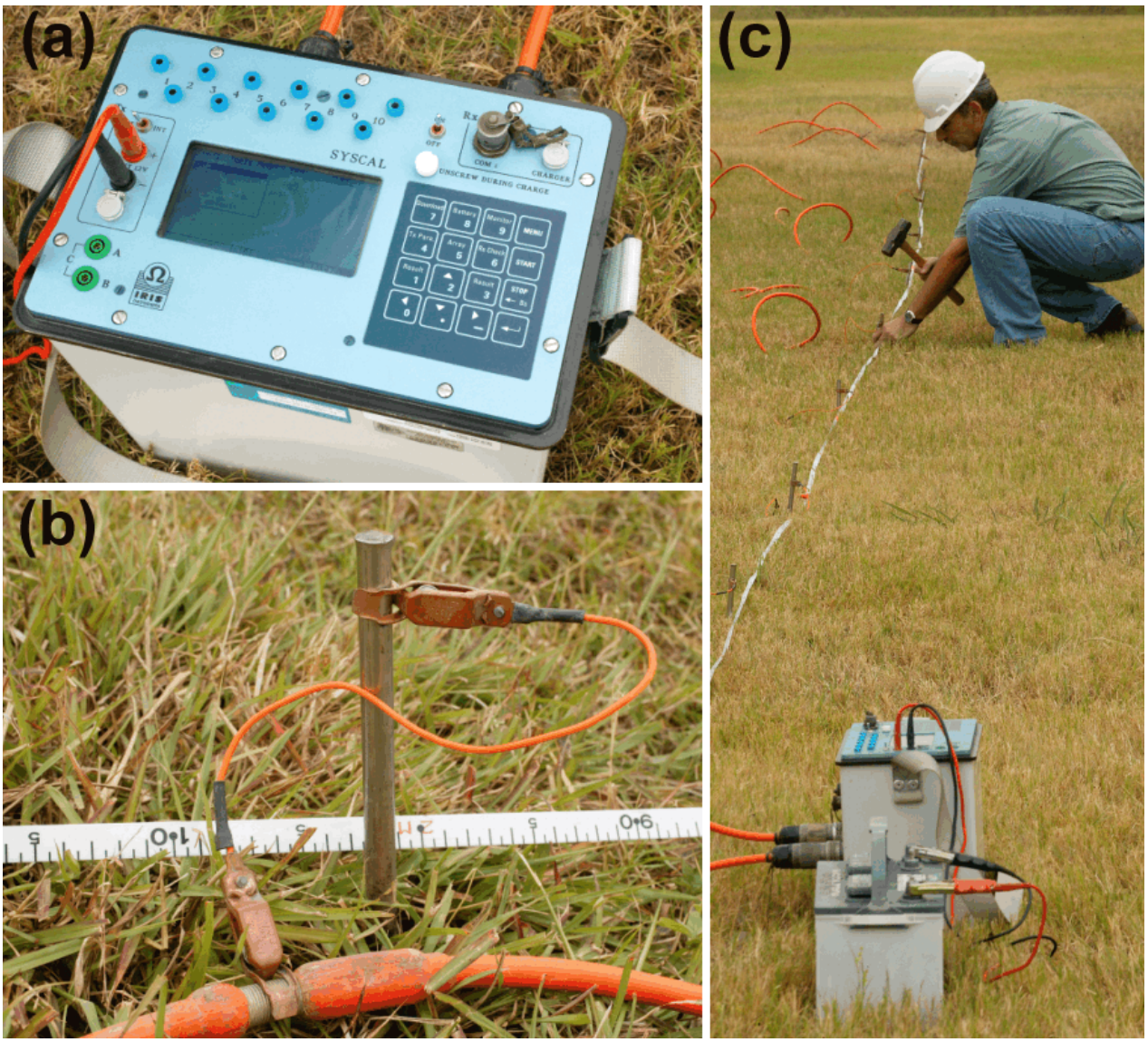

Figure 3-26. Multi-Electrode Resistivity: (a) SYSCAL-PRO 10 Channel Multi-Electrode Resistivity Measurement System (see http://www.heritagegeophysics.com/resistivity/resistivity_meters.htm for System Description), (b) Close-Up of Electrode Field Installation, and (c) Field Deployment of Multi-Electrode Array [Photographs Courtesy of R. Green, Geosciences and Engineering Division, Southwest Research Institute®]

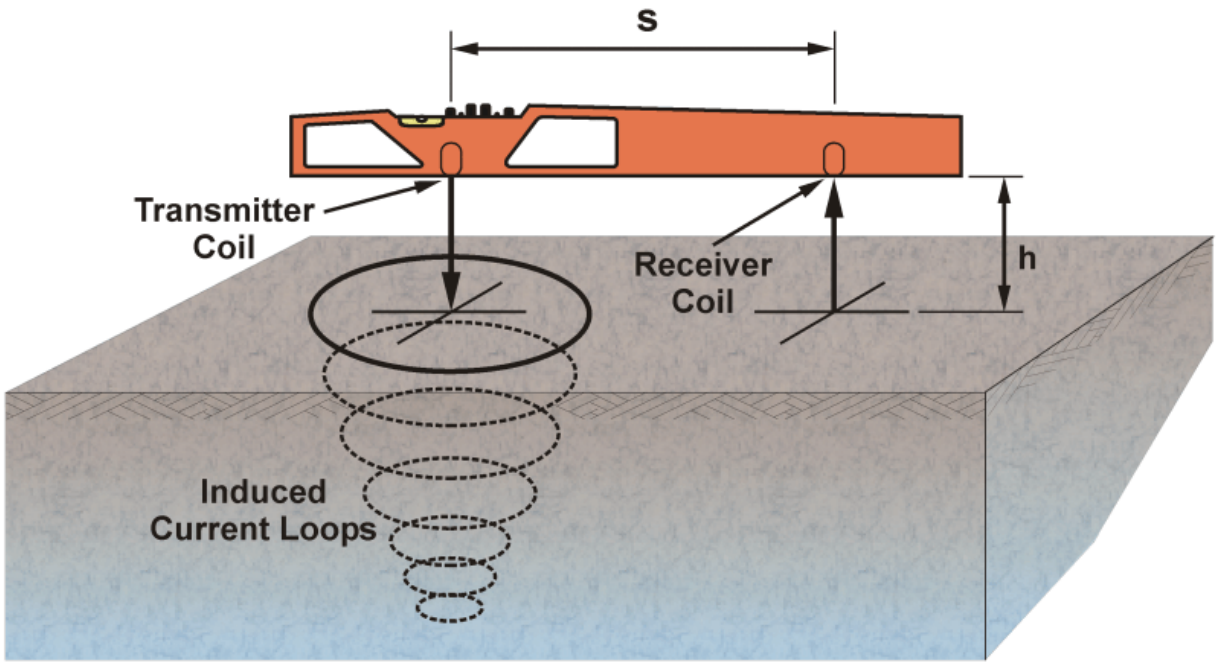

Figure 3-27. Electromagnetic Induction Method [Illustration Copyright 2005 From "Field Methods for Monitoring Solute Transport" by Tuller and Islam, 2005. Reproduced by Permission of Routledge/Taylor & Francis Group, LLC.]

An alternative to the surface-based electrical resistivity method for determining depth-dependent EC_a was introduced by Rhoades and van Schilfgaarde (1976). They developed a single probe with four equally spaced electrodes mounted as annular rings. The probe that is pushed into the soil to the desired depth provides higher measurement resolution. A drawback, however, is the small sampling volume; a large number of measurements are necessary to obtain representative values of EC_a. Application of this probe is advantageous when a precise measurement of salinity within a small localized region is required. Surface-positioned electrodes are better suited for determining a soil salinity index for larger areas.

Observations of soil or rock electrical conductivity to greater depths can be achieved with borehole electrical resistivity tomography, where arrays of current and potential electrodes (pole-dipole) mounted on cables are lowered into boreholes. Low frequency electrical current is injected into the subsurface, and the resulting potential distribution is measured for many different current and potential electrode orientations. Robust regularized nonlinear inverse methods (Binley, et al., 2002) allow the reconstruction of two- and three-dimensional electrical resistivity distributions within the soil volume between two or more boreholes (cross-borehole electrical resistivity tomography). In special cases, the current and potential electrodes are placed in a single borehole (in-line electrical resistivity tomography). While electrical resistivity tomography was successfully applied to qualitatively study flow and transport in porous media (Daily, et al., 1995, 1992) and fractured porous media (Slater, et al., 1997), quantitative assessment of transport characteristics in soils and rocks from electrical resistivity tomography data is still being developed (Binley, et al., 1996; Slater, et al., 2000).

3.4.2 Electromagnetic Induction Methods

Another widely applied method used to measure apparent electrical conductivity of sediment and rock is based on electromagnetic induction. In contrast to the electrical resistivity methods discussed in the previous section, current is applied to the geological formation (rock or sediment) through electromagnetic induction; thus, no direct contact with the ground surface is required (Corwin and Lesch, 2003). Common instruments consist of a transmitter coil that, when energized with alternating current at audio frequency, produces an electromagnetic field. Figure 3-27 illustrates the method. The time-varying electromagnetic field emitted from the transmitter coil induces weak circular eddy current loops in the conducting medium, which in turn generate a secondary electromagnetic field that differs in amplitude and phase from the primary field (McNeill, 1980). The magnitude of amplitude and phase differences between the primary and secondary field depends on medium properties such as texture, structure, water content, and solute concentration, as well as spacing between transmitter and receiver coil, distance between coils and ground surface, and coil orientation (parallel or perpendicular to the ground surface). The effect of rock or soil magnetic permeability is relatively minor (de Jong, et al., 1979) unless the soil contains a large amount of magnetic components (Huang and Fraser, 2002).

The primary and secondary fields are sensed as apparent electrical conductivity at the receiver coil, *m*, according to (McNeill,1980)

$$m = \frac{4}{\omega \mu_0 s^2} \left(\frac{H_s}{H_p} \right) \tag{3-22}$$

where

ω	—	angular operating frequency (radians per second) of the instrument
μ_0	—	magnetic permeability of free space (1.2566×10^{-6} H m^{-1}; H = Henries)
s	—	coil spacing (m)
H_s and H_p	—	sensed intensities of the primary and secondary fields at the receiver coil (A m^{-1})

The apparent electrical conductivity defined in Eq. (3-22) is equal to EC_a when (i) the distance between the coils and the ground surface is zero; (ii) the soil is homogeneous with uniform bulk electrical conductivity, EC_a; and (iii) the induction number N_B is much smaller than 1 ($N_B << 1$). The induction number is defined as

$$N_B = \frac{s}{\delta} \tag{3-23}$$

where δ is the skin depth, defined as the depth where the primary magnetic field has been attenuated to 1/e of its original strength (i.e., 37 percent; e is the base of the natural logarithm) (Hendrickx, et al., 2002).

Assuming that $N_B << 1$, depth-dependent bulk electrical conductivity $EC_a(z)$ can be calculated for horizontal and vertical coil orientation by solving the following Fredholm integral equations of the

first kind (McNeill, 1980; Borchers, et al., 1997; Hendrickx, et al., 2002)

$$m^H(h) = \int_0^\infty \phi^H(z+h)\, EC_a(z)\, dz \tag{3-24}$$

with the sensitivity function $\phi^H(z)$ given as

$$\phi^H(z) = 2 - \frac{4z}{(4z^2+1)^{1/2}} \tag{3-25}$$

and

$$m^v(h) = \int_0^\infty \phi^v(z+h)\; EC_a(z)\, dz \tag{3-26}$$

with the sensitivity function $\phi^V(z)$ given as

$$\phi^v(z) = \frac{4z}{(4z^2+1)^{3/2}} \tag{3-27}$$

where

H and *V*	—	horizontal and vertical coil orientation, respectively
h	—	distance between the coils and the ground surface (Figure 3-27)
m(*h*)	—	apparent electrical conductivity (S m^{-1})

The sensitivity functions represent the relative contribution of the electrical conductivity at depth *z* to the instrument reading *m*(*h*). In practice it may be difficult to solve the inverse problem given in Eqs. (3-24) through (3-27), because the continuous functions *m*(*h*) are not known (only a finite sets of measurements at different heights *h* are available), and small variations in *m*(*h*) might lead to large changes in $EC_a(z)$. Borchers, et al. (1997) applied a second-order Tikhonov regularization method to solve the inverse problem for EC_a profiles in layered soils.

Hendrickx, et al. (2002) present a nonlinear model, based on solutions of Maxwell's equations in the frequency domain, that relate electromagnetic induction measurements to depth-dependent EC_a when the assumption $N_B << 1$ is violated.

It is not clear that the physical models discussed above that describe the electromagnetic response in homogeneous media are applicable to heterogeneous field conditions. Hendrickx, et al. (2002) note that attempts to use electromagnetic measurements to determine vertical EC_a distributions are hindered by the nonuniqueness typical of inverse procedures, but the lack of understanding of physical relationships between the vertical distribution of electrical conductivity and the response of electromagnetic-induction ground conductivity meters under heterogeneous field conditions may further exacerbate the situation.

Electromagnetic induction meters are commercially available from a number of geophysical instrumentation companies. A comprehensive literature review suggests that the most commonly applied systems in vadose zone hydrology and soil science are the GEONICS, Ltd.,

EM–31 and EM–38 ground conductivity meters. The EM–31 has a coil spacing of 3.66 m [12.0 ft], which results in a penetration depth of approximately 3 m [9.8 ft] when the coils are oriented parallel to the ground surface (horizontal), and 6 m [19.7 ft] when the coils are perpendicular to the surface (vertical orientation). The coil spacing of the EM–38 (shown in Figure 3-28) is exactly 1 m [3.3 ft], which leads to penetration depths of 0.75 and 1.0 m [2.5 and 3.3 ft] when operated in horizontal and vertical mode, respectively. Note that the horizontal mode is obtained by simply turning the instrument 90 degrees. Both instruments are lightweight and can be easily operated by a single person. Corwin and Lesch (2003) mount the instrument on a sled that is pulled by an all-terrain vehicle, which may be more convenient for large-scale resistivity surveys.

Recent applications of the electromagnetic induction method in soil and environmental science are reported by Hendrickx, et al. (1992), Triantafilis, et al. (2000), Hendrickx, et al. (2002), Lesch and Corwin (2003), Corwin and Lesch (2003), and Sudduth, et al. (2003).

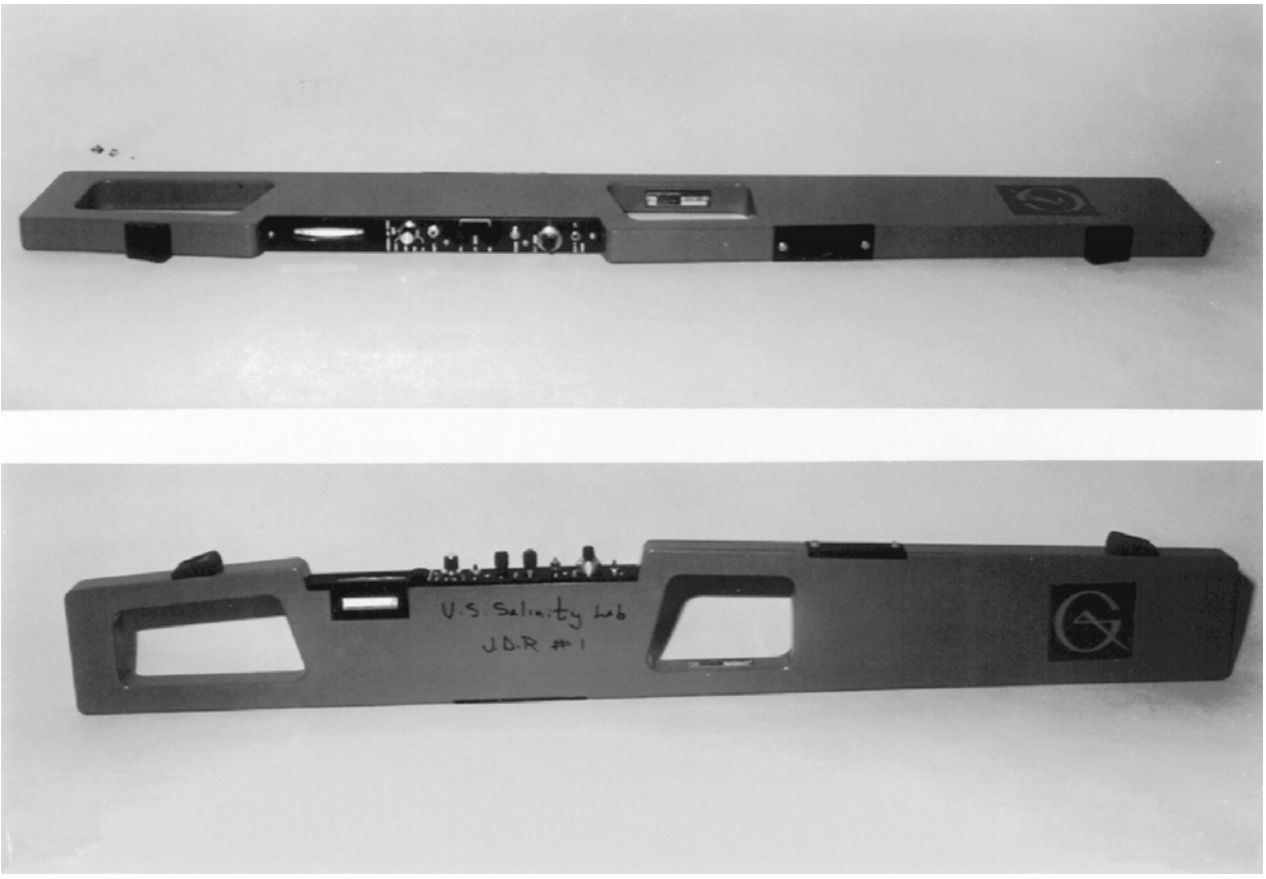

Figure 3-28. Commercially Available Electromagnetic Induction Meter: Handheld EM-38 Ground Conductivity Meter (Geonics, Ltd.) With Horizontal Coil Orientation (Top) and Vertical Coil Orientation (Bottom) [Reproduced From Corwin and Lesch (2003) With Permission]

3.4.3 Fiber Optic Sensors

Rapid advancements in fiber optic sensor applications offer the promise of expanded capabilities for monitoring transport of dissolved constituents (solutes and tracers). Yet-to-be-developed multipurpose probes may be able to simultaneously measure relative humidity, moisture content, temperature, and CO_2, and detect fluorescent tracers in soils and fractured rock (see also fiber optic thermometry and chilled mirror techniques discussed in Section 3.5.4).

The fiber optic technique directs a constant light beam through optical fibers (input leg) to a target location within a porous matrix, where it is partially adsorbed and partially reflected back into the probe. The reflected light is guided through a separate fiber bundle (output leg) from the probe to a photodetector that quantifies light intensity and converts the optical signal to an electrical signal that can be recorded with a computer or datalogger as shown in Figure 3-29. Narrow and broad band filters are employed to condition the outgoing and reflected light beams respectively (Ghodrati, 1999). Given that the intensity of the ingoing light remains constant with time, the intensity of the reflected beam will be constant if the system under investigation is in equilibrium (Krohn, 1988). Perturbations of the equilibrium state will cause a change in output

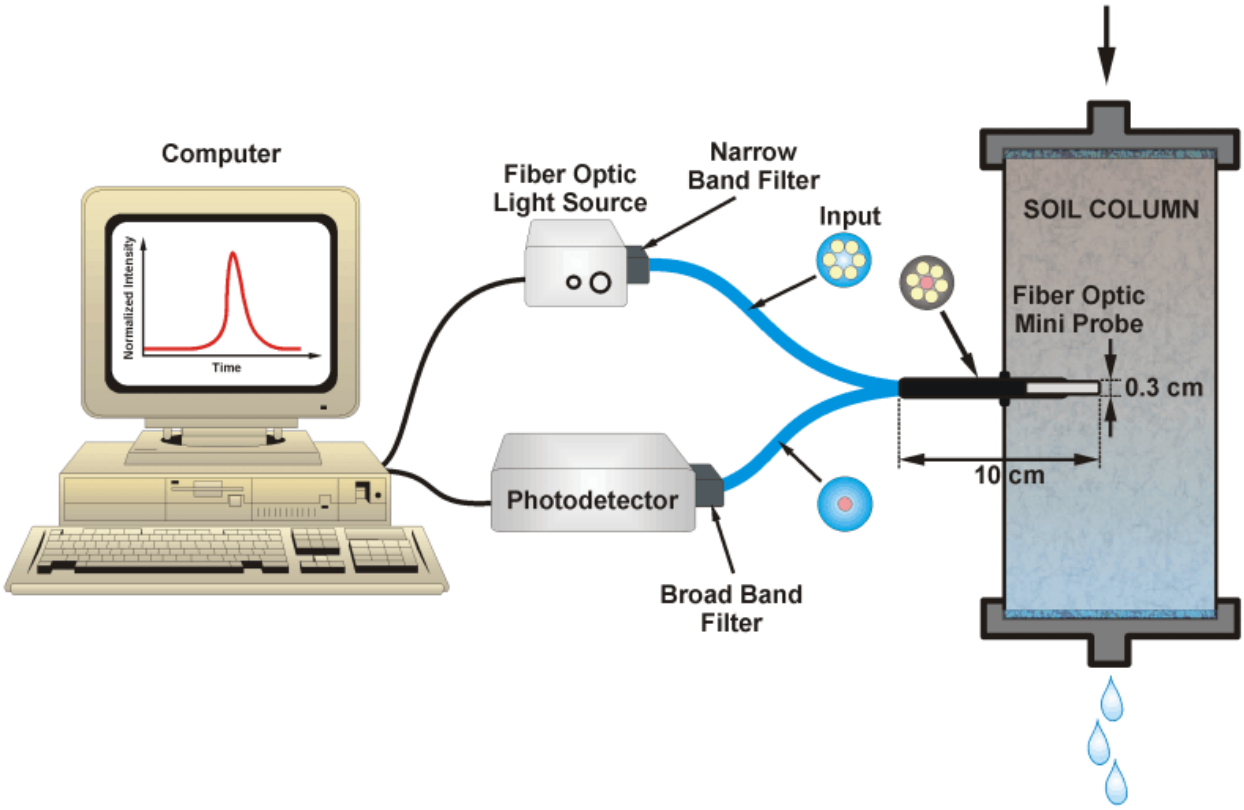

Figure 3-29. Design of a Fiber Optic Miniprobe Measurement System [Reproduced From Ghodrati (1999) With Permission]

light intensity that can be analyzed to quantify the perturbation-causing process, based on calibration relationships that must be established for each probe and the process of interest (e.g., change in solute concentration or water content).

Fiber optic sensors have been applied for measuring soil water content (Alessi and Prunty, 1986; Garrido, et al., 1999), but characterization of solute transport phenomena in porous media via fluorescent tracers (Ghodrati, 1999) may be the most promising application for vadose zone and environmental science.

Garrido, et al. (2000) provide calibration procedures for laboratory and field experiments that relate tracer concentration to output light intensity with the assumption of a rigid and stable soil matrix (no particle rearrangement or swelling). The conventional calibration procedure for laboratory experiments consists of stepwise leaching a column filled with the porous medium of interest with several pore volumes of tracer with known concentration. Once the photodetector indicates stable output intensity for a certain tracer concentration, the column is flushed with a solution of $CaCl_2$ and the procedure is repeated for the next tracer concentration, until several points are established on the calibration curve. A second order polynomial function may be fitted to the measurements to establish a continuous calibration relationship (Ghodrati, et al. 1999).

This calibration procedure may not be practical for field application because of the large amount of tracer that would be required. Garrido, et al. (2000) developed a point calibration device that allows site-specific calibration of fiber optic sensors. The device consists of a stainless steel tube that either forms a jacket around or is attached to the outside of the miniprobe, allowing injection of a small known amount of tracer directly into the medium in front of the fiber optics. The tracer injection tube is connected to a peristaltic pump or a syringe. The calibration curve is constructed in the same manner as for the conventional method. A comparison of both methods in the laboratory shows good agreement (Garrido, et al., 2000).

Studies by Kulp, et al. (1988), Nielsen, et al. (1991), Campbell, et al. (1999), Ghodrati (1999), and Ghodrati, et al. (2000), and a comprehensive review of fiber optic sensors and applications for environmental monitoring by Rogers and Poziomek (1996), reveal great potential for this technique, but extensive testing and calibration under field conditions and further sensor development is required before continuous real time monitoring of environmental parameters is feasible.

3.5 Temperature Measurement

Temperature can be measured via a diverse variety of sensors. All of these sensors infer temperature by sensing some change in a physical characteristic. The most common types that are used in porous media are: thermocouples, resistive temperature devices, thermistors, and fiber-optic sensors.

3.5.1 Thermocouples

A thermocouple consists of a double junction of two dissimilar metals, and provides a simple and efficient means of measuring temperature. Two junctions subjected to different temperatures generate a voltage difference, explained by the *Seebeck effect* (Seebeck, 1921). This voltage difference can be read using an analog to digital converter (or any voltmeter), and the temperature can be inferred from standard calibration tables.

In principle, a thermocouple can be made from almost any two metals. In practice, several thermocouple types have become standard because of desirable qualities, including linearity of the voltage drop as a function of temperature and large voltage-to-temperature ratio. The most common types are the E, J, K, R, S, and T types, with their characteristics summarized in Table 3-2. Each type has a different temperature range and environment, although the maximum temperature varies with the diameter of the wire used in the thermocouple. A field bank of thermocouples is shown in Figure 3-30, demonstrating how small these devices are.

3.5.2 Resistance Temperature Detectors

Resistance temperature detectors are sensors used to measure temperature by correlating the resistance of the resistance temperature detector element with temperature. Most resistance temperature detector elements consist of fine coiled wire of known length wrapped around a ceramic or glass core. The element is usually quite fragile, so it is often placed inside a sheathed probe for protection. The resistance temperature detector element is made from a pure material whose resistance at various temperatures has been documented. The material has a predictable change in resistance as the temperature changes, and it is this predictable change that is used to determine temperature. Common materials for resistance temperature detectors are platinum (most popular and accurate), nickel, or copper. A rugged commercially

Table 3-2. Measurement Range and Calibration Coefficients for E, J, K, R, S, and T-Type Thermocouples

Calibration Coefficients	Type E	Type J	Type K	Type R	Type S	Type T
	Nickel-10% Chromium (+) and Constantan (–)	**Iron (+) and Constantan (–)**	**Nickel-10% Chromium (+) and Nickel-5% (–) (Aluminum Silicon)**	**Platinum-13% Rhodium (+) and Platinum (–)**	**Platinum-10% Rhodium (+) and Platinum (–)**	**Copper (+) and Constantan (–)**
	–100 to 1,000 °C [–148 to –1,832 °F] ± 0.5 °C [1.8 °F] 9th Order	0 to 760 °C [32 to 1,400 °F] ± 0.1 °C [0.4 °F] 5th Order	0 to 1,370 °C [–32 to 2,498 °F] ± 0.7 °C [2.5 °F] 8th Order	0 to 1,000 °C [32 to 1,832 °F] ± 0.5 °C [1.8 °F] 8th Order	0 to 1,750 °C [32 to 3,182 °F] ± 1 °C [3.6 °F] 9th Order	–160 to 400 °C [–256 to –752 °F] ± 0.5 °C [1.8 °F] 7th Order
a_0	0.104967248	–0.048868252	0.226584602	0.263632917	0.927763167	0.100860910
a_1	17189.45282	19873.14503	24152.10900	179075.491	169526.5150	25727.94369
a_2	–282639.0850	–218614.5353	67233.4248	–48840341.37	–31568363.94	–767345.8295
a_3	12695339.5	11569199.78	2210340.682	1.90002×10^{10}	8990730663	780225595.81
a_4	–448703084.6	–264917531.4	–860963914.9	-4.82704×10^{12}	-1.63565×10^{12}	–9247486589
a_5	1.10866×10^{10}	2018441314	4.83506×10^{10}	7.62091×10^{14}	1.88027×10^{14}	6.97688×10^{11}
a_6	-1.76807×10^{11}	—	-1.18452×10^{12}	-7.20026×10^{16}	-1.37241×10^{16}	-2.66192×10^{13}
a_7	1.71842×10^{12}	—	1.38690×10^{13}	3.71496×10^{18}	6.17501×10^{17}	3.94078×10^{14}
a_8	-9.19278×10^{12}	—	-6.33708×10^{13}	-8.03104×10^{19}	-1.56105×10^{19}	—
a_9	2.06132×10^{13}	—	—	—	1.69535×10^{20}	—

Notes: Temperature conversion equation: $T = a_0 + a_1x + a_2x^2 + ...+ a_nx^n$.
Nested polynomial form: $T = a_0 + x(a_1 +x(a_2 + x(a_3 + x(a_4 + a_5x))))$ (5th order) where x is in volts, T is in °C.

Figure 3-30. Thermocouples Connected to a Datalogger and Embedded in the Soil, With a Thermocouple Junction Held up for Viewing [Photograph Courtesy of J. Wraith, Montana State University]

available resistance temperature detector probe is shown in Figure 3-31, which is suitable for installation in soil and rock.

The resistance temperature detector is one of the most accurate temperature sensors with a measurement range from 200 to 850 °C [392 to 1,562 °F]. Not only does it provide good accuracy, it also provides excellent stability and repeatability. Resistance temperature detectors are also relatively immune to electrical noise, thus are well-suited for temperature measurement in industrial environments, especially around motors, generators and other high voltage equipment. The resistance temperature detector is a more linear device than the

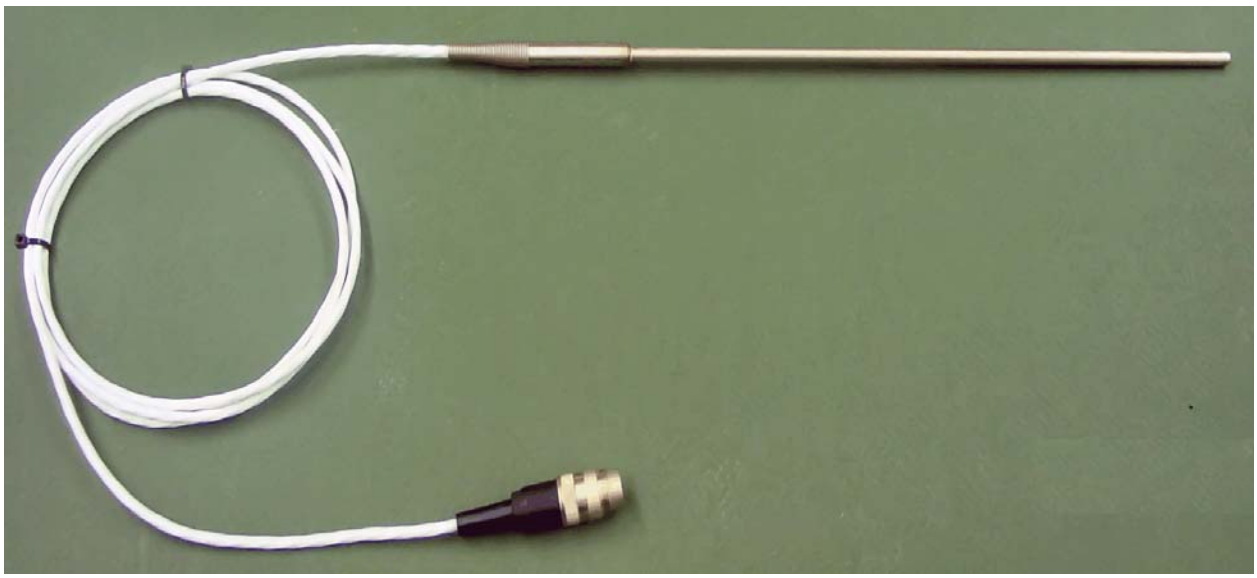

Figure 3-31. Commercially Available Resistance Temperature Detector Probe (Omega Engineering, Inc.) [Photograph by M. Tuller]

thermocouple, but it still requires curve-fitting. The Callendar-Van Dusen equation is commonly used to approximate the resistance temperature detector temperature response

$$R_T = R_0 + R_0\alpha\left[T - \delta - \left(\frac{T}{100} - 1\right)\left(\frac{T}{100}\right) - \beta\left(\frac{T}{100} - 1\right)\left(\frac{T}{100}\right)^3\right] \tag{3-28}$$

where

R_T	—	resistance at a given temperature T
R_0	—	resistance at 0 °C [32 °F]
α, δ, and β	—	temperature coefficients determined from testing the resistance temperature detector at four temperatures and solving the associated Callendar-Van Dusen equations

3.5.3 Thermistors

The thermistor is a thermally sensitive variable resistor. The thermistor exhibits a much larger parameter change with temperature than either resistance temperature detectors or thermocouples. Thermistors are generally composed of semiconductor materials. Although positive temperature coefficient units are available, most thermistors have a negative temperature coefficient (i.e., their resistance decreases with increasing temperature). The negative temperature coefficient can be as large as several percent per degree Celsius, allowing the thermistor circuit to detect minute changes in temperature that could not be observed with a resistance temperature detector or thermocouple circuit. The price paid for this increased sensitivity is loss of linearity. The thermistor is an extremely nonlinear device that is highly dependent upon process parameters. Consequently, manufacturers have not standardized thermistor curves to the extent that resistance temperature detectors and thermocouple curves have been standardized.

An individual thermistor curve can be closely approximated with the Steinhart-Hart equation

$$\frac{1}{T} = A + B \ln R + C (\ln R)^3 \tag{3-29}$$

where

R	—	resistance at temperature T
A, B, and C	—	coefficients determined from a three-point calibration

3.5.4 Fiber Optic Thermometry

Fiber optic thermometry is based on measuring the decay time of an inorganic (ceramic) photoluminescent sensor material (i.e., a “phosphor”). The phosphor sensor is attached to the end of a quartz fiber, which is cabled with a Teflon® sheath to ensure high dielectric integrity. The sensor is subjected to excitation by hundreds of light pulses per second, generated by a high intensity light-emitting diode at the appropriate wavelength.

The phosphor sensor emits light over a broad spectrum in the near infrared region when stimulated with red light from the light emitting diode, as shown in Figure 3-32a. The time required for the fluorescence to decay is dependent on the temperature of the sensor, illustrated in Figure 3-32b. After the light-emitting diode is turned off, the decaying fluorescent signal continues to transmit through the fiber to the instrument, where it is focused onto a detector. The signal from the detector is amplified and sampled after the light-emitting diode is turned off.

The measured decay time is then converted to temperature using a calibrated conversion table. Different calibration tables are used depending on the temperature range and application, but the overall temperature range capability of this optical sensor technology is currently −200 to 330 °C [−328 to 626 °F].

Fiber optic probes can be relatively small because the excitation light signal and the fluorescent decay signal pass along the same optical path. Fiber optic probes are compact because the excitation light signal and the fluorescent decay signal pass along the same optical path. The tip detail for a typical fiber optic probe is shown in Figure 3-33a, and a variety of commercially available fiber optic probe tips is shown in Figure 3-33b.

3.6 Relative Humidity Measurement in Cavities

Measurements of relative humidity within a porous medium were discussed in Section 3.2.6, because relative humidity provides a method for estimating matric potential in a dry medium. The Performance Confirmation Program also requires relative humidity measurements in drifts and within other subterranean cavities to assess conditions giving rise to corrosion, microbial activity, and the potential for condensation and dripping. Although measurements in a porous medium using psychrometers provide direct estimates of relative humidity values within the porous medium, other methods may be required for relative humidity determination in drifts, because temperature differences between psychrometer junctions may be adversely influenced by mass exchange between the rock and air in drifts with active ventilation.

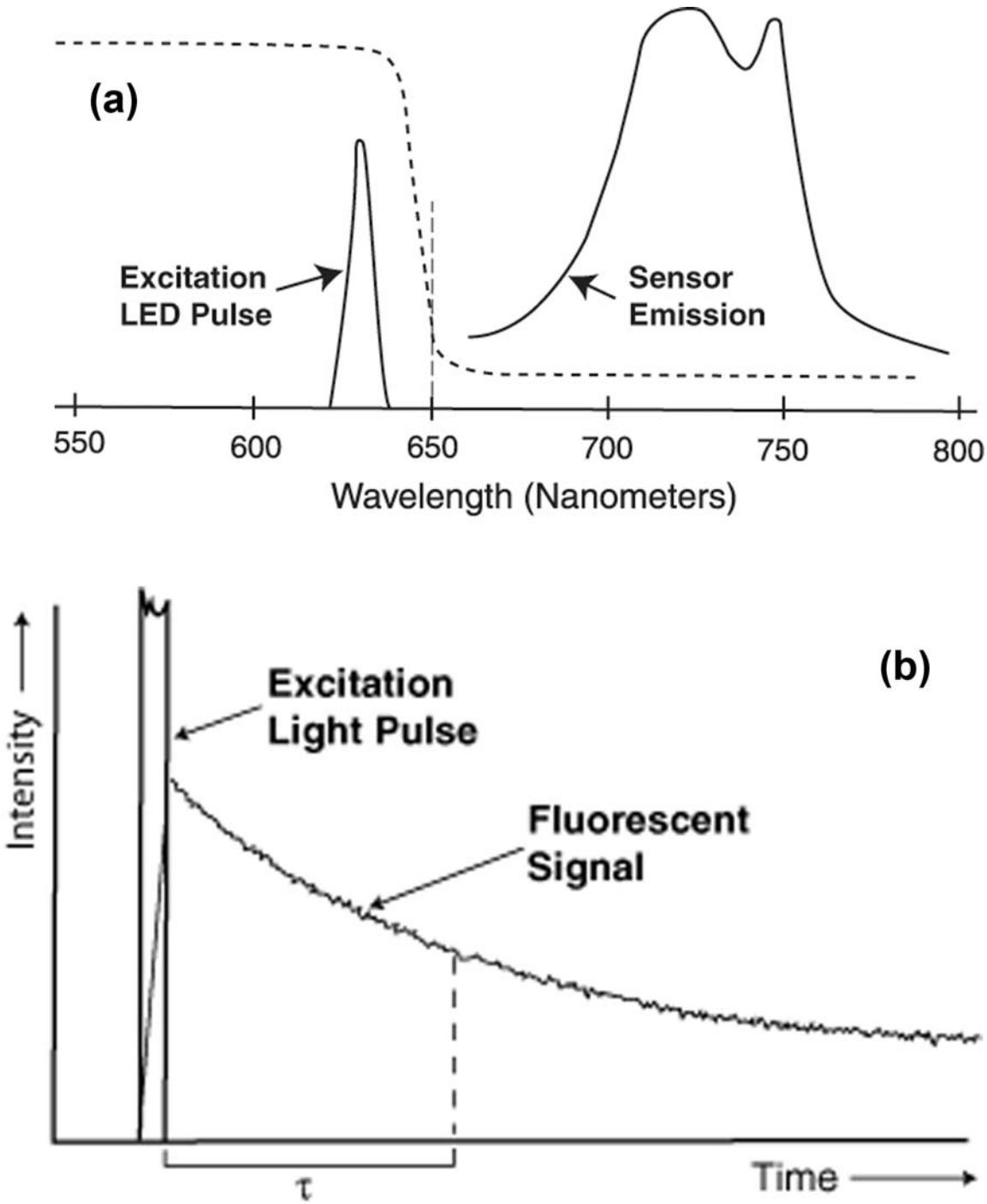

Figure 3-32. Fiber Optic Thermometry: (a) Wavelengths of an Excitation Light Pulse From a Light-Emitting Diode, and the Resulting Light Emitted by the Sensor; and (b) Decay of Sensor-Emitted Fluorescent Signal [Images Courtesy of Luxtron Corporation]

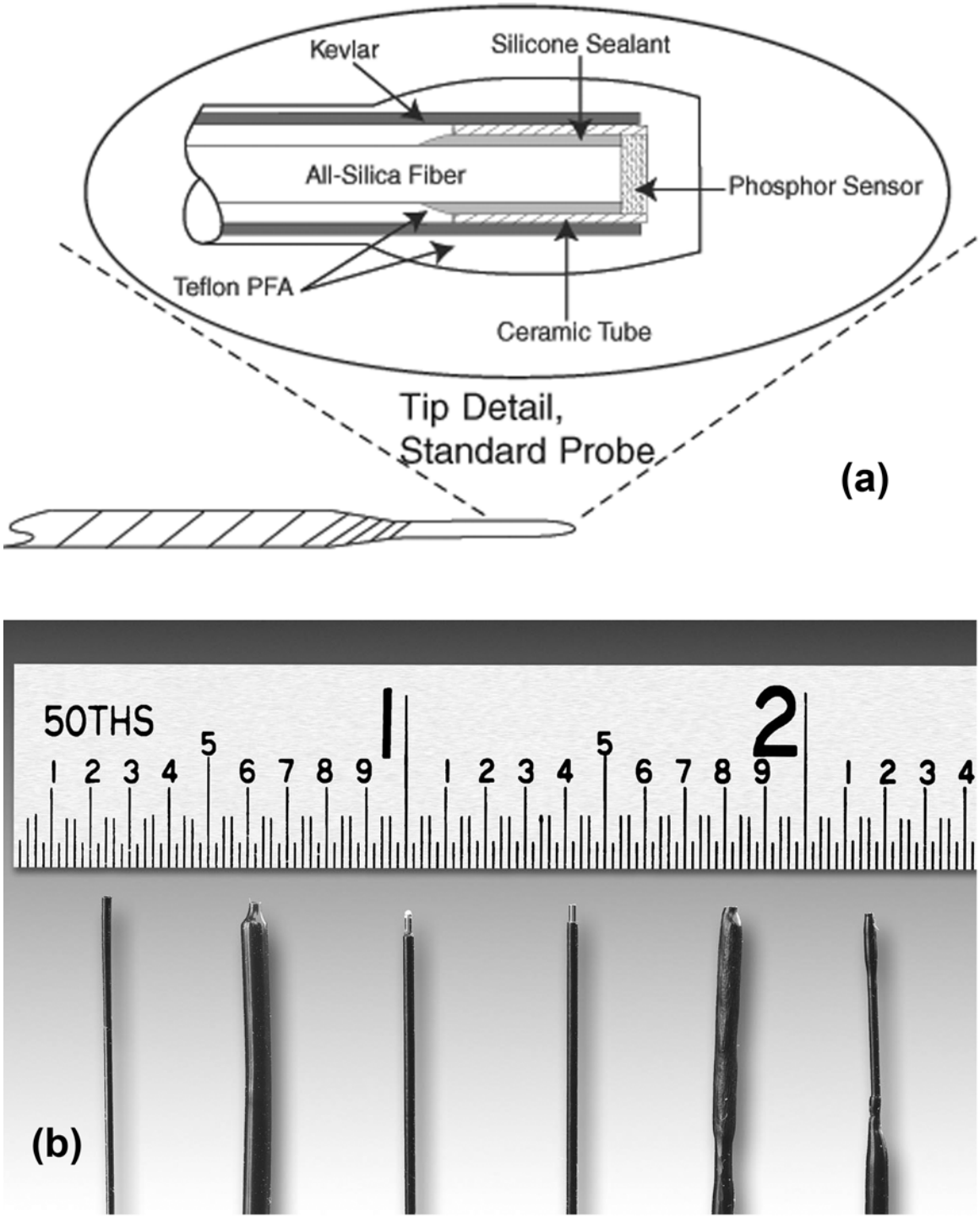

Figure 3-33. Fiber Optic Probes: (a) Tip Detail of a Fiber Optic Probe, and (b) Representative Commercially Available Probes [Images Courtesy of Luxtron Corporation]

Five methods for measuring relative humidity in cavities are discussed in this section.

Psychrometer theory is reviewed briefly. Like psychrometers, chilled mirror hygrometers also manipulate sensor temperatures to achieve vapor condensation, but use a different sensor approach. Capacitive humidity sensors measure the difference in capacitance of the surrounding air due to changes in relative humidity. Resistive humidity sensors measure changes in electrical resistivity in a hygroscopic medium. Thermal conductivity sensors measure changes in atmospheric thermal conductivity.

3.6.1 Psychrometers

Psychrometers were introduced in Section 3.2.4. These sensors measure relative humidity, from which matric potential in a porous medium can be inferred, but of course psychrometers can be used when relative humidity itself is the quantity of interest. Psychrometers are used to infer the relative humidity from the difference between dry bulb and wet bulb temperatures. The dry bulb temperature is that of the ambient air (nonevaporating surface). The wet bulb temperature is that of an evaporating surface; this temperature is generally lower than the dry bulb temperature because of latent heat loss in the evaporation process.

For typical use in porous media, one junction of the thermocouple psychrometer is suspended in a thin-wall ceramic or stainless screen cup embedded in the porous material (Figure 3-34), while the other junction is embedded in an insulated plug to measure the ambient temperature at the same location. The suspended thermocouple is cooled below the dew point by means of an electrical current until pure water condenses on the junction. This is called *Peltier cooling*. The cooling then stops, and as water evaporates it draws heat in the form of latent heat of vaporization from the junction, cooling the junction below the temperature of the surrounding air until the junction attains a wet bulb temperature. The warmer and dryer the surrounding air, the higher the evaporation rate and the greater the wet bulb temperature depression. The difference in temperatures between the insulated dry bulb and the wet bulb thermocouples is measured and used to infer the relative humidity or relative vapor pressure using the psychrometer equation

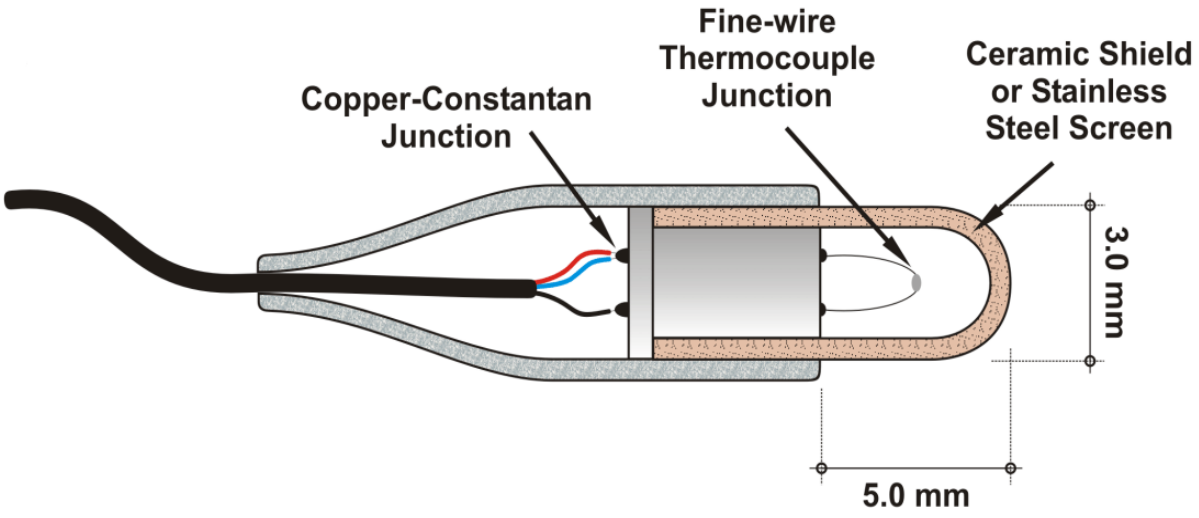

Figure 3-34. Design of a Psychrometer Used for Porous Media Applications

$$\mathrm{RH} = \frac{e}{e_0} = 1 - \frac{s+\gamma}{e_0}\Delta T \tag{3-30}$$

where

RH	—	relative humidity
e_0	—	water vapor pressure at saturation (kPa)
e	—	water vapor pressure (kPa)
s	—	slope of the saturation water vapor pressure curve
γ	—	psychrometric constant {approximately 0.067 kPa K^{-1} at 20 °C [68 °F]}
ΔT	—	temperature difference (°C)

The slope s is temperature-dependent and can be approximated as (Brutsaert, 1982)

$$s = \frac{de_0}{dT} = \frac{373.15 e_0}{T^2}(13.3185 - 3.952\tau - 19335\tau^2 - 0.5196\tau^3) \tag{3-31}$$

where $\tau = 1 - 373.15/T$. The saturated vapor pressure e_0 is also temperature dependent and is estimated from the integral of Eq. (3-31) as

$$e_0 = 101.325 \exp\left(13.3185\tau - 19760\tau^2 - 0.6445\tau^3 - 0.1299\tau^4\right) \tag{3-32}$$

3.6.2 Chilled Mirror Hygrometers (Dew-Point Technique)

A chilled mirror hygrometer makes a direct measurement of the dew point temperature of a gas by allowing a sample of gas of unknown water vapor content to condense on an inert, chilled, mirror-polished metal surface. Thermoelectric modules (e.g., using the Peltier effect) are typically used to chill the surface. The chilled mirror is used to reflect a beam of light from a light-emitting diode into a photodetector, as shown in Figure 3-35. The presence of condensed fine water droplets markedly alters the properties of the reflected beam. A commercially available chilled mirror dewpoint sensor is shown in Figure 3-36.

The mirror is maintained, using a feedback system, at the temperature at which the rate of dew condensation exactly equals the rate of dew evaporation. In this state, the mass of the dew layer neither increases nor decreases, and the layer achieves dynamic equilibrium with the water vapor in the surrounding gas sample to define the dew point temperature of the sample. Under such conditions, the surface temperature of the metallic condensation surface represents the saturation temperature of the water vapor in the gas being measured. A second detector is sometimes used to monitor the polarization of the scattered light, which allows automatic determination of the phase of the condensate (i.e., dew point or frost point).

A typical chilled mirror hygrometer can be made very inert, in contrast to many other humidity sensors, rendering it virtually indestructible and minimizing the need for recalibration. A full-range dew point sensor is capable of handling dew points from >100 °C [>212 °F] to as low as −70 °C [−94 °F]. The gas sample contacts only inert materials: a glass or quartz lens, a Teflon® O-ring, and a stainless steel housing and metallic condensation surface. Some of the inert mirror materials include gold, chromium-plated silver or copper, and titanium nitride. A

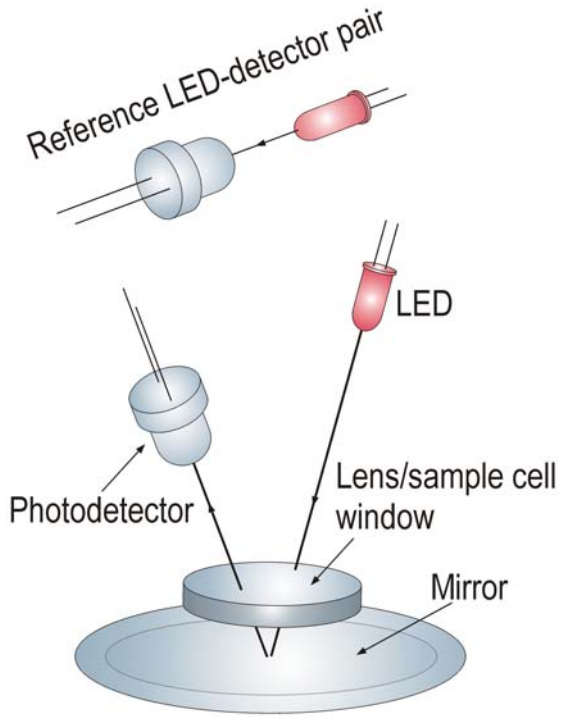

Figure 3-35. Chilled Mirror Hygrometer Method

Figure 3-36. Commercially Available Chilled Mirror Dewpoint Sensor (GE General Eastern Instruments) [Image Courtesy of GE Sensing]

copper or silver mass covered by a thin, polished stainless steel sheath is commonly used for mirrors in harsh environments.

The chilled mirror hygrometer has several advantages over other water vapor sensing technologies:

- A chilled mirror hygrometer provides a direct physical measurement of humidity. This technique is the most precise method for determining water vapor content of a gas with more than 5-percent relative humidity.

- The chilled mirror hygrometer optical sensor is a totally inert device. The sample gas contacts glass and non-reactive metals, thus, the device is easily cleaned and may last indefinitely.

- A chilled mirror hygrometer sensor does not lose its calibration, unlike polymer relative humidity sensors, lithium chloride dew cells, and other chemically-based sensors.

- The dew/frost point temperature defines the saturation point for the water vapor in the gas. From this unique equilibrium temperature, all other reporting formats of gas humidity can be derived.

3.6.3 Capacitive Humidity Sensors

Capacitive relative humidity sensors, such as the sensor shown in Figure 3-37, are widely used in industrial, commercial, and weather telemetry applications. Capacitive relative humidity sensors consist of a substrate on which a thin film of polymer or metal oxide is deposited between two conductive electrodes. The sensing surface is coated with a porous metal electrode to protect it from contamination and exposure to condensation. The substrate is typically glass, ceramic, or silicon. The incremental change in the dielectric constant of a capacitive humidity sensor is nearly directly proportional to the relative humidity of the surrounding environment. The change in capacitance is typically 0.2–0.5 pF for a 1-percent relative humidity change, while the bulk capacitance is between 100 and 500 pF at 50-percent relative humidity at 25 °C [77 °F]. Capacitive sensors are characterized by (i) low temperature coefficient, (ii) ability to function at high temperatures {up to 200 °C [392 °F]}, (iii) full recovery from condensation, and (iv) moderate resistance to chemical vapors. The response time ranges from 30 to 60 seconds for a 63-percent relative humidity step change.

State-of-the-art techniques for producing capacitive sensors take advantage of many of the principles used in semiconductor manufacturing to yield sensors with minimal long-term drift and hysteresis. Thin film capacitive sensors may include monolithic signal conditioning circuitry integrated onto the substrate. The most widely used signal conditioner incorporates a complementary metal oxide semiconductor timer to pulse the sensor and to produce a near-linear voltage output.

The typical uncertainty of capacitive sensors is ± 2 percent relative humidity from 5 to 95 percent relative humidity with two-point calibration. Unwanted capacitive effects in cables limit the distance between the sensing element (the capacitor) and signal conditioning circuitry to <3 m [<10 ft].

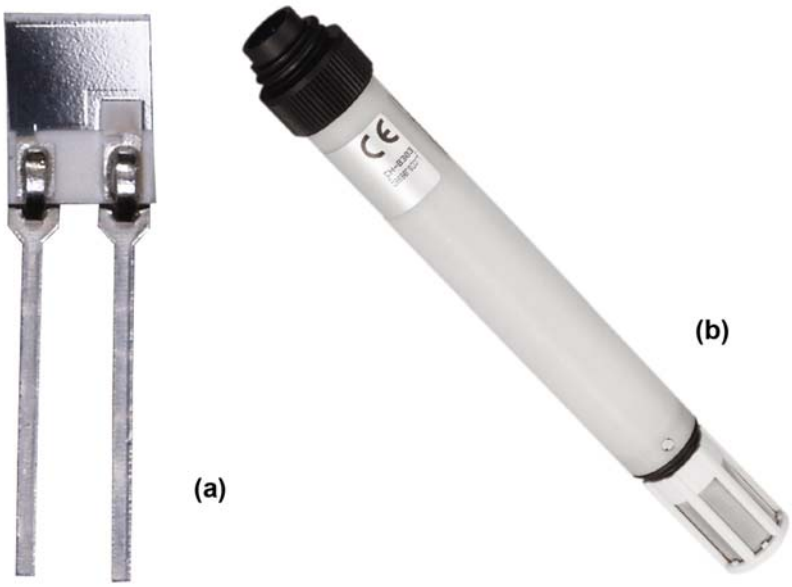

Figure 3-37. Commercially Available Capacitive Relative Humidity Sensor: (a) Relative Humidity Sensor and (b) Relative Humidity Probe [Images Courtesy of ROTRONIC Instrument Corp., Huntington, New York]

3.6.4 Resistive Humidity Sensors

Resistive humidity sensors measure the change in electrical impedance of a water-absorbing (hygroscopic) medium such as a conductive polymer, salt, or treated substrate. The impedance change typically exhibits an inverse exponential relationship with humidity.

Resistive sensors usually consist of either noble metal electrodes deposited on a substrate or wire-wound electrodes on a plastic or glass cylinder. The substrate is coated with a salt or conductive polymer, or the substrate may be treated with activating chemicals such as acid. Ionic functional groups are dissociated as the sensor absorbs water vapor, resulting in an increase in electrical conductivity. The response time for most resistive sensors ranges from 10 to 30 seconds for a 63-percent step change. The impedance range of typical resistive elements varies from 1 kΩ to 100 MΩ.

Most resistive sensors use a symmetrical alternating current excitation voltage with no direct current bias to prevent polarization of the sensor. The resulting current flow is converted and rectified to a direct current voltage signal for additional scaling, amplification, and linearization. Nominal excitation frequency is from 30 Hz to 10 kHz.

A distinct advantage of resistive relative humidity sensors is their interchangeability, usually within ± 2 percent relative humidity, which allows the electronic signal conditioning circuitry to be calibrated by a resistor at a fixed relative humidity value. This property eliminates the need for humidity calibration standards, hence, resistive humidity sensors are generally field replaceable. The accuracy of individual resistive humidity sensors may be confirmed by testing them in a

relative humidity calibration chamber or with a computer-based data acquisition system referenced to a standardized humidity-controlled environment. The nominal operating temperature of resistive sensors ranges from −40 to 100 °C [−40 to 212 °F].

A limitation of some resistive sensors with a water soluble coating is a tendency to shift values when exposed to condensation. Resistive humidity sensors have significant temperature dependencies when installed in an environment with large {> 5.5 °C [> 10 °F]} temperature fluctuations. Simultaneous temperature compensation is incorporated to improve accuracy.

3.6.5 Thermal Conductivity Humidity Sensors

Thermal conductivity sensors measure absolute humidity (mass of water vapor per unit volume of dry air) by quantifying the difference between the thermal conductivity of a reference gas and ambient air. The rate of heat loss or gain in air is a function of the air vapor content. Thermal conductivity humidity sensors (or absolute humidity sensors) consist of two matched negative temperature coefficient thermistor elements in a bridge circuit; one is hermetically sealed in dry nitrogen and the other is exposed to the ambient air. When current is passed through the thermistors, resistive heating increases their temperature to > 200 °C [> 392 °F]. More heat is dissipated from the sealed thermistor than from the exposed thermistor due to the difference in the thermal conductivity of the air water vapor relative to dry nitrogen. The difference in heat dissipation results in a difference in operating temperatures and in thermistor resistance that is proportional to absolute air humidity.

A simple resistor bridge circuit provides a voltage output range corresponding to absolute humidity in the range of 0 to 0.13 kg (water)/m^3 of air at 60 °C [140 °F]. Calibration is performed by placing the sensor in moisture-free air or nitrogen and adjusting the output to zero. Absolute humidity sensors are very durable, operate at temperatures up to 300 °C [575 °F] and are resistant to chemical vapors by virtue of the inert materials used for their construction (i.e., glass, semiconductor material, high-temperature plastics, or aluminum).

3.7 *In Situ* Water Flux Measurement

It is extremely difficult to directly measure fluxes within a porous medium, so water fluxes usually are inferred from point measurements of water potential obtained from different locations, from which a gradient of water potential may be estimated. With knowledge of the hydraulic properties of the porous medium, Darcy's law can be applied to estimate water flux. There are two methods, however, for directly measuring water fluxes.

A water flux meter is simply a version of the passive capillary sampler (discussed in Section 3.3.4) without water sampling capabilities. A heat pulse sensor determines water flux from the temperature response following application of a heat pulse; moving water carries heat, which changes the temperature response.

3.7.1 Water Flux Meter

Water flux meters are typically used in an unconsolidated medium, such as soil or sediment. Water flux meters use a conical collector (filled with the native medium) to intersect flow from a predetermined area. The flow converges into the funnel, which is filled with a fiberglass wick that is capable of applying capillary suction. Water flux is measured directly by placing a transducer

at or near the distal end of the wick. The top 15 cm [6 in] of the wick material is separated into single strands, which are used to line the interior of the collector. A thin layer of diatomaceous earth is placed in the bottom of the funnel above the wick to prevent overlying material from filtering through the funnel and the wick. The wick, which extends vertically 60 cm [2 ft] below the collector, is analogous to a hanging water column applying a suction of 60 cm [2 ft] at the base of the collector. Figure 3-38 shows a cross-sectional view of a typical water flux meter with divergence control.

3.7.2 Heat Pulse Sensors—Water Content, Thermal Properties, and Water Flux

The dual probe heat pulse method was first proposed by Campbell, et al. (1991) for measurement of water content from volumetric heat capacity, which is linearly related to volumetric water content. Campbell, et al. (1991) proposed a sensor with two parallel hollow tubes. One tube contained a thermocouple and the other contained an enamel-coated

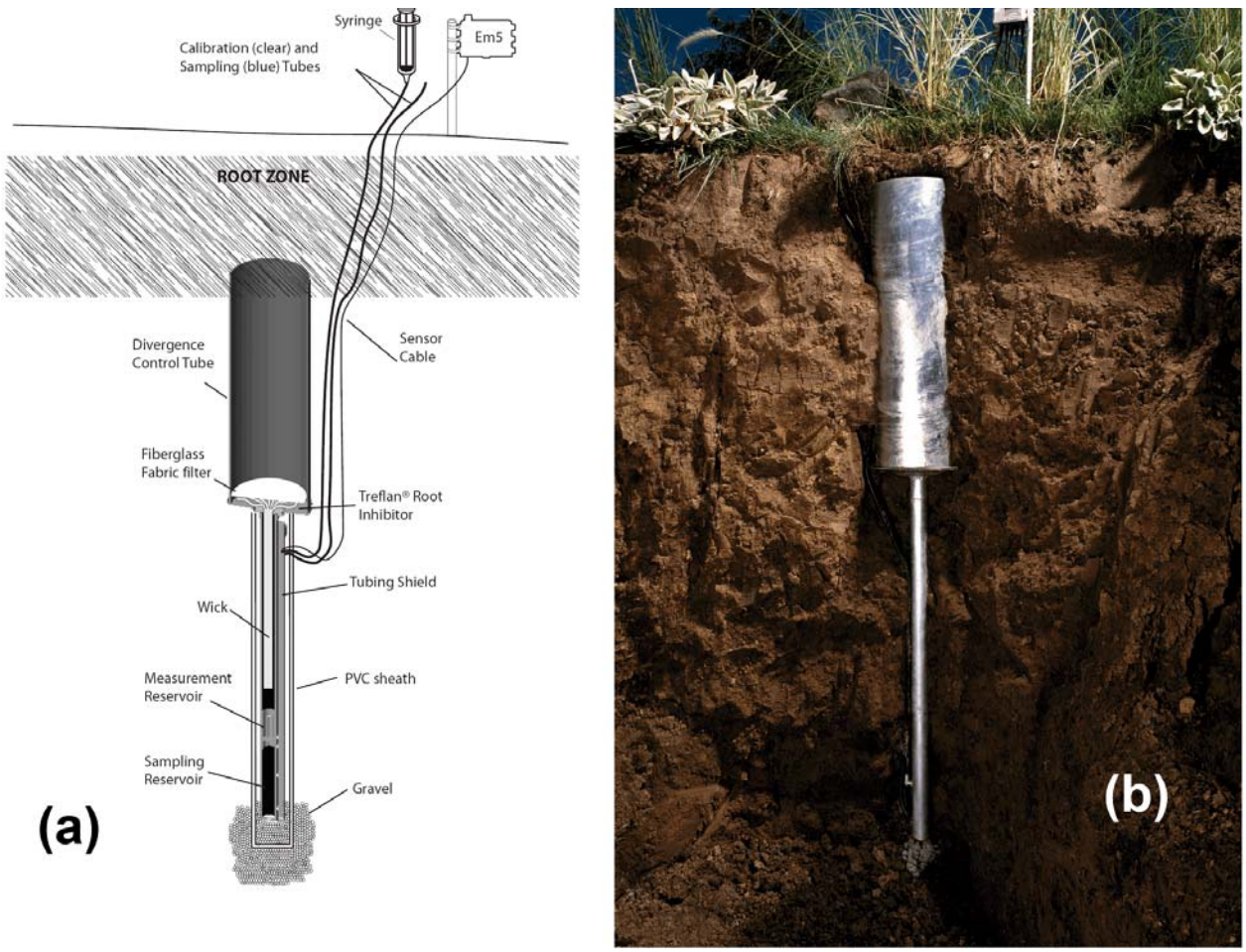

Figure 3-38. Water Flux Meter Proposed by Gee, et al. (2005): (a) Flux Meter Design, and (b) Field Installation [(a) Reproduced With Permission From Decagon Devices, and (b) Courtesy of Decagon Devices. Photocredit: phtoboy.biz; Reproduced With Permission From Decagon Devices]

resistance wire used to introduce a heat impulse as illustrated in Figure 3-39. Considering the sensor as an instantaneous and infinitely long thermal line source in an isothermal, homogeneous medium, they developed an expression that relates the maximum temperature rise measured at the probe and volumetric heat capacity of the medium

$$\rho C = \frac{q}{e\pi r^2 T_m} \tag{3-33}$$

where

ρC	—	volumetric (bulk) heat capacity (J m^{-3} C^{-1})
q	—	heat input per unit length of heater (J m^{-1})
e	—	base of natural log [2.71828]
r	—	radial distance from the heat source (m)
T_m	—	maximum temperature rise (°C) observed at r

In practice, r may be considered as an apparent spacing rather than the geometrical probe spacing, and r may be determined from measurements in a medium of known heat capacity. Hence, only measurement of T_m is needed to calculate ρC if q is known, Knight and Kluitenberg

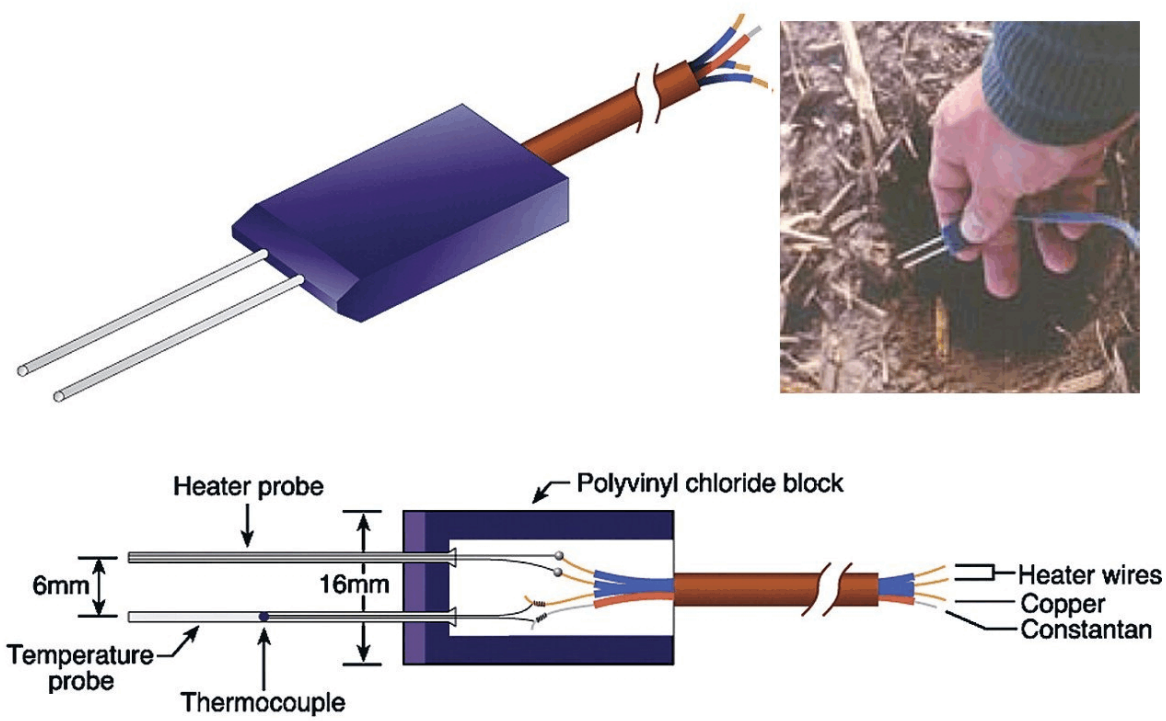

Figure 3-39. Dual Probe Heat Pulse Sensor: Design and Field Installation [Reproduced From Heitman, et al. (2003) With Permission]

(2004) presented an expression for heat capacity that offers the advantage of considering the time interval of heating:

$$\rho C = \frac{q}{e\pi r^2 T_m}\left[1+\frac{\varepsilon^2}{8}\left[\frac{1}{3}+\varepsilon\left(\frac{1}{3}+\frac{\varepsilon}{8}\left\langle\frac{5}{2}+\frac{7\varepsilon}{3}\right\rangle\right)\right]\right] \tag{3-34}$$

where

ε	—	t_o/t_m
t_o	—	duration of the heat pulse
t_m	—	time from the initiation of heating to the occurrence of the maximum temperature rise

Campbell, et al. (1991) also suggested that measurements of ρC might be useful for measuring water content. Assuming that the heat capacity of the gas phase is negligible, ρC becomes a weighted sum of the heat capacities of the water and solid constituents, yielding (Knight and Kluitenberg, 2004)

$$\theta_v = \frac{\rho C - \rho_b C_s}{(\rho C)_W} \tag{3-35}$$

where

ρ_b	—	bulk density of the solid constituents
C_s	—	specific heat capacity of the solid constituents
$(\rho C)_W$	—	volumetric heat capacity of water.

Equation (3-35) assumes that bulk density and solid specific heat capacity remain constant.

Ren, et al. (2000) introduced an application of the heat pulse method for estimating water flux density in a porous medium. The operational expression developed by Wang, et al. (2002) relates steady-state temperature differences between locations upstream and downstream of a heat source to the steady water flux density, J_w

$$J_w = \frac{2(\rho C)\alpha}{(\rho C)_w (r_d + r_u)} \ln\left(\frac{T_d}{T_u}\right) \tag{3-36}$$

where

α	—	porous medium thermal diffusivity (m^2/s)
r_u, r_d	—	upstream and downstream distances from the heat source
T_u, T_d	—	upstream and downstream measured temperatures

In theory, the expression is suitable for fluxes in the range of 0.1 to 5.0 m/day. Thermal dispersion should be considered for high water fluxes. Current methods can reliably determine temperature differences of approximately 0.01 °C, implying that this method cannot observe water fluxes less than 0.06 m/day (Mori, et al., 2003). Mori, et al. (2003) performed a series of

tests using the method, with results that suggest the method may not be reliable for unsaturated conditions but may perform better for saturated conditions, perhaps in part because higher fluxes were tested under saturated conditions.

3.8 *In Situ* Gas Flux Measurement

The primary methods for gaseous measurements within porous media include direct pore air sampling at different depths (Buyanowski and Wagner, 1983) and laboratory analysis of core samples (Cortassa, et al., 2001). Measurements of surface CO_2 flux are typically based on the "closed-chamber method," whereby surface flux is determined from changes in gas concentration within an enclosed volume on the ground surface (de Jong, et al., 1979; Cropper, et al., 1985; Drewitt, et al., 2002). Portable devices such as the Li-6400 systems by Li-COR Biosciences (shown in Figure 3-40) are capable of measuring soil CO_2 fluxes using high accuracy research-grade instrumentation (Dugas, 1993).

Among the primary limitations of soil chamber measurements are the lack of continuous observations, manual setup, and impact on surface boundary conditions that could alter the nature of the diffusive flux (Davidson, et al., 1998). Attempts to improve temporal coverage (de Jong, et al., 1979; Cropper, et al., 1985; Freijer and Bouten, 1991) by continuous air pumping from the enclosure to a gas analyzer resulted in significant alteration of the ground surface boundary conditions due to variations in air pressures within the chamber (Lund, et al., 1999) and perturbation of natural conditions at the surface (e.g., gas concentration gradients, precipitation, radiation).

Recently, automated surface chamber designs have been proposed for capturing short-term changes in soil respiration. Such systems were developed for customized experiments (Ambus and Robertson, 1998) or by specialized companies (i.e., the LI-8100 system by Li-COR Biosciences, Lincoln, Nebraska). However, these quasi-continuous systems still present short-time surface boundary-condition changes and biases due to air pumping and short-time pressure differences between soil and the chamber, and are difficult to calibrate. Moreover, surface chamber measurements only consider surface CO_2 fluxes without measuring subsurface CO_2 fluxes. The need for accurate determination of soil CO_2 flux and associated concentration profiles for extended periods is widely recognized as key to reliable integration of total CO_2 exchange between soil and the atmosphere (Ouyang and Boersma, 1992).

3.9 Sensor Pairing for *In Situ* Characterization and Monitoring

Certain characterization and monitoring activities rely on multiple sensor measurements within the same volume of medium. This is particularly important for *in situ* determination of various transport properties, such as hydraulic conductivity and liquid retention characteristics, and for continuous monitoring of fluxes.

Sensor pairs, such as time domain reflectometry probes and tensiometers, may be used for simultaneously determining water content and matric potential within the same volume. The limitations of most sensor pairing techniques stem from (i) differences in the volumes sampled by each sensor (e.g., large volume averaging by a neutron probe versus small volume averaging by a heat dissipation sensor or psychrometer); (ii) different equilibration times for each sensor (e.g., many *in situ* water content measurement methods are instantaneous but matric potential sensors require time for equilibrium, so that the two measurements may not be indicative of the

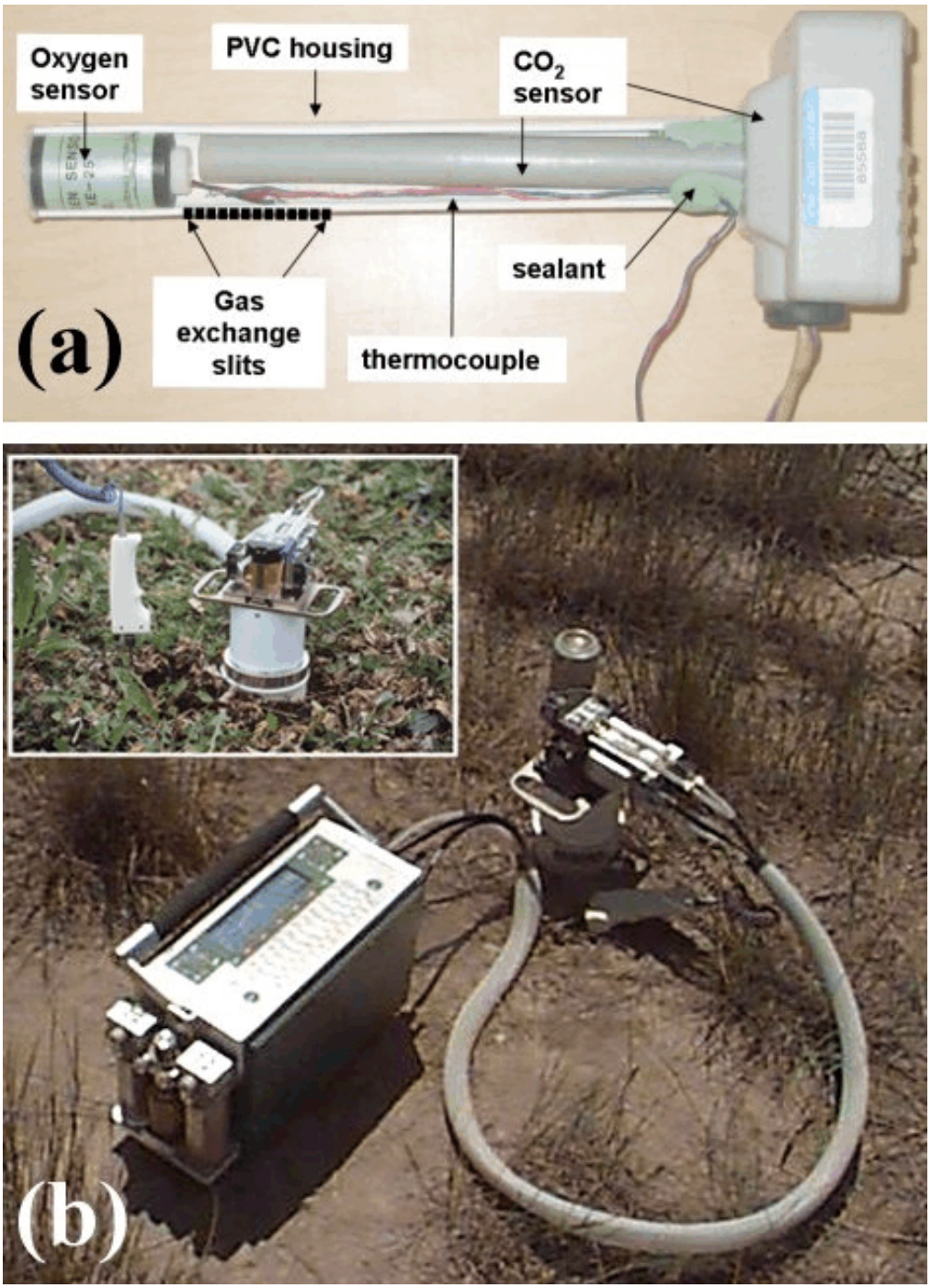

Figure 3-40. Gas-Flux Sensors: (a) Detailed View of Gas-Flux Sensor Arrangement With CO_2 and O_2 Sensors [Turcu, et al. (2005)], (b) Gas Flux Measurement System Li-8500 with Special Surface Chamber (See www.licor.com/env/ for System Description), and (Inset) a Thermocouple Inserted in the Soil Profile [(a) Reproduced From Turcu, et al. (2005) With Permission; Photographs in (b) by D. Or]

same conditions); (iii) limited parameter ranges; and (iv) deteriorating sensor accuracy, often resulting in limited overlap in retention information and interpretation difficulty due to measurement errors within the range of overlap (Or and Wraith, 1999).

A visual summary of the methods available for matric potential measurement and their range of application is presented in Figure 3-41. The figure illustrates that most available techniques have a limited range and many ranges do not overlap. Some of the methods shown in Figure 3-41 are laboratory methods unsuitable for *in situ* field applications. In addition, various methods and combinations of sensor pairs have widely variable accuracy, adding to the complexity of data interpretation.

The Performance Confirmation Plan suggests that DOE will rely on highly variable and strongly nonlinear transport properties to estimate some quantities of interest. For example, the Plan suggests that deep percolation flux and gaseous fluxes will be estimated using unsaturated hydraulic conductivity and the unsaturated gaseous diffusion coefficient, respectively. The use of such parameters may lead to highly unreliable estimates. For example, Hubbell, et al. (2004) estimated downward liquid flux in the deep vadose zone {30 to 70 m [98 to 230 ft]} using the Darcian approach, combining *in situ* water potential measurements with laboratory estimates for unsaturated hydraulic conductivity, but the estimates were hindered by large uncertainty in the

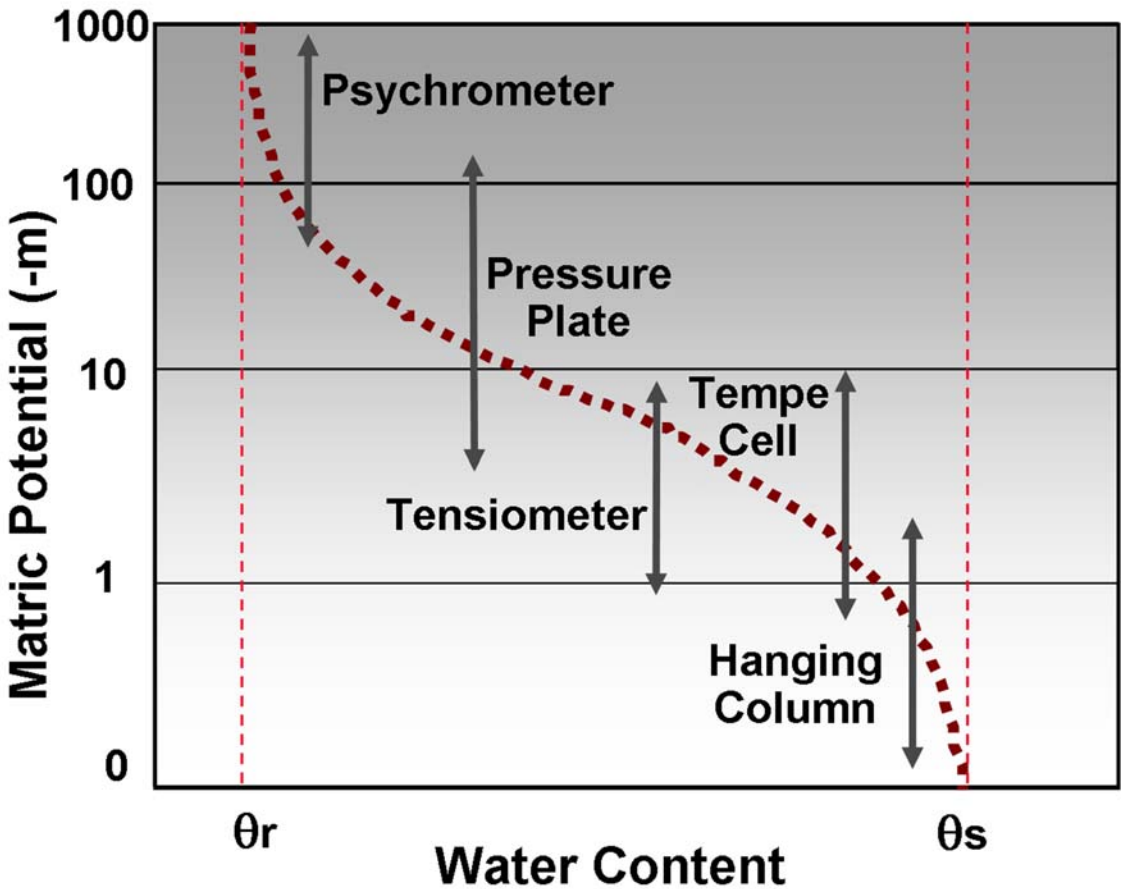

Figure 3-41. The Effective Measurement Range of Commonly Used Matric Potential Measurement Methods

values of unsaturated hydraulic conductivity. Even though the existence of a unit hydraulic gradient in the formation was confirmed by remarkably stable tensiometer data over nearly 30 months, flux estimates (shown in Figure 3-42) ranged over four orders of magnitude. The highest flux value was approximately 500 times the mean precipitation of 22 cm/yr [8.7 in/yr]. It is anticipated that techniques based on transport properties may feature improved flux estimates using *in situ* characterization of the transport properties. *In situ* characterization of transport properties invariably relies on use of sensor pairs for repetitive and non-destructive measurements of properties and dynamics within the same volumes of a porous medium. The following are typical examples:

- Figure 3-43 shows an experimental set-up using time domain reflectometry probes in close proximity to tensiometers for concurrent measurement of water content and matric potential dynamics (with plant root uptake in this experiment). The information is used to delineate an important region of the water characteristic curve *in situ* {albeit in the narrow range of matric potentials from 0 to −10 m [0 to −33 ft]}.

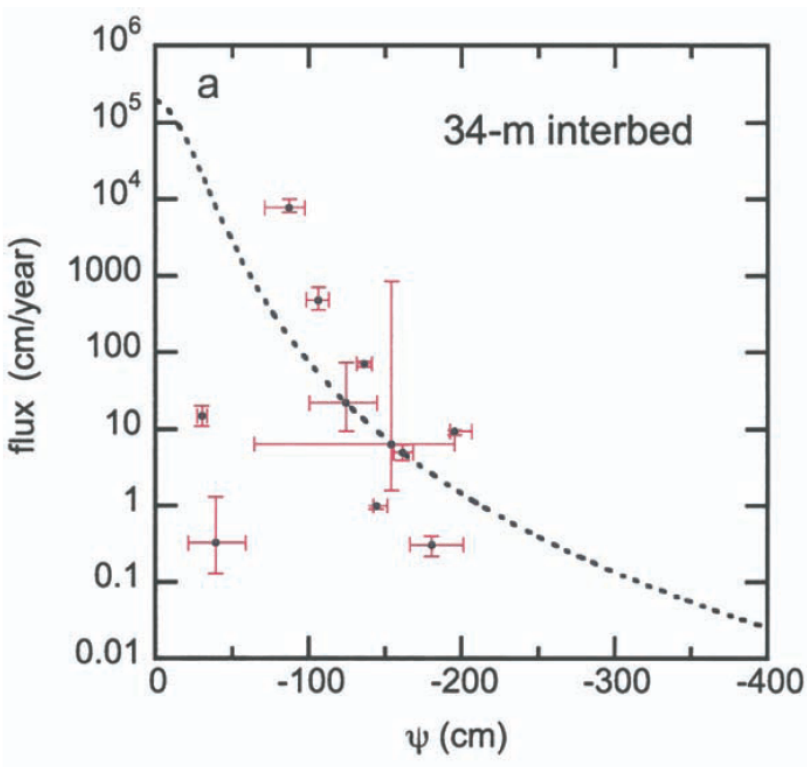

Figure 3-42. Vertical Flux Estimates from a Site in Idaho Exhibiting a Unit Gradient. Horizontal Bars Represent the Range of Water Potentials Measured at a Location, With the Solid Dot Placed at the Mean. Vertical Bars Represent the Range of Hydraulic Conductivity *K*(ψ) Estimated From Those Values. The Dashed Lines Represent the Generic Curves Developed in Earlier Studies (Hubbell, et al., 2004). [Reproduced From Hubbell, et al. (2004) With Permission]

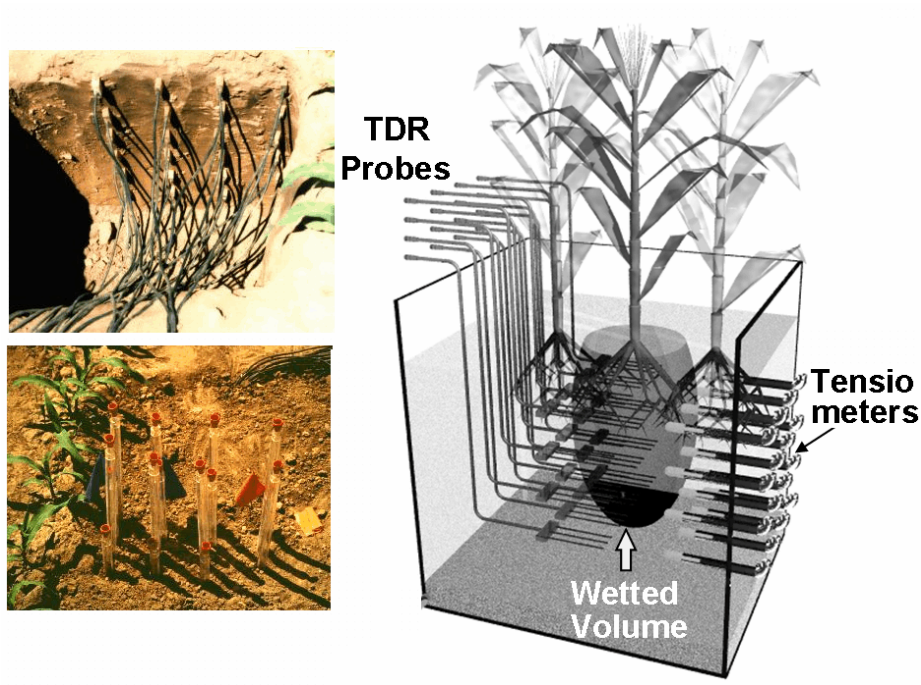

Figure 3-43. Time Domain Reflectometry Probes and Tensiometers Combined to Continuously Monitor Soil Water Dynamics in the Plant Root Zone [Photographs by D. Or]

- Similar sensor pairing methodology may also be used for monitoring percolation fluxes and *in situ* determination of unsaturated hydraulic conductivity using the so-called instantaneous profile method. Figure 3-44 illustrates typical spatial and temporal data obtained from sensor pairs (neutron probe and tensiometers) that is subsequently used to deduce the unsaturated hydraulic conductivity from a transient water flow experiment by the instantaneous profile method.

Figure 3-42 illustrates the inherent noise associated with field data, and the resultant need for averaging and integration to obtain quantities sufficiently reliable for flow parameter estimation. In addition to limited and non-overlapping measurement ranges of different sensors (e.g., Figure 3-41), experimentalists often encounter data with nonuniform error structure such as obtained from psychrometer measurements (where errors vary with water potential range). Differences in automation potential and in sampling intervals required for different sensors (rapid tensiometer sampling versus slow neutron probe measurements) complicate matters. These issues of range, error, and sampling interval compatibility become particularly important for extended monitoring periods.

In summary, each of the issues related to single-sensor accuracy are present when using multiple sensors. The use of multiple sensors to determine a quantity creates additional issues about the accuracy and representativeness of the desired quantity, because (i) the sensors typically have significantly different characteristics that may strongly affect data interpretation, and (ii) the likelihood of sensor deterioration is proportional to the number of sensors used.

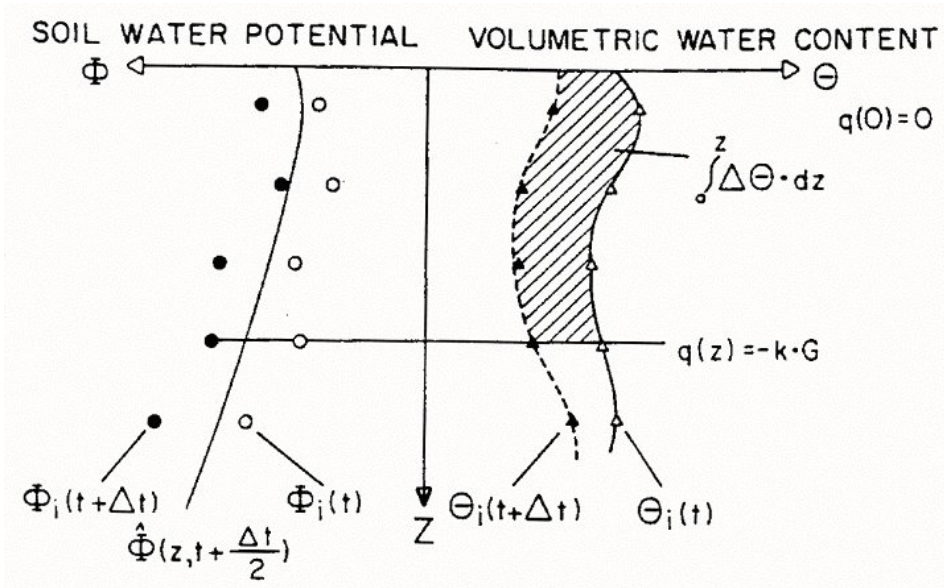

Figure 3-44. The Instantaneous Profile Method for Measurement of Hydraulic Conductivity *In Situ* Using Concurrent Measurements of Water Content and Matric Potential From Sensor Pairs [Reproduced From Flühler, et al. (1976) With Permission]

3.10 Characterization and Monitoring in the Vadose Zone

The measurement and characterization methods reviewed in this section use diverse operating principles and have widely varying sensitivities and accuracies. Vadose zone measurement methods are most commonly used for applications such as water management (agricultural), estimating recharge (hydrology and water resources), pollution mitigation and remediation (environmental), and infrastructure monitoring (geotechnical). These applications usually consider shallow vadose zone processes in unconsolidated material. Each of these applications feature (i) a relatively short duration for continuous use (days to months), (ii) ready accessibility for data retrieval and servicing, and (iii) relatively simple replacement and upgrading. The current generation of technology reflects these application fields, thus the most mature technology is designed for relatively short-term use in near-surface soils or sediments. Hard and fractured rock is inherently more difficult to access and instrument than unconsolidated material; however, technology applied in hard and fractured rock is usually modified from methods first proven in shallow unconsolidated materials.

Characterization activities typically require intensive sampling and observations for a relatively short period of time, using equipment that is highly sensitive to the measured quantities. Ongoing characterization of the potential repository at Yucca Mountain has used current technology, and in principle more of the reviewed techniques may be modified for characterization studies in hard and fractured rock. Specific examples where current technology could be adapted for characterization in fractured rock are discussed in Section 4. It is reasonable to expect that the normal pace of technological development will produce enhanced sensors and methodology for the shallow subsurface that may be adapted to hard and fractured rock, even if such applications are not the primary driver for sensor development.

Monitoring activities may have different objectives than characterization activities. Monitoring activities may require reliable, robust sampling over many years with little or no maintenance, but these attributes were not a priority in developing the current generation of characterization technology. Indeed, sensitivity and robustness are often conflicting design parameters. Reliability and robustness become even more important when monitoring the near field of a hot repository, because the equipment would be placed in a harsh environment with little or no opportunity for maintenance and upgrading. Market forces have produced relatively reliable and robust sensors in areas that are important to industry, such as temperature and humidity sensors, and these market forces would presumably continue to operate. However, it is not clear that most current technology used to measure properties of porous media can be easily adapted to achieve monitoring goals, even in relatively benign environments far from the near field of a hot repository. It is doubtful that market forces will emphasize development of reliable, robust monitoring technology that can withstand the harsh conditions typical of the near field of a hot repository.

It appears fair to conclude that relatively short-term characterization activities under ambient conditions in both unconsolidated media and fractured rock are supported by current technology or straightforward modifications of current technology, and it is likely that commercial sensor development will continue to improve sensors for characterization activities. It is also fair to conclude that long-term monitoring activities are not well supported by commercially available technology. It is clear that sensor choices are far more restricted under harsh near-boiling conditions, even for short-term studies. Furthermore, it is not clear that market forces are acting to dramatically improve sensor longevity and robustness, nor is it clear that market forces will provide sensors that can withstand near-field conditions.

4 EXAMPLE APPLICATIONS USING CURRENT TECHNOLOGY

There are a wide variety of vadose zone processes that occur at a geologic repository that may require characterization and monitoring, but the deep percolation flux passing through the repository horizon is one of the most fundamental hydrologic quantities affecting repository performance. Several representative approaches to estimating deep percolation flux are discussed in Section 4, demonstrating how currently available technology might be used for characterization or monitoring activities at a hypothetical geologic repository. The first example illustrates how applied tracers might be used to quantify fluxes, lateral diversion, and fast pathways within the vadose zone. The second example illustrates how current technology might be used to quantify water fluxes in the shallow subsurface.

4.1 Tracers and Fractured Rock

The period of atmospheric atomic testing provided an unexpected benefit to environmental science. As a result of atomic testing, radioactive materials entered the subsurface during precipitation, providing an unmistakable bomb-pulse signature that has helped (i) differentiate pre-bomb-pulse waters from post-bomb-pulse waters and (ii) fingerprint fast pathways through the subsurface. However, the bomb-pulse signature was derived from application over an extended period of time, and background levels of cosmogenically produced radionuclides make it difficult at times to interpret observations.

An improved signature can be obtained by marking surface water with periodic applications of environmentally benign tracers with negligible background concentrations. Controlled tracer application is a relatively simple and inexpensive procedure that allows the age of waters to be precisely dated deep in the geologic profile. A sampling network installed at depth may be used to identify tracer pulses via pore water extraction methods, allowing deep percolation rates to be quantified and the presence of preferential flow paths to be identified. Fiber optic methods may be an alternative to pore water extraction in the near future.

Applied tracers can also be used to identify and quantify lateral flow in the natural environment. Long-term tracer studies can identify lateral flow if several zones along a transect receive different tracers. The presence of a tracer outside of the application zone would strongly suggest that lateral diversion is occurring. The distance between an observation of the tracer and the application zone gives a minimum estimate for diversion distance. A better estimate could be derived by using several observation locations, or by applying different tracers at different distances from an observation location.

In general, tracer solutions for vadose zone hydrological studies can be applied to the soil surface or directly injected into the soil or rock, depending on the specific purpose of the tracer experiment.

4.1.1 Tracers

Long-term monitoring of deep percolation would be enhanced if a suite of tracers of different chemical composition were applied to the ground surface. A series of clearly distinguishable pulses would result from well-separated tracer applications (e.g., at intervals of 5 to 10 years), and each individual application would be clearly differentiated if a different tracer was used for

each application. Systematic marking of shallow subsurface water provides an excellent way of dating deep water, which is extremely useful in identifying water velocity.

Desirable characteristics for tracers include:

- Conservative and nonreactive movement (e.g., similar to water)
- Minimal background concentrations, so that signals may be clearly distinguished
- Insensitivity to changes in pH, alkalinity, or ionic strength of the aqueous solution
- Detectability by chemical analysis or visual observation (e.g., dyes)
- Minimal biological and chemical impact, so that the study environment is not damaged

Comprehensive reviews compiled by Drew (1968), Knutsson (1968), Käss (1998), and Flury and Wai (2003) suggest, in light of the desirable characteristics listed above, that stable isotopes (^{2}H, ^{13}C, ^{15}N, ^{18}O, and ^{34}S), ethanol, benzoate, and fluorobenzoates are useful tracers.

Deuterium ($^{2}H_2O$) at low concentrations is considered an ideal aqueous tracer; however, like most other stable isotopes, sophisticated instrumentation is required for chemical analysis and quantification.

Malcolm, et al. (1980) conducted a series of recharge and injection experiments using ethanol and benzoate as tracers; they found that both tracers mimicked the conservative, non-sorbing character of bromide. Malcolm, et al. (1980) recommended benzoate as a groundwater tracer due to its high sensitivity to spectrophotometry. Benzoate and benzenesulfonic acids have been used as geothermal groundwater tracers (Adams, et al., 1989). A variety of fluorinated benzoate compounds proposed as tracers (Stetzenbach, et al., 1982; Bowman, 1984; Bowman and Gibbens, 1992) are shown in Figure 4-1. Bowman (1984) and Bowman and Gibbens (1992) compared the performance of the benzoate tracers (using bromide as a reference tracer), finding that each benzoate tracer exhibited negligible sorption to the soil and aquifer materials in laboratory column tests, and the mobility of the benzoates mimicked that of bromide. However, some of the benzoate tracers appeared to degrade under field conditions. On the basis of their resistance to degradation, Bowman and Gibbens (1992) ranked the fluorobenzoates shown in Figure 4-1 in the following order, with PFBA being the best tracer:

- PFBA
- 2,6-DFBA
- 2,3-DFBA, 2,5-DFBA, 3,4-DFBA, and 3,5-DFBA
- o-TFMBA
- m-TFMBA

Sorption and transport of the benzoate tracers depends on pH, because these tracers contain a carboxylic acid group. The pK_a values for these tracers are relatively low (pK_a is $-\log K_a$, where K_a is the equilibrium constant for acid dissociation), so that under most environmental conditions the tracers should be predominantly negatively charged. Results from sorption and transport experiments indicate that benzoate tracers behave conservatively as long as the pH of the pore

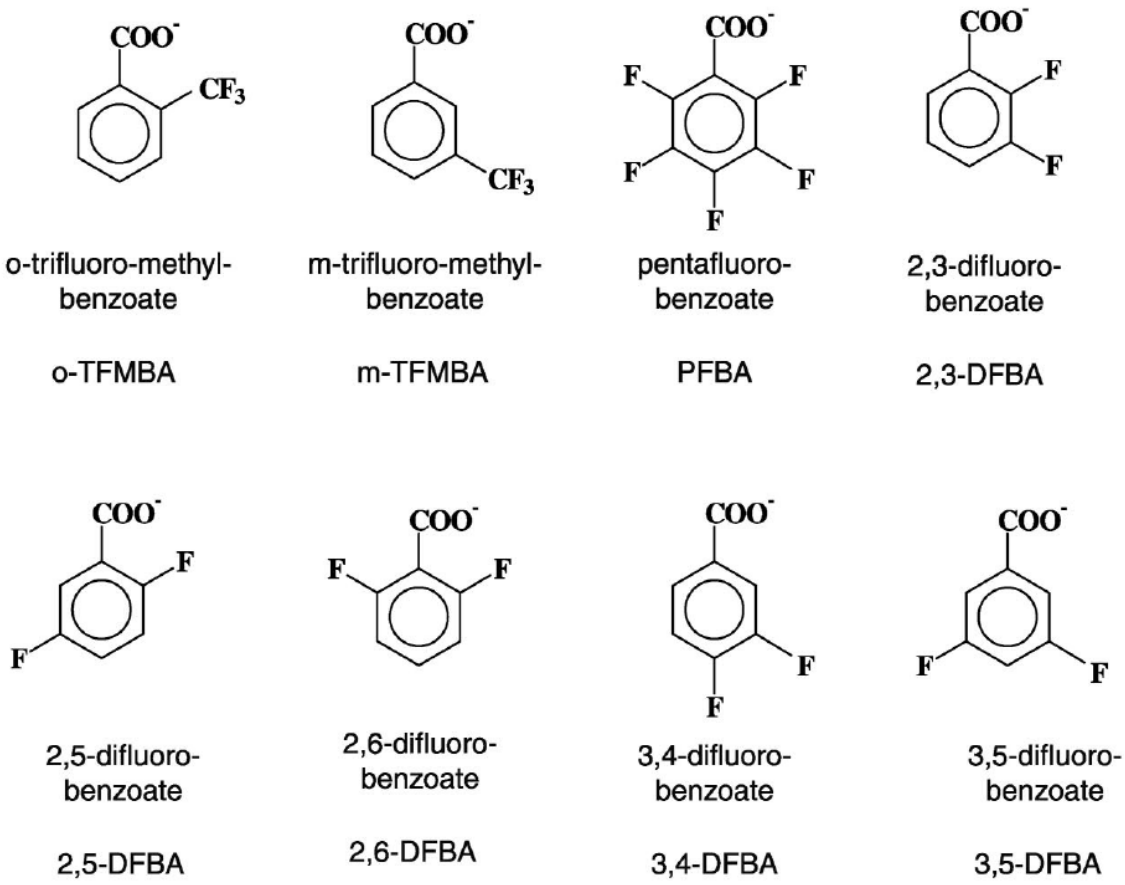

Figure 4-1. Fluorobenzoate Tracers [Reproduced From Flury and Wai (2003) With Permission]

solution remains about two pH units above the pK_a of the tracer (McCarthy, et al., 2000). Flury and Wai (2003) found that benzoate and fluorobenzoates migrate similarly to bromide under most pH conditions found in soils and aquifers, but mobility usually decreases under low pH conditions. Because sorption and transport of fluorobenzoates can be affected by organic carbon, clay, and Fe-oxide content, it is useful to evaluate the tracer behavior with sorption or column tests before running field experiments where these compounds may occur.

4.1.2 Measurement and Sampling in Fractured Rock

Tracer sampling is particularly difficult within unsaturated fractured rock masses. Usually sampling occurs within small-diameter boreholes drilled into the host rock. Two issues must be considered: One, how is the tracer extracted from unsaturated rock, given that water does not enter a cavity under unsaturated conditions? Two, is a sample location more representative of matrix conditions or fracture conditions?

Absorber methods are the most reliable current technology for obtaining tracer samples. As described in Section 3.3.5, it is important to ensure that absorber elements maintain contact with the borehole wall to avoid evaporative concentration of the tracer, which leads to erroneous

concentration estimates. Contact is assured by pressing the absorbers to the borehole wall using inflatable packers, as illustrated in Figure 4-2. Continuous monitoring of gas pressure in the packers and absorbers allows detection of gas leakage. The absorbers are removed after a pre-determined time interval, and analyzed for the tracer. Other absorber placement techniques, such as those outlined in Section 3.3.5, could be modified and applied. The next generation of sampling technology may replace absorbers with procedures for directly measuring tracer concentrations. For example, fiber optic spectrometry (see Section 3.4.3) offers the potential to enable direct measurement of tracer concentrations at the borehole walls.

Sections of the borehole that contain fractures can be determined from core analysis or video imagery, but these methods cannot distinguish between fractures that are connected to a larger network and fractures that dead-end. Gas permeameter testing provides a straightforward method for finding sections of a borehole with fractures connecting to a larger fracture network. A small section of the borehole can be isolated with inflatable packers and pressurized with a gas such as N_2, as shown in Figure 4-3. Gas permeability can be calculated from measured gas flux and the pressure history in the test section. Zones with high gas permeability typically correspond to zones with connected fractures, although some care in interpretation is needed for zones near open cavities.

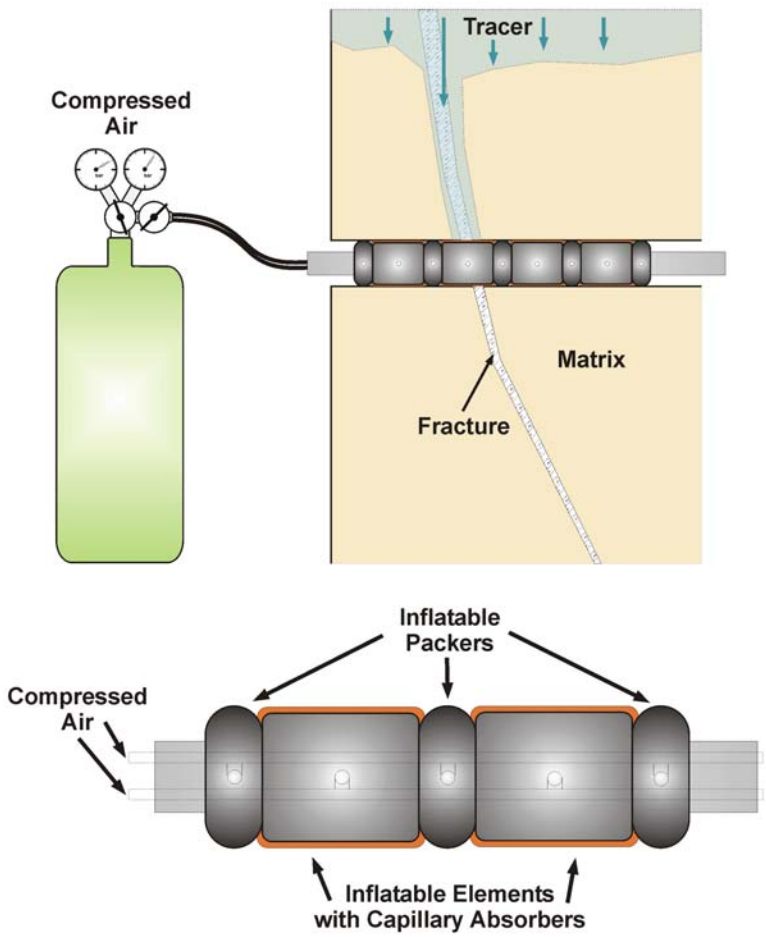

Figure 4-2. Potential Design and Placement of Capillary Absorbers for Solution Sampling From Boreholes

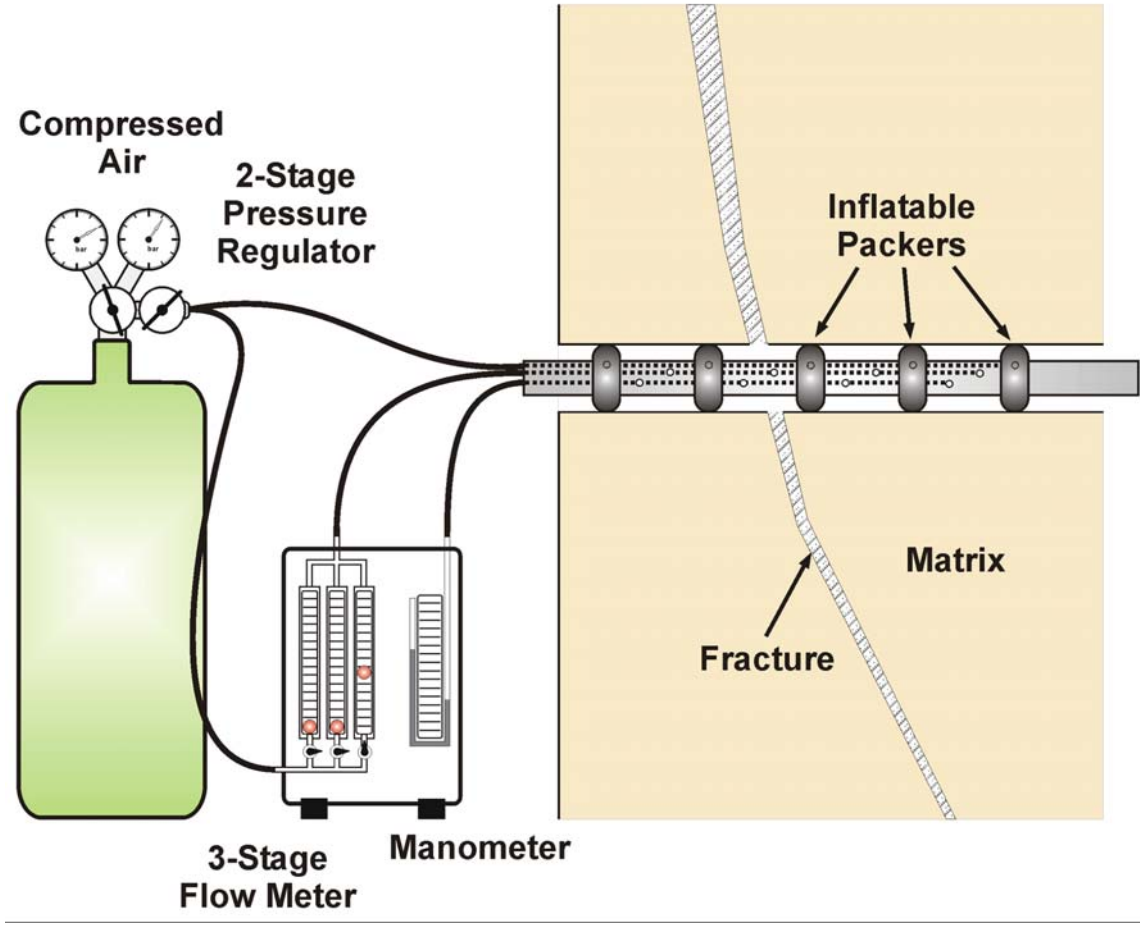

Figure 4-3. A Setup for Gas Permeability Mapping in a Borehole Using Inflatable Packers

4.2 Near-Surface Water Fluxes

Vadose zone measurement technology may be most fully developed in the shallow subsurface (the realm of soil scientists), and several approaches may be taken to quantify net infiltration (the source of deep percolation fluxes in the vadose zone).

Atmospheric flux measurements, which are used as forcing functions in soil water-balance closure models, provide an indirect method for estimating deep percolation flux. The difference between annual precipitation and measured annual evapotranspiration provides an estimate for the annual deep percolation flux in the atmospheric-flux-based method. Direct measurements of actual evapotranspiration are made using a method such as the eddy covariance technique (Massman and Lee, 2002). The error in this estimation method is approximately 20 percent due to limitations in the eddy covariance technique for estimating evapotranspiration; however, the accuracy of this estimate may be increased with the aid of shallow soil water content measurements; for example, by using a neutron probe as illustrated on the right side of Figure 4-4. Errors in atmospheric-flux-based deep percolation estimates supplemented with soil

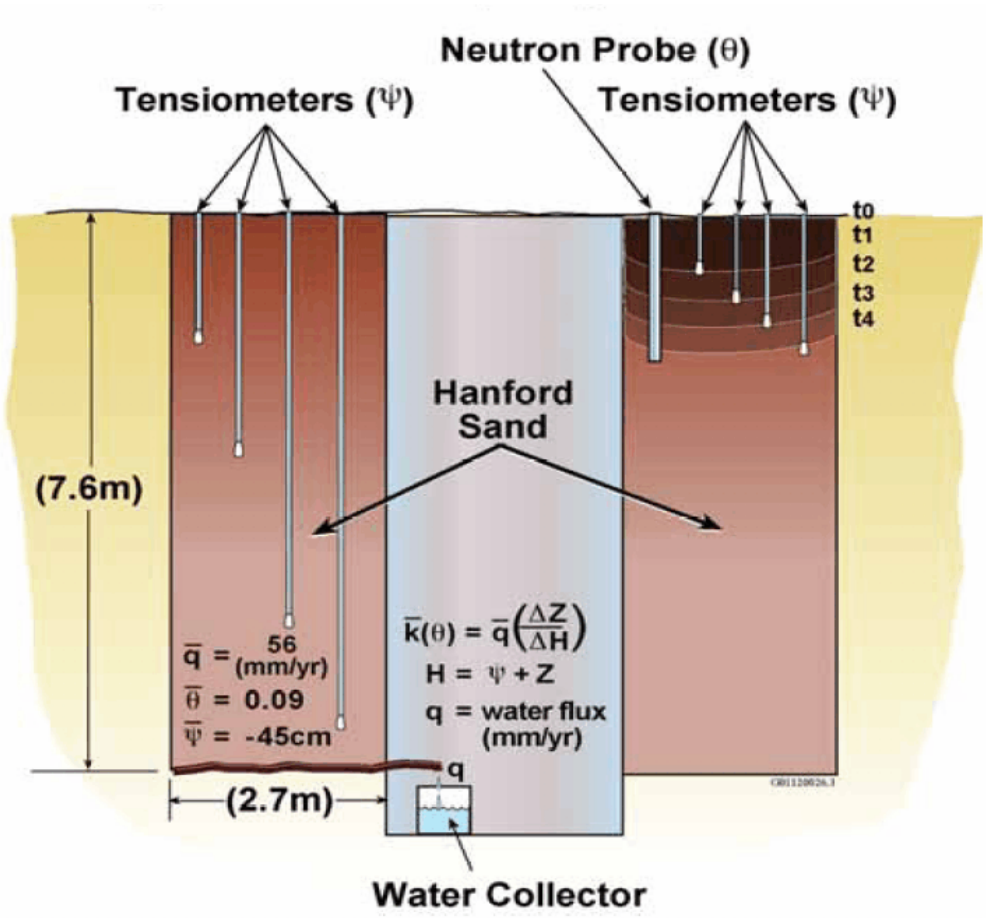

Figure 4-4. Indirect Flux Measurement Using Tensiometers and a Neutron Probe (Right), and Direct Flux Measurement Using Deep Tensiometers and a Lysimeter (Left) [Reproduced With Permission From Glendon Gee]

moisture measurements are approximately 10 percent. Note that evapotranspiration measurements are representative of a larger area than are soil-water measurements; soil-water measurements provide “point” values that may vary considerably with soil type and vegetation cover.

Another near-surface approach for quantifying deep percolation flux relies on monitoring of hydraulic gradients well below the influence of surface processes and plant roots. Monitoring is accomplished with tensiometers (or psychrometers for drier conditions), such as the bank of tensiometers on the right side of Figure 4-4 (Hubbell, et al., 2004). A reliable independent estimate of unsaturated hydraulic conductivity is required to estimate water fluxes using Darcy’s Law, which is a significant limitation to this approach.

Deep lysimeters (hydrologically isolated blocks of soil or rock) overcome the need for a reliable estimate of unsaturated hydraulic conductivity, especially for locations with deep alluvial cover. The left side of Figure 4-4 represents a lysimeter with tensiometers emplaced to monitor the

actual hydraulic gradients within the soil or rock mass in the lysimeter. Psychrometers may be appropriate for drier conditions. Water flux is intercepted and directly measured as drainage from the lysimeter, thus it is not necessary to use unsaturated hydraulic conductivity to estimate fluxes. Installation and maintenance of a lysimeter is expensive, especially in fractured rock, and the accuracy of this method is strongly dependent on the extent of disturbance to the natural hydrological setting.

5 SUMMARY AND RECOMMENDATIONS

The DOE Performance Confirmation Plan (Bechtel SAIC Company, LLC, 2004) documents recent DOE intentions for performance confirmation activities at the potential repository at Yucca Mountain. The Performance Confirmation Plan does not represent a final plan for confirmation activities, and technical details of the activities have not been fully developed. A preliminary review of the Performance Confirmation Plan identified several ongoing and planned future performance confirmation activities that would occur in the vadose zone. All of the planned vadose-zone activities are identified as occurring in facilities at the repository horizon. By implication, all characterization and monitoring activities in the vadose zone during performance confirmation will use sensors emplaced in fractured rock (most likely within boreholes drilled from the repository) or cavities in the rock (e.g., drifts, niches, and alcoves). Many of the sensors used for performance confirmation will experience elevated temperatures in the thermally accelerated drifts used to mimic postclosure conditions, where access for maintenance and upgrades may be severely restricted.

5.1 Summary of Measurement Technology

The activities listed in the Performance Confirmation Plan suggest that DOE may wish to use sensors for measuring water content, matric potential, temperature, relative humidity, and water and gas fluxes, and DOE may also wish to obtain pore water for additional analyses. The current state of the art in sensor technology for these applications is reviewed in this document in order to provide baseline information on the suite of sensors that are available for characterization and monitoring activities in the vadose zone.

The widest variety of approaches are brought to bear on obtaining water content, taking advantage of the distinct physical, electrical, and thermal properties of liquid water compared to air and solid grains. Most of the techniques take advantage of the large dielectric constant of liquid water relative to air and solid grains, using an electromagnetic pulse or wave to estimate bulk dielectric constant, but the neutron-scattering and heat-pulse methods probe the system using a radioactive source and a heat source, respectively. Fiber optic sensors probe the system with light. Dielectric and electric measurement methods may be applied in a direct and an indirect way. The direct method makes measurements in a calibrated engineered porous medium that is in equilibrium with the natural medium, while sensors in the indirect method interrogate the natural medium without benefit of a direct calibrated relationship between water content and the sensed quantity.

Matric potential is also determined with a variety of methods. Tensiometers are the most direct method for obtaining matric potential, but only work under relatively wet conditions. Heat dissipation and electrical resistivity sensors probe water content in an engineered porous medium in equilibrium with the bulk medium, using a thermal or electrical signal; the relationship between the signal and matric potential is calibrated before sensor emplacement. Psychometers measure relative humidity instead of water content, using an equilibrium relationship between matric potential and vapor density. No single method works over the entire range of potentials that may be observed in the field.

Pore water samples are difficult to obtain from the vadose zone, as water is held within the pore space by capillary forces. Sampling techniques induce a gradient in matric potential (e.g., through vacuum extraction, hanging wicks, or pressing a dry medium to the bulk medium)

to draw out the pore water. Solute concentrations can also be obtained by allowing a known quantity of distilled water to come to equilibrium with the bulk solution. Obtaining samples can be time-consuming, leaving laboratory extraction from samples as the alternative under dry conditions.

Temperature sensors infer temperature from the known response of an engineered component to temperature. Thermocouples measure temperature differences by generating voltage from dissimilar metals subjected to the same temperature difference. Resistance temperature detectors and thermistors relate the change in electrical resistance to temperature. Fiber optic sensors use the decay time of a phosphor after excitation from a light-emitting diode to estimate temperature.

Some relative humidity sensors (psychrometers and chilled mirror hygrometers) use the difference between ambient temperature (dry bulb temperature) and the temperature at which water vapor evaporates (wet bulb temperature) to estimate relative humidity. Capacitive and resistive humidity sensors relate changing electrical properties to relative humidity. Thermal conductivity sensors compare the thermal response of a reference gas and the ambient gas to estimate absolute humidity, from which relative humidity is obtained by comparison to the known response of saturated absolute humidity to temperature.

Direct *in situ* measurement of water flux is extremely difficult, especially in the vadose zone. A water flux meter can be used in an unconsolidated medium, using a hanging wick at the bottom of a funnel to induce a water potential unit gradient that pulls water through the funnel. Heat pulse sensors estimate water fluxes based on differential thermal responses at probes surrounding a heat source.

Direct *in situ* measurement of gas-species flux is even more difficult. Current practice within a porous medium infers fluxes from point concentration measurements and a diffusion coefficient that depends on water content. Fluxes across an interface between a medium and the atmosphere are quantified using the closed-chamber method, which quantifies flux by using the change in concentration within the chamber, but the presence of the measurement device has been found to significantly alter the flow fields being measured.

5.2 Discussion

The current state of the art in vadose-zone measurement methods is dominated by characterization applications from the shallow subsurface. Vadose-zone measurement methods are most commonly used for applications such as water management (agricultural), estimating recharge (hydrology and water resources), pollution mitigation and remediation (environmental), and infrastructure monitoring (geotechnical), all of which tend to consider shallow vadose-zone processes in unconsolidated material. These applications tend to feature (i) a relatively short duration for continuous use (days to months), (ii) ready accessibility for data retrieval and servicing, and (iii) relatively simple replacement and upgrading—current sensor technologies for characterization do not emphasize long-term maintenance-free operation. The current generation of technology reflects these fields of application, and is generally designed for relatively short-term use in near-surface unconsolidated porous media under ambient temperatures. Some of the technology is used in a wider context, such as temperature and relative humidity sensors that may be used for long-term monitoring, and in these fields market forces have provided sensor technology that is more robust and requires less maintenance.

Hard and fractured rock is inherently more difficult to access and instrument than unconsolidated material, thus technology applied in hard and fractured rock to date is usually modified from methods first proven in shallow unconsolidated environments. Accordingly, the technology applied to hard and fractured rock tends to be less developed than technology intended for unconsolidated media.

Measurement activities occurring in fractured vadose-zone rock under ambient temperatures, with time horizons up to perhaps a few years, may be able to use current technology with little modification as long as appropriate maintenance access is available. It is reasonable to expect that the normal pace of technological development will continue to produce enhanced sensors and methodologies for the shallow subsurface that may be adapted to hard and fractured rock, even if the rock applications themselves do not drive sensor development.

Current technology may not be adequate for some measurement activities with time horizons of years to decades, particularly if maintenance access is not available or elevated temperatures will occur. Sensors adapted from industry, such as temperature and relative humidity sensors, may be relatively robust and reliable under these conditions. Sensors with a less wide-spread applicability, such as water content, matric potential, water and gas flux sensors, and pore water samplers, may require significant further development before the technology is capable of handling extended emplacement, especially under elevated temperatures. As there is a quite limited market for such products, it is reasonable to expect that technological development may only slowly produce enhanced sensors and methodology suitable for these more demanding conditions.

6 REFERENCES

Adams, M.C., W.R. Benoit, C. Doughty, G.S. Bodvarsson, and J.N. Moore. "The Dixie Valley, Nevada Tracer Test." *Geothermal Resources Council Transactions*. Vol. 13. pp. 215–220. 1989.

Adams, F., C. Burmester, N.V. Hue, and F.L. Long. "A Comparison of Column-Displacement and Centrifuge Methods for Obtaining Soil Solutions." *Soil Science Society of America Journal*. Vol. 44. pp. 733–735. 1980.

Alberts, E.E., R.E. Burwell, and G.E. Schuman. "Soil Nitrate-Nitrogen Determined by Coring and Solution Extraction Techniques." *Soil Science Society of America Journal*. Vol. 41. pp. 90–92. 1977.

Alessi, R.S. and G.A. Prunty. "Soil Water Determination Using Fiber Optics." *Soil Science Society of America Journal*. Vol. 50. pp. 860–863. 1986.

Ambus, P. and G.P. Robertson. "Automated Near-Continuous Measurement of CO_2 and N_2O Fluxes With a Photoacoustic Infra-Red Spectrometer and Flow-Through Soil Cover Boxes." *Soil Science Society of America Journal*. Vol. 62. pp. 394–400. 1998.

Andraski, B.J. and B.R. Scanlon. "Thermocouple Psychrometry." *Methods of Soil Analysis Part 4—Physical Methods*. 5th Edition. J.H. Dane and G.C. Topp, eds. Madison, Wisconsin: Soil Science Society of America, Inc. pp. 609–642. 2002.

ASTM International. "Standard Guide for Conducting a Terrestrial Soil-Core Microcosm Test." *ASTM E1197–87 (1998): Annual Book of ASTM Standards. Volume 11.05: Water and Environmental Technology: Biological Effects and Environmental Fate, Biotechnology; Pesticides*. Published on CD ROM. West Conshohocken, Pennsylvania: ASTM International. 1998.

Barnes, H.E. "Soil Investigation Employing a New Method of Layer-Value Determination for Earth Resistivity Interpretation." *Highway Research Board Bulletin*. Vol. 65. pp. 26–36. 1952.

Bechtel SAIC Company, LLC. "Performance Confirmation Plan." TDR–PCS–SE–000001. Rev. 05 ICN 00. Las Vegas, Nevada: Bechtel SAIC Company, LLC. 2004.

Bergström, L.F. "Use of Lysimeters to Estimate Leaching of Pesticides in Agricultural Soils." *Environmental Pollution*. Vol. 67: pp. 325–347. 1990.

Best, J.A., and J.B. Weber. "Disappearance of S-Triazines as Affected by Soil pH Using a Balance-Sheet Approach. *Weed Science*. Vol. 22. pp. 364–373. 1974.

Binley, A., G. Cassiani, R. Middleton, and P. Winship. "Vadose Zone Flow Model Parameterization Using Cross-Borehole Radar and Resistivity Imaging." *Journal of Hydrology*. Vol. 267, No. 34. pp. 147–159. 2002.

Binley, A., S. Henry-Poulter, and B. Shaw. "Examination of Solute Transport in An Undisturbed Soil Column Using Electrical Resistance Tomography." *Water Resources Research*. Vol. 32, No. 4. pp. 763–769. 1996.

Boll, J., T.S. Steenhuis, and J.S. Selker. "Fiberglass Wicks for Sampling of Water and Solutes in the Vadose Zone." *Soil Science Society of America Journal*. Vol. 56. pp. 701–707. 1992.

Boll, J., J.S. Selker, B.M. Nijssen, T.S. Steenhuis, J. Van Winkle, and E. Jolles. "Water Quality Sampling Under Preferential Flow Conditions." Proceedings of the ASCE International Symposium on Lysimetry: Lysimeters for Evapotranspiration and Environmental Measurement. R.G. Allen, et al., eds. New York City, New York. pp. 290–298. 1991.

Borchers, B., T. Uram, and J.M.H Hendrickx. "Tikhonov Regularization of Electrical Conductivity Depth Profiles in Field Soils." *Soil Science Society of America Journal*. Vol. 61. pp. 1,004–1,009. 1997.

Bowman, R.S. "Evaluation of Some New Tracers for Soil Water Studies." *Soil Science Society of America Journal*. Vol. 48. pp. 897–993. 1984.

Bowman, R.S. and J.F. Gibbens. "Difluorobenzoates as Nonreactive Tracers in Soil and Ground Water." *Ground Water*. Vol. 30. pp. 8–14. 1992.

Brandi-Dohrn, F.M., R.P. Dick, M. Hess, and J.S. Selker. "Field Evaluation of Passive Capillary Samplers." *Soil Science Society of America Journal*. Vol. 60. pp. 1,705–1,713. 1996.

Briggs, L.J. and A.G. McCall. "An Artificial Root for Inducing Capillary Movement of the Soil Moisture." *Science*. Vol. 20. pp. 566–569. 1904.

Bristow, K.L., G.S. Campbell, and K. Calissendorff. "Test of a Heat-Pulse Probe for Measuring Changes in Soil Water Content." *Soil Science Society of America Journal*. Vol. 57. pp. 930–934. 1993.

Brown, K.W., J.C. Thomas, and M.W. Holder. "Development of a Capillary Unsaturated Zone Water Sampler." CR812316–01–0. Las Vegas, Nevada: EPA, Environmental Monitoring Systems Laboratory. 1986.

Buoyoucos, G.J. and A.H. Mick. "An Electrical Resistance Method for the Continuous Measurement of Soil Moisture Under Field Conditions." Technical Bulletin 172. East Lansing, Michigan: Michigan Agricultural Experiment Station. 1940.

Buyanowski, G.A. and G.H. Wagner. "Annual Cycles of Carbon Dioxide Level in Soil Air." *Soil Science Society of America Journal*. Vol. 47. pp. 1,139–1,145. 1983.

Calder, I.R., I, Reid, T. Nisbet, A. Armstrong, J. Green, and G. Parkin "Study of the Potential Impacts on Water Resources of Proposed Afforestation." Final Report to Department of Environment, Food & Rural Affairs Contract CWO 633-I and Contract CWO 633-II. United Kingdom: Loughborough University. p. 179. 2002.

Campbell, C.G., M. Ghodrati, and F. Garrido. "Comparison of Time Domain Rreflectometry, Fiber Optic Mini-Probes, and Solution Samplers for Real Time Measurement of Solute Transport in Soil." *Soil Science Society of America Journal*. Vol. 164, No. 3. pp. 156–170. 1999.

Campbell, G.S., C. Calissendorff, and J.H. Williams. "Probe for Measuring Soil Specific Heat Using a Heat-Pulse Method." *Soil Science Society of America Journal*. Vol. 55. pp. 291–293. 1991.

Cepuder, P., and M. Tuller. "Simple Field-Testing Sites to Determine the Extent of Nitrogen Leaching From Agricultural Areas." *Nitrogen Economy in Tropical Soils*. N. Ahmad, ed. Dordrecht, The Netherlands: Kluwer Academic Publishers. pp. 355–361. 1996.

Chow, T.L. "A Porous Cup Soil-Water Sampler With Volume Control." *Soil Science Society of America Journal*. Vol. 124, No. 3. pp. 173–176. 1977.

Cole, D.W. "A System for Measuring Conductivity, Acidity, and Rate of Water Flow in a Forest Soil." *Water Resources Research*. Vol. 4, No. 5. pp. 1,127–1,136. 1968.

Corey, A.T. and A. Klute. "Application of the Potential Concept to Soil Water Equilibrium and Transport." *Soil Science Society of America Journal*. Vol. 49. pp. 3–11. 1985.

Cortassa, S., M.A. Aon, and P.F. Villon. "A Method for Quantifying Rates of O_2 Consumption and CO_2 Production." *Soil Science Society of America Journal*. Vol. 166. pp. 68–77. 2001.

Corwin, D.L. and S.M. Lesch. "Application of Soil Electrical Conductivity to Precision Agriculture: Theory, Principles, and Guidelines." *Agronomy Journal*. Vol. 95. pp. 455–471. 2003.

Cropper, W.P., K.C. Ewel, and J.W. Raich. "The Measurement of Soil CO_2 Evolution ." *Pedobiologia*. Vol. 28. pp. 35–40. 1985.

Daily, W.D., A.L. Ramirez, D.J. LaBrecque, and W. Barber. "Electrical Resistance Tomography Experiments at the Oregon Graduate Institute." *Journal of Applied Geophysics*. Vol. 33. pp. 227–237. 1995.

Daily, W.D., A.L. Ramirez, D.J. LaBrecque, and J. Nitao. "Electrical Resistivity Tomography of Vadose Water Movement: Electrical Resistivity Tomography of Vadose Water Movement." *Water Resources Research*. Vol. 28, No. 5. 1,429–1,442. 1992.

Davidson, E.A., E. Belk, and R.D. Boone. "Soil Water Content and Temperature as Independent or Confounded Factors Controlling Soil Respiration in a Temperate Mixed Hardwood Forest." *Global Change Biology*. Vol. 4, No. 2. pp. 217–277. 1998.

Davis, J.L. and A.P. Annan. "Ground-Penetrating Radar for High Resolution Mapping of Soil and Rock Stratigraphy." Geophysical Prospecting. Vol. 37. pp. 531–551. 1989.

Day, P.R., G.H. Bolt, and D.M. Anderson. "Nature of Soil Water." *Irrigation of Agricultural Lands*. R.M. Hagan, H.R. Haise, and T.W. Edminster, eds. Madison, Wisconsin: American Society of Agronomy. pp. 193–208. 1967.

de Jong, E., A.K. Ballantyne, D.R. Cameron, and D.W.L. Read. "Measurement of Apparent Electrical Conductivity of Soils By An Electromagnetic Induction Probe." *Soil Science Society of America Journal*. Vol. 43. pp. 810–812. 1979.

Dobson, M.C., F.T. Ulaby, M.T. Hallikainen, and M.A. El-Rayes. "Microwave Dielectric Behavior of Wet Soil II: Dielectric Mixing Models." *IEEE Transactions on Geoscience and Remote Sensing*. Vol. GE–23. pp. 35–46. 1985.

Dolan, P.W., B. Lowery, K.J. Fermanich, N.C. Wollenhaupt, and K. McSweeney. "Nitrogen Placement and Leaching In A Ridge-Tillage System." Proceedings on Agricultural Research to Protect Water Quality Conference, Minneapolis, Minnesota, February 21–24, 1993. Ankeny, Iowa. Soil Water Conservation Society. pp. 176–183. 1993.

Drew, B.P. A Review of the Available Methods for Tracing Underground Waters." *Proceedings of the British Speleological Association*. Vol. 6. pp. 1–19. 1968.

Drewitt, G.B., T.A. Black, Z. Nesic, E.R. Humphreys, E.M. Joek, R. Swanson, G.J. Ethier, T. Griffis, and K. Morgenstern. "Measuring Forest Floor CO_2 Fluxes in a Douglas-Fir Forest." *Agricultural and Forest Meteorology*. Vol. 110. pp. 299–317. 2002.

Dugas, W.A. "Micrometeorological and Chamber Measurements of CO_2 Flux from Bare Soil." *Agricultural and Forest Meteorology*. Vol. 67. pp. 115–128. 1993.

Essert, S. and J.W. Hopmans. "Combined Tensiometer-Solution Sampling Probe." *Soil & Tillage Research*. Vol. 45. pp. 299–309. 1998.

Evett, S.R. and J.L. Steiner. "Precision of Neutron Scattering and Capacitance Type Moisture Gauges Based on Field Calibration." *Soil Science Society of America Journal*. Vol. 59. pp. 961–968. 1995.

Ferré, P.A., G. von Glinski, and L.A. Ferré. "Monitoring the Maximum Depth of Drainage in Response to Pumping Using Borehole Ground Penetrating Radar." *Vadose Zone Journal*. Vol. 2. pp. 511–518. 2003.

Flint, A L., G.S. Campbell, K.M. Ellett, and C. Calissendorff. "Calibration and Temperature Correction of Heat Dissipation Matric Potential Sensors." *Soil Science Society of America Journal*. Vol. 66. pp. 1,439–1,445. 2002.

Flühler, H., M.S. Ardakani, and L.H. Stolzy. "Error Propagation in Determining Hydraulic Conductivities from Successive Water Content and Pressure Head Profiles." *Soil Science Society of America Journal*. Vol. 40. pp. 830–836. 1976.

Flury, M. and N.N. Wai. "Dyes as Tracers for Vadose Zone Hydrology." *Reviews of Geophysics*. Vol. 41, No. 1. pp. 2–5. 2003.

Freijer, J.I. and W.A. Bouten. "A Comparison of Field Methods for Measuring Soil Carbon Dioxide Evolution: Experiments and Simulation." *Plant and Soil*. Vol. 135. Vol. 133–142. 1991.

Fuentes, A., M. Lloréns, J. Sáez, A. Soler, M.I. Aguilar, J.F. Ortuño, and V.F. Meseguer. "Simple and Sequential Extractions of Heavy Metals From Different Sewage Sludges." *Chemosphere*. Vol. 54. pp. 1,039–1,047. 2004.

Furman, A., T.P.A. Ferré, and A.W. Warrick. "A Sensitivity Analysis of Electrical Resistivity Tomography Array Types Using Analytical Element Modeling." *Vadose Zone Journal*. Vol. 2. pp. 416–423. 2003.

Furth, R. "Application of 14C-Labeled Herbicides in Lysimeter Studies." *Weed Science*. Vol. 33, Supplement 2. pp. 11–17. 1985.

Gardner, W.H. "Water Content." *Methods of Soil Analysis Part 1: Physical and Mineralogical Methods*. 2nd Edition. A. Klute, ed. Agronomy Series No. 9. Madison, Wisconsin: American Society of Agronomy. pp. 493–544. 1986.

Garrido, F., M. Ghodrati, and C.G. Campbell. "Method for Field Calibration of Fiber Optic Miniprobes." *Soil Science Society of America Journal*. Vol. 64. pp. 836–842. 2000.

Garrido, F., M. Ghodrati, and M. Chendorain. "Small-Scale Measurement of Soil Water Content Using a Fiber Optic Sensor. *Soil Science Society of America Journal*. Vol. 63. pp. 1,505–1,512. 1999.

Gaskin, G.D. and J.D. Miller. "Measurement of Soil Water Content Using Simplified Impedance Measuring Technique. *Journal of Agricultural Engineering Research*. Vol. 63. pp. 153–160. 1996.

Gee, G. W., J.M. Keller, and A.L. Ward. "Measurement and Prediction of Deep Drainage from Bare Sediments at a Semiarid Site." *Vadose Zone Journal*. Vol. 4. pp. 32–40. 2005.

Ghodrati, M. "Point Measurement of Solute Transport Processes in Soil Using Fiber Optic Sensors." *Soil Science Society of America Journal*. Vol. 63. pp. 471–479. 1999.

Ghodrati, M., F. Garrido, C.G. Campbell, and M. Chendorain. "A Multiplexed Fiber Optic Miniprobe System for Measuring Solute Transport in Soil." *Journal of Environmental Quality*. Vol. 29. pp. 540–550. 2000.

Grimm, R.E., E. Heggy, S. Clifford, C. Dinwiddie, R. McGinnis, and D. Farrell. "Absorption and Scattering in Ground-Penetrating Radar: Analysis of the Bishop Tuff." *Journal of Geophysical Research*. Vol. 111. doi: 10.1029/2005JE002619. 2006.

Halvorson, A.D. and J.D. Rhoades. "Assessing Soil Salinity and Identifying Potential Saline-seep Areas with Field Soil Resistance Measurements." *Soil Science of America Proceedings*. Vol. 38. pp. 576–581. 1974.

Hanks, R.J. *Applied Soil Physics*. 2nd Edition. New York City, New York: Springer Verlag Publishers. 1992.

Heitman, J.L., Basinger, J.M., Kluitenberg, G.J., Ham, J.M., Frank, J.M., Barnes, and P.L. Field. "Evaluation of the Dual-Probe Heat-Pulse Method for Measuring Soil Water Content." *Vadose Zone Journal*. Vol. 2. pp. 552–560. 2003.

Hendrickx, J.M.H., B. Borchers, D.L. Corwin, S.M. Lesch, A.C. Hilgendorf, and J. Schlue. "Inversion of Soil Conductivity Profiles from Electromagnetic Induction Measurements: Theory and Experimental Verification." *Soil Science Society of America Journal*. Vol. 66. pp. 673–685. 2002.

Hendrickx, J.M.H., B. Baerends, Z.I. Raza, M. Sadig, and M. Akram Chaudhry. "Soil Salinity Assessment by Electromagnetic Induction of Irrigated Land." *Soil Science Society of America Journal*. Vol. 56. pp. 1,933–1,941. 1992.

Hilhorst, M.A., C. Dirksen, F.W.H. Kampers, and R.A. Feddes. "Dielectric Relaxation of Bound Water Versus Soil Matric Pressure." *Soil Science Society of America Journal*. Vol. 65. pp. 311–314. 2001.

Holder, M., K.W. Brown, J.C. Thomas, J.C., D. Zabcik, and H.E. Murray. "Capillary-Wick Unsaturated Zone Soil Pore Water Sampler." *Soil Science Society of America Journal*. Vol. 55, No. 5. pp. 1,195–1,202. 1991.

Huang, H. and D.C. Fraser. "Dielectric Permittivity and Resistivity Mapping Using High Frequency Helicopter-Borne EM Data." *Geophysics*. Vol. 67, No. 3. pp. 727–738. 2002.

Hubbell, J.M., M.J. Nicholl, J.B. Sisson, and D.L. McElroy. "Application of a Darcian Approach to Estimate Liquid Flux in a Deep Vadose Zone." *Vadose Zone Journal*. Vol. 3. pp. 560–569. 2004.

Iwata, S., T. Tabuchi, and B.P. Warkentin. *Soil Water Interactions*. New York City, New York: M. Dekker Publishers. 1988.

Jemison, J.M. and R.H. Fox. "Nitrate Leaching from Nitrogen Fertilized and Manured Corn Measured With Zero-Tension Pan Lysimeters." *Journal of Environmental Quality*. Vol.23. pp. 337–343. 1994.

Joffe, J.S. "Lysimeter Studies I: Moisture Percolation Through Soil Profiles." *Soil Science*. Vol. 34. pp. 123–143. 1932.

Karnok, K.J. and R.T. Kucharski. "Design and Construction of Rhizotron-Lysimeter Facility at the Ohio State University." *Agronomy Journal*. Vol. 74. pp. 152–156. 1982.

Käss, W. *Tracing Technique in Geohydrology*. Brookfield, Vermont: A.A. Balkema. 1998.

Keller, C. and J.M.H. Hendrickx. "Capillary Absorbers." *Methods of Soil Analysis Part 4—Physical Methods*. W.A. Dick, J.H. Dane, and G.C. Topp, eds. Madison, Wisconsin: Soil Science Society of America Inc. pp. 1,308–1,311. 2002.

Keller, C. and B. Travis. “Evaluation of the Potential of Fluid Absorber Mapping of Contaminants in Ground Water.” Proceedings of the Seventh National Outdoor Action Conference and Exposition. Dublin, Ohio: National Groundwater Association. p. 421. 1993.

Kilmer, V.J., O.E. Hays, and R.J. Muckenhirn. “Plant Nutrients and Water Losses from Fayette Silt Loam as Measured by Monolith Lysimeters.” *Journal of American Society of Agronomy*. Vol. 36. pp. 249–263. 1944.

Knight, J.H. and G.J. Kluitenberg. “Simplified Computational Approach for Dual-Probe Heat-Pulse Method.” *Soil Science Society of America Journal*. Vol. 68. pp. 447–449. 2004.

Knutson, J.H. and J.S. Selker. “Fiberglass Wick Sampler Effects on Measurement of Solute Transport in the Vadose Zone.” *Soil Science Society of America Journal*. Vol. 60. pp. 420–424. 1996.

———. “Unsaturated Hydraulic Conductivities of Fiberglass Wicks and Designing Capillary Pore-water Samplers.” *Soil Science Society of America Journal*. Vol. 58. pp. 721–729. 1994.

Knutson, J.H., S.B. Lee, W.Q. Zhang, and J.S. Selker. “Fiberglass Wick Preparation for Use in Passive Capillary Wick Soil Pore-Water Samplers.” *Soil Science Society of America Journal*. Vol. 57. pp. 1,474–1,476. 1993.

Knutsson, G. “Tracers for Ground Water Investigations.” *Groundwater Problems*. E. Eriksson, Y. Gustavsson, and K. Nilsson, eds. New York City, New York: Pergamon Publishers. pp. 123–152. 1968.

Koglin, E.N., E.J. Poziomek, and M.L. Kram. “Emerging Technologies for Detecting and Measuring Contaminants in the Vadose Zone.” *Handbook of Vadose Zone Characterizing and Monitoring*. L.G. Wilson, L.G. Everett, and S.J. Cullen., eds. Boca Raton, Florida: Lewis Publishers. pp. 657–700. 1995.

Kohnke, H., F.R. Dreibelbis, and J.M. Davidson. “A Survey and Discussion of Lysimeters and a Bibliography on Their Construction and Performance.” Publication No. 374. Washington, DC: Department of Agriculture. 1940.

Kowalsky, M.B., J. Peterson, J. Birkholzer, S. Finsterle, S. Mukhopadhyay, and Y. Tsang. “Joint Inversion of Ground-Penetrating Radar and Thermal-Hydrological Data Collected During a Large-Scale Heater Test.” *EOS Transactions of American Geophysical Union*. Vol. 86, No. 52. Fall Meeting Supplement. 2005.

Krohn, D.A. “Chemical Analysis.” *Fiber Optic Sensors: Fundamentals and Applications*. Research Triangle Park, North Carolina: Instrument Society of America. pp.193–209. 1988.

Krone, R.B., H.F. Ludwig, and J.F. Thomas. “Porous Tube Device for Sampling Soil Solutions During Water Spreading Operations.” *Soil Science Society of America Journal*. Vol. 73. pp. 211–219. 1951.

Kulp, T.J., D. Bishop, and S.M. Angel. “Column-Profile Measurements Using Fiber Optic Spectroscopy.” *Soil Science Society of America Journal*. Vol. 52. pp. 624–627. 1988.

Kutilek, M. and D.R. Nielsen. *Soil Hydrology*. Cremlingen-Destedt, Germany: Catena Verlag, GeoScience Publisher. 1994.

Lesch, S.M, and D.L. Corwin. "Using the Dual-pathway Conductance Model to Determine How Different Soil Properties Influence Conductivity Survey Data." *Agronomy Journal*. Vol. 95. pp. 365–379. 2003.

Louie, M.J., P.M. Shelby, J.S. Smesrud, L.O. Gatchell, and J.S. Selker. "Field Evaluation of Passive Capillary Samplers for Estimating Groundwater Recharge." *Water Resources Research*. Vol. 36, No. 9. pp. 2,407–2,416. 2000.

Lund, C.P., W.J. Riley, L.L. Pierce, and C.B. Field. "The Effects of Chamber Pressurization on Soil-Surface CO_2 Efflux and the Implications for NEE Measurements Under Elevated CO_2." *Global Change Biology*. Vol. 5. pp. 269–281. 1999.

Majer, E.L., K.H. Williams, J.E. Peterson, and T.M. Daley. "High Resolution Imaging of Vadose Zone Transport Using Crosswell Radar and Seismic Methods." LBNL–13792. Berkeley, California: Lawrence Berkeley National Laboratory. 2002.

Malcolm, R.L., G.R. Aiken, E.M. Thurman, and P.A. Avery. "Hydrophilic Organic Solutes as Tracers in Groundwater Recharge Studies." *Contaminants and Sediments*. R.A. Baker, ed. pp. 71–88. Woburn, Massachusetts: Butterworth-Heinemann. 1980.

Martens, D.A. "Identification of Phenolic Acid Composition of Alkali-Extracted Plants and Soils." *Soil Science Society of America Journal*. Vol. 66. pp. 1,240–1,248. 2002.

Massman, W.J. and X. Lee. "Eddy Covariance Flux Corrections and Uncertainties in Long-Term Studies of Carbon and Energy Exchanges." *Agricultural and Forest Meteorology*. Vol. 113, No. 1-4. pp. 121–144. 2002.

McCarthy, J.F., K.M. Howard, and L.D. Mckay. "Effect of pH on Sorption and Transport of Fluorobenzoic Acid Ground Water Tracers." *Journal of Environment Quality*. Vol. 29. pp. 1,806–1813. 2000.

McElroy D.L. and J.M. Hubbell. "Evaluation of the Conceptual Flow Model for a Deep Vadose Zone System Using Advanced Tensiometers." *Vadose Zone Journal*. Vol. 3. pp. 170–182. 2004.

McMahon, M.A. and G.W. Thomas. "Chloride and Tritiated Water Flow in Disturbed and Undisturbed Soil Cores." *Soil Science of America Proceedings*. Vol. 38. pp. 727–732. 1974.

McNeill, J.D. *Electromagnetic Terrain Conductivity Measurement at Low Induction Numbers*. Technical Note TN–6. Ontario, Canada: Geonics Limited, Mississauga. 1980.

Mori, Y., J.W. Hopmans, A.P. Mortensen, and G.J. Kluitenberg. "Multi-Functional Heat Pulse Probe for the Simultaneous Measurement of Soil Water Content, Solute Concentration, and Heat Transport Parameters." *Vadose Zone Journal*. Vol. 2. pp. 561–571. 2003.

Morrison, R.D., K. Lepic, and J. Baker. "Vadose Zone Monitoring at a Hazardous Waste Landfill." Proceedings of the Characterization and Monitoring of the Vadose Zone. Las Vegas, Nevada: National Well Association. pp. 517–528. 1983.

Moutonnet, P. and J.C. Fardeau. "Inorganic Nitrogen in Soil Solution Collected with Tensionic Samplers." *Soil Science Society of America Journal*. Vol. 61. pp. 822–825. 1997.

Moutonnet, P., J.F. Pagenel, and J.C. Fardeau. "Simultaneous Field Measurement of Nitrate-Nitrogen and Matric Pressure Head." *Soil Science Society of America Journal*. Vol. 57. pp. 1,458–1,462. 1993.

Moutonnet, P., G. Guiraud, and C. Marol. "Le Tensiomètre et La Teneur En Nitrates De La Solution De Sol." *Milieux Poreux Transferts Hydriques*. Vol. 26. pp. 11–29. 1989.

Moyer, J.W., L.S. Saporito, and R.R. Janke. "Design, Construction, and Installation of an Intact Soil Core Lysimeter." *Agronomy Journal*. Vol. 88. pp. 253–256. 1996.

Nadler, A. "Determining the Volume of Sampled Soil When Using the Four-Electrode Technique." *Soil Science Society of America Journal*. Vol. 44. pp. 1,186–1,190. 1980.

Nakashima, M., M. Inoue, K. Sawada, and C. Nicholl. "Measurement of Soil Water Content by Amplitude Domain Reflectometry Method and its Calibrations." *Cikasui Gakkaishi*. Vol. 40. pp. 509–519. 1998.

Neal, A. "Ground-Penetrating Radar and Its Use in Sedimentology: Principles, Problems, and Progress." *Earth-Science Reviews*. Vol. 66. pp. 261–330. 2004.

Nielsen, J.M., G.F. Pinder, T.J. Kulp, and S.M. Angel. "Investigation of Dispersion in Porous Media Using Fiber-Optic Technology." *Water Resources Research*. Vol. 27, No. 10. pp. 2,743–2,749. 1991.

Nitao, J.J. and J. Bear. "Potentials and Their Role in Transport in Porous Media." *Water Resources Research*. Vol. 32. pp. 225–250. 1996.

Or, D. "Irrigation Management Considering Soil Variability and Climatic Uncertainty (Abstract)." Ph.D. dissertation. Utah State University. Logan, Utah. 1990.

Or, D. and J.M. Wraith. "Soil Water Content and Water Potential Relationships." *Soil Physics Companion*. A Warrick, ed. Boca Raton, Florida: CRC Press. pp. 49–84. 2002.

———. "Soil Water Content and Water Potential Relationships." *Handbook of Soil Science*. M. Sumner, ed. Boca Raton, Florida: CRC Press. pp. A53–A85. 1999.

Ouyang, Y. and L. Boersma. "Dynamic Oxygen and Carbon Dioxide Exchange Between Soil and Atmosphere: I. Model Development." *Soil Science Society of America Journal*. Vol 56. pp. 1,695–1,702. 1992.

Paltineanu, I.C. and J.L. Starr. "Real-Time Soil Water Dynamics Using Multisensor Capacitance Probes: Laboratory Calibration." *Soil Science Society of America Journal*. Vol. 61. pp. 1,576–1,585. 1997.

Parizek, R.R. and R.E. Lane. "Soil-Water Sampling Using Pan and Deep Pressure-Vacuum Lysimeters." *Journal of Hydrology*. Vol. 11, No. 1. pp. 1–21. 1970.

Phene, C.J., G.J. Hoffman, and S.L. Rawlins. "Measuring Soil Matric Potential by Sensing Heat Dissipation Within a Porous Body: I. Theory and Sensor Construction." *Soil Science of America Proceedings*. Vol. 35. pp. 27–33. 1971.

Pueyo, M., J. Sastre, E. Hernández, M. Vidal, J.F. López-Sánchez, and G. Rauret. "Prediction of Trace Element Mobility in Contaminated Soils by Sequential Extraction." *Journal of Environmental Quality*. Vol. 32. pp. 2,054–2,066. 2003.

Reece, C.F. "Evaluation of a Line Heat Dissipation Sensor for Measuring Soil Matric Potential." *Soil Science Society of America Journal*. Vol. 60. pp. 1,022–1,028. 1996.

Reeder, J.D. "A Nonweighing Lysimeter Design for Field Studies Using Nitrogen-15. *Soil Science Society of America Journal*. Vol. 50. pp. 1,224–1,227. 1986.

Rehm, B., B. Christel, T. Stolzenberg, D. Nichols, B. Lowery, and B. Andraski. "Field Evaluation of Instruments of Unsaturated Hydraulic Properties of Fly Ash." Palo Alto, California: Electric Power Research Institute. 1986.

Ren, T., G.J. Kluitenberg, and R. Horton. "Determining Soil Water Flux and Pore Water Velocity by a Heat Pulse Technique." *Soil Science Society of America Journal*. Vol. 64. pp. 552–560. 2000.

Rhoades, J.D. "Monitoring Soil Salinity: A Review of Methods." *Establishment of Water Quality Monitoring Programs*. L.G. Everett and K.D. Schmidt, eds. St. Paul, Minnesota: American Water Resources Association. pp. 150–165. 1978.

Rhoades, J.D. and A.D. Halvorson. "Electrical Conductivity Methods for Detecting and Delineating Saline Seeps and Measuring Salinity in Northern Great Plains Soils." USDA ARS–42. Washington, DC: U.S. Government Printing Office. 1977.

Rhoades, J.D. and R.D. Ingvalson. "Determining Salinity in Field Soils with Soil Resistance Measurements." *Soil Science of America Proceedings*. Vol. 35. pp. 54–60. 1971.

Rhoades, J.D. and J.D. Oster. "Solute Content." *Methods of Soil Analyses Part 1—Physical and Mineralogical Methods*. 2nd Edition. A. Klute, ed. Madison, Wisconsin: Soil Science Society of America, Inc. 1986.

Rhoades, J.D. and J. van Schilfgaarde. "An Electrical Conductivity Probe for Determining Soil Salinity." *Soil Science Society of America Journal*. Vol. 40. pp. 647–651. 1976.

Rimmer, A., T.S. Steenhuis, and J.S. Selker. "Wick Samplers: An Evaluation of Solute Travel Times." *Soil Science Society of America Journal*. Vol. 59. pp. 235–243. 1995.

Rimmer, A., T.S. Steenhuis, and J.S. Selker. "One-Dimensional Model to Evaluate the Performance of Wick Samplers in Soils. *Soil Science Society of America Journal*. Vol. 59. pp. 88–92. 1995.

Robinson, D.A., S.B. Jones, J.M. Wraith, D. Or, and S.P. Friedman. "A Review of Advances in Dielectric and Electrical Conductivity Measurement in Soils Using Time Domain Reflectometry." *Vadose Zone Journal*. Vol. 2. pp. 444–475. 2003.

Rogers, K.R. and E.J. Poziomek. "Fiber Optic Sensors for Environmental Monitoring." *Chemosphere*. Vol. 33, No. 6. pp. 1,151–1,174. 1996.

Roth, K., R. Schulin, H. Fluhler, and W. Attinger. Calibration of Time Domain Reflectometry for Water Content Measurement Using Composite Dielectric Approach. *Water Resources Research*. Vol. 26, No. 10. pp. 2,267–2,273. 1990.

Rust, A.C. and J.K. Russell. "Detection of Welding in Pyroclastic Flows with Ground-Penetrating Radar: Insights From Field and Forward Modeling Data." *Journal of Volcanology and Geothermal Research*. Vol. 95. pp. 23–34. 2006.

Saragoni, H., R. Poss, and R. Oliver. "Dynamique et Lixiviation Des Éléments Minéraux Dans Les Terres De Barre du Sud du Togo." *Agron. Trop*. (Paris). Vol. 45. pp. 259–273. 1990.

Seebeck, T.J. "Über den Magnetismus der Galvenischen Kette." *Abh. K. Akad*. (Wiss. Berlin) 289. 1921.

Selker, J.S. "Passive Capillary Samplers." *Methods of Soil Analysis Part 4—Physical Methods*. W.A. Dick, et al., eds. Madison, Wisconsin: Soil Science Society of America, Inc. pp. 1,266–1,269. 2002.

Sentek Pty Ltd. "Calibration Manual of Sentek Pty Ltd Soil Moisture Sensors." Stepney, South Australia: Sentek Pty Ltd. p. 12. 2001.

Slater, L., A. Binley, W. Daily, and W.R. Johnson. "Cross-Hole Electrical Imaging of a Controlled Saline Tracer Injection." *Journal of Applied Geophysics*. Vol. 44. pp. 85–102. 2000.

Slater, L., A. Binley, and D. Brown. "Electrical Imaging of Fractures Using Ground-Water Salinity Change." *Ground Water*. Vol. 35. pp. 436–442. 1997.

Spaans, E.J.A., and J.M. Baker. "Calibration of Watermark Soil Moisture Sensors for Soil Matric Potential and Temperature." *Plant Soil*. Vol. 143. pp. 213–217. 1992.

Stetzenbach, K.J., S.L. Jensen, and G.M. Thompson. "Trace Enrichment of Fluorinated Organic Acids Used as Groundwater Tracers by Liquid Chromatography." *Environmental Science Technology*. Vol. 16. pp. 250–254. 1982.

Stone, D.M., and J.L. Robl. "Construction and Performance of Rugged Ceramic Cup Soil Water Samplers." *Soil Science Society of America Journal*. Vol. 60. pp. 417–420. 1996.

Sudduth, K.A., N.R. Kitchen, G.A. Bollero, D.G. Bullock, and W.J. Wiebold. "Comparison of Electromagnetic Induction and Direct Sensing Soil Electrical Conductivity." *Agronomy Journal*. Vol. 95. pp. 472–482. 2003.

Thompson, M.L., and R.L., Scharf. "An Improved Zero-Tension Lysimeter to Monitor Colloid Transport in Soils." *Journal of Environmental Quality*. Vol. 23. pp. 378–383. 1994.

Topp, E. and W. Smith. "Sorption of Herbicides Atrazine and Metolachlor to Selected Plastics and Silicone Rubber." *Journal of Environmental Quality*. Vol. 8, No. 2. pp. 316–317. 1992.

Topp, G.C., J.L. Davis, and A.P. Annan. "Electromagnetic Determination of Soil Water Content: Measurements in Coaxial Transmission Lines." *Water Resources Research*. Vol. 16. pp. 574–582. 1980.

Triantafilis, J., G.M. Laslett, and A.B. McBratney. "Calibrating an Electromagnetic Induction Instrument to Measure Salinity Under Irrigated Cotton." 2000.

Tuller, M. and M.R. Islam. "Field Methods for Monitoring Solute Transport." *Soil-Water-Solute Process Characterization: An Integrated Approach*. J. Álvarez-Benedí and R. Muñoz-Carpena, eds. Boca Raton, Florida: CRC Press. pp. 309–355. 2005.

Turcu, V.E., S.B. Jones, and D. Or. "Continuous Soil Carbon Dioxide and Oxygen Measurements and Estimation of Gradient-based Gaseous Flux." *Vadose Zone Journal*. Vol. 4. pp. 1,161–1,169. doi: 10.2136/vzj2004.0164. 2005.

Tyler, D.D. and G.W., Thomas. "Lysimeter Measurements of Nitrate and Chloride Losses from Soil under Conventional and No-Tillage Corn." *Journal of Environmental Quality*. Vol. 6. pp. 63–66. 1977.

Villar-Mir, J.M., P. Villar-Mir, C.O. Stockle, F. Ferrer, and M. Aran. "On-Farm Monitoring of Soil Nitrate-Nitrogen in Irrigated Cornfields in the Ebro Valley (Northeast Spain)." *Agronomy Journal*. Vol. 94. pp. 373–380. 2002.

Wang, Q., T.E. Ochsner, and R. Horton. "Mathematical Analysis of Heat Pulse Signals for Soil Water Flux Determination." *Water Resources Research*. Vol. 38. p. 10. 2002.

Warrick, A.W., and A. Amoozegar-Fard. "Soil Water Regimes Near Porous Cup Water Samplers." *Water Resources Research*. Vol. 13, No. 1. pp. 203–207. 1977.

Weber, J.B. "Physicochemical and Mobility Studies with Pesticides." *Agrochemical Environmental Fate Studies: State of the Art*. M.L. Leng, E.M.K. Leovey, and P.L. Zubkoff, eds. Boca Raton, Florida: CRC Press. pp. 99–115. 1995.

Winton, K. and J.B. Weber. "A Review of Field Lysimeter Studies to Describe the Environmental Fate of Pesticides." *Weed Technology*. Vol. 10. pp. 202–209. 1996.

Wood, W.W. "A Technique Using Porous Cups for Water Sampling at Any Depth in the Unsaturated Zone." *Water Resources Research*. Vol. 9, No. 2. pp. 486–488. 1973.